FUNCTION AND MECHANISM OF CHROMATIN BOUNDARIES IN DROSOPHILA HOX GENE COMPLEXES

by

MO LI

(Under the Direction of Haini N. Cai)

ABSTRACT

Chromatin boundaries or insulators partition the genome into structurally and functionally autonomous domains. The mechanism of boundary function is unclear. Based on the observations that the *gypsy* retrotransposon, which contains the su(Hw) insulator, and the su(Hw) insulator proteins, SUHW and MOD(MDG4), cluster near the nuclear periphery, it was proposed that the function of su(Hw) depends on its localization to the nuclear periphery. Using fluorescent in situ hybridization (FISH), we show that transgenes containing the su(Hw) insulator do not preferentially localize near the nuclear periphery. Immunostainings show that SUHW and MOD(MDG4) are not restricted to the nuclear periphery. Additionally, the enhancer-blocking activity of suHw remains intact during heat shock, which disrupts the cluster of insulator proteins at the nuclear periphery. Our data show that su(Hw) can function in the nuclear interior, possibly through interactions with other insulators or nuclear structures. To understand how endogenous insulators regulate gene expression, I studied the SF-1 insulator in the *Antennapedia* complex (ANT-C). Using a cell-based insulator assay, we show that

Ebx/NURF301 and Iswi modulate the activity of multiple *Drosophila* insulators including SF-1, su(Hw), Fab-7 and Fab-8. Reduced levels of Ebx/NURF301 or Iswi disrupts the enhancer-blocking activity of SF1 and su(Hw) in transgenic embryos. Our findings provide the first evidence that a nucleosome-remodeling complex participates in the enhancer-blocking mechanism of insulators. To gain insights into the role of insulators in Hox gene regulation, we studied the genomic organization of *Drosophila* Hox complexes using Chromosome Conformation Capture (3C) and FISH. First, we find that SF-1 interacts with multiple regions in ANT-C, and show that these regions contain novel insulators. Second, we find that the *lab* and *Antp* gene in ANT-C are closely associated with each other inside the nucleus despite the large linear distance. Third, we find an interaction between promoter regions of *Antp* in ANT-C and *Abd-B* in BX-C. This interaction occurs in posterior tissues, where both genes are expressed, or in tissues where both genes are ectopically activated due to mutations in the *Polycomb* group proteins. This is the first documented example of a developmentally regulated, long-range physical interaction between Hox clusters.

INDEX WORDS: *Drosophila*, transcription, enhancer, promoter, chromatin boundary, insulator, SF-1, RNAi, Hox gene, ANT-C, BX-C, 3C, FISH.

FUNCTION AND MECHANISM OF CHROMATIN BOUNDARIES IN DROSOPHILA HOX GENE COMPLEXES

by

MO LI

B.S., Peking University, China, 2001

A Dissertation Submitted to the Graduate Faculty of The University of Georgia in Partial Fulfillment of the Requirements for the Degree

DOCTOR OF PHILOSOPHY

ATHENS, GEORGIA

2007

FUNCTION AND MECHANISM OF CHROMATIN BOUNDARIES IN DROSOPHILA HOX GENE COMPLEXES

by

MO LI

Major Professor: Haini N. Cai

Committee: Michael Bender
Scott T. Dougan
Edward T. Kipreos
Boris Striepen

Electronic Version Approved:

Maureen Grasso
Dean of the Graduate School
The University of Georgia
August 2007

TABLE OF CONTENTS

LIST OF FIGURES

Page

CHAPTER 1

INTRODUCTION AND LITERATURE REVIEW

Eukaryotic Gene Regulation

Animal development consists of numerous programs that determine when and where to activate or repress certain genes. In eukaryotes, genes are controlled by cis-regulatory elements known as enhancers and promoters, which contain binding sites for protein factors that control gene transcription. Enhancers can activate gene promoters over distances as great as several hundred kilo base pairs (Jack and DeLotto, 1995; Liu et al., 1991) and in extreme cases, across different chromosomes (Lomvardas et al., 2006). Furthermore, many enhancers can promiscuously interact with heterologous promoters. These properties of enhancers could potentially lead to a spillover of the activation effect. The expression of eukaryotic genes is also influenced by the structure of chromatin, which contains condensed domains known as heterochromatin that repress transcription. The spread of heterochromatin is an important mechanism to repress gene repression at specific locations such as centromeres and telomeres. If left unchecked, the propagation of heterochromatin can invade open chromatin domains and ectopically silence genes therein (Fig. 1.1). These long-range activating or repressive transcriptional influences present a challenge for independent gene regulation.

Insulators, also known as chromatin boundaries, are DNA elements found in most eukaryotic organisms from yeast to humans that partition the genome into functionally and structurally autonomous domains. Insulators can block the interaction between an enhancer and a promoter when situated in between the two (enhancer blocking) and act as barriers to encroaching condensed chromatin domains (Fig. 1.1). Over a decade of research has demonstrated the important role that insulators play in many aspects of biology, including regulation of key developmental genes such as Hox genes, gene imprinting, and escape from X-chromosome inactivation (Filippova et al., 2005).

Insulators in flies, vertebrates and yeast

Two of the first insulator elements identified in *Drosophila* are the *scs* and *scs'* insulators that flank the 87A7 *hsp70* locus. The 87A7 hsp70 locus on polytene chromosome decondenses to form a puff when the *hsp70* gene expression is induced by heat shock. The *scs* and *scs'* elements were initially discovered as nuclease hypersensitive sites that coincide with the borders of the chromosome puff under heat shock conditions (Udvardy et al., 1985). Their nuclease sensitivity profiles were found to be altered by heat shock. Based on these observations, it was proposed that *scs* and *scs'* functions as boundaries of the active *hsp70* domain. The *scs* and *scs'* elements were characterized by two assays. The first assay tested for their ability to protect a reporter gene from chromosomal position effects (CPE). The *mini-white* gene is required for the production of the red pigment in fly eyes and traditionally used for CPE-

protection assay in Drosophila. An unprotected mini-white gene gives rise to a wide range of eye color when randomly inserted into the genome, indicating that the expression of *mini-white* is influenced by the chromosomal environment of the insertion site. When *mini-white* is flanked by either *scs* or *scs'* on both sides, it produced a uniform eye color independent of the insertion site, suggesting that *scs* and *scs'* can protect trangenes against CPE. The second assay tested for the ability of *scs* and *scs'* to block enhancer-promoter communication. The *scs* and *scs'* elements were shown to block an enhancer from activating a promoter when inserted in between the enhancer and promoter (Kellum and Schedl, 1992b).

Additional insulators were later identified in a wide range of genetic locations in *Drosophila*, including the su(Hw) insulator in the *gypsy* retrotransposon, the Fab-7 and Fab-8 insulators in the *Abd-B* locus, the SF-1 insulator in the *Scr-ftz* locus and an insulator in the *evenskipped* promoter (Ohtsuki and Levine, 1998b). Like *scs* and *scs'*, these insulators also contain nuclease hypersensitive sites and possess the ability to protect trangenes against CPE and block enhancers. Interestingly, the insulators identified in *Drosophila* so far share little sequence similarity, and require distinct protein factors, suggesting that diverse mechanisms may be at play.

Insulators are also believed to be widely present in vertebrate genomes. It is worth noting that the chromosomal position effects that transgenes experience in vertebrates are not identical to those in *Drosophila*. Unlike *Drosophila*, the vertebrate genome has constitutive heterochromatin domains outside of telomeres and centromeres. Transgenes randomly inserted into vertebrate genomes become

repressed over time by formation of condensed chromatin. Consequently, the CPE protection assay in vertebrates measures the ability of insulators to shield transgenes from long-term repression (barrier activity). One of the best-characterized vertebrate insulators is the 5'HS4 element in the chicken *β-globin* locus (Bell et al., 1999; Pikaart et al., 1998). The enhancer-blocking activity of the 5'HS4 insulator is dependent on the CTCF protein. Interestingly, CTCF is the only vertebrate insulator component identified to date, and is used by many different vertebrate insulators. The *Drosophila* homolog of CTCF, dCTCF, is also an insulator protein of the Fab-8 insulator. It is unclear why among many *Drosophila* insulator proteins only CTCF is conserved in higher animals. Interestingly, the barrier activity of 5'HS4 is separable from its enhancer-blocking activity and requires distinct protein factors (Recillas-Targa et al., 2002; West et al., 2004). Such separation of the two activities has not been demonstrated in *Drosophila.*

Chromatin boundaries in yeast function primarily as barriers that block spread of heterochromatin and telomeric silent domains. The formation of silent chromatin domains provides an important mechanism for gene repression in yeast. In the haploid budding yeast *Saccharomyces cerevisiae,* the mating-type specific genes *MATa* and *MAT*α in the HMR and HML loci, respectively, are silenced by two flanking silencers through Sir2/3/4 protein complex-mediated spread of heterochromatin (Haber, 1998). Boundary elements identified on both sides of the two sliencers, such as HMR $tRNA^{Thr}$ and *Chal* UAS, have been shown to restrict the silent chromatin domain to the HM loci (Donze et al., 1999; Donze and Kamakaka, 2001). The STAR (sub-telomeric anti-silencing region) element, which is located between the X and Y' sub-telomeric repeats

represents another type of yeast boundary that can block sub-telomeric silencing. Boundary elements in yeast share little similarity in DNA sequence and most of them consist of clusters of binding sites for distinct proteins. All chromatin boundaries in yeast identified to date exhibit barrier activity but not enhancer-blocking activity. The reason may be that yeast, being single-cell organisms with a compact genome, do not have long-range enhancers, and use short sequences called UAS (upstream activating sequence) close to promoters to activate genes instead.

Mechanism of enhancer blocking

Although many insulators have been characterized in diverse organisms, the mechanisms underlying insulator function are still unknown. The insulators identified so far show little sequence similarities and require distinct protein components, suggesting that they may function via different mechanisms. In this section, current views on how insulators function as enhancer-blocker and barriers will be presented together with supporting evidence.

Our limited knowledge on how enhancers work is the major hindrance to understanding how insulators block enhancers. Several models attempting to explain enhancer blocking are closely connected to often-conflicting notions of how enhancers work. One school of thought proposes that enhancer activity relies on "tracking" along DNA/chromatin to the promoter in the form of physical interactions between enhancer-nucleoprotein complex and intervening sequences. According to this model, an insulator sitting in between the enhancers and promoters would disrupt this tracking

process, leading to enhancer blocking. Evidence from the Drosophila *cut* locus supports this model. An insertion of the su(Hw) insulator has been shown to block the wing margin enhancer of the *cut* gene that is 85 kb upstream of the *cut* promoter and result in the cut-wing phenotype (Dorsett, 1993). The ability of the su(Hw) insulator to block the wing margin enhancer is enhanced by mutations in the Drosophila CHIP protein, which has been shown to interact with numerous transcription factors and facilitates enhancer action (Morcillo et al., 1997; Morcillo et al., 1996). It is proposed that CHIP is recruited to enhancers by other activators and facilitates enhancer-promoter communications by binding to sites spread along the intervening chromatin fiber (Gause et al., 2001). According to this view, the interaction observed between suHw and *Chip* could stop the CHIP-enhancer complex on its track to the promoter, leading to enhancer blocking.

Enhancers can also emit processive signals that gradually open up the chromatin between the enhancer to the promoter. The locus control region (LCR) of the *β-globin* locus, which contains long-range enhancers of the *β-globin* genes, has been found to recruit RNA polymerase II (Gause et al., 2001; Johnson et al., 2003; Routledge and Proudfoot, 2002; Tuan et al., 1992). Additionally, non-genic transcripts by Pol II are detected within the LCR and upstream of the *β-globin* genes, suggesting that the transcription machinery is first recruited to the enhancers and then delivered to the promoters (Ashe et al., 1997; Gribnau et al., 2000; Tuan et al., 1992). Intergenic transcription may be a mechanism by which enhancers can open up chromatin between the enhancer and the promoter for active transcription. An insulator situated in between

the enhancer and promoter could possibly act as a roadblock against the delivery of Pol II to the promoter, therefore blocking activation. Consistent with the "roadblock model", insertion of the 5'HS4 insulator between the HS2 enhancer in the human *β-globin* LCR and a downstream *ε-globin* gene greatly reduces the level of Pol II found at the promoter. On the other hand, Pol II is accumulated in the region from the HS2 enhancer to the 5'HS4 insulator (Zhao and Dean, 2004; Zhao et al., 2006). Together, this suggests that 5'HS4 blocks the processive transfer of Pol II from HS2 to the promoter. Recently, CTCF has been shown to interact with the largest subunit of Pol II, providing a possible mechanism for CTCF-dependent insulators to intercept the delivery of Pol II from enhancers to promoters (Chernukhin et al., 2007).

Enhancers can also create active chromatin domains through histone modifications. For example, the recruitment of histone acetyltransferases (HATs) to the human growth hormone locus control region (hGH LCR) is essential for establishing a 32 kb domain of acetylated chromatin that originates from LCR and spreads to the *hGH-N* gene (Elefant et al., 2000a; Elefant et al., 2000b; Ho et al., 2002). The 5'HS4 insulator has also been shown to block the spreading of active histone modifications from an enhancer to a promoter, possibly through formation of a nucleosome-free gap within the insulator (Zhao et al., 2006).

Another model based on "enhancer-tracking" suggests that an insulator can trap the enhancer by mimicking a functional promoter and therefore preventing activation of the true target promoter. This model is often referred to as the promoter decoy model (Geyer, 1997a). Consistent with the promoter decoy model, many Drosophila insulators

contain promoter-like sequences. However, there are enhancers that can activate two tandem genes without being blocked by the authentic promoters most proximal to the enhancer, meaning additional mechanisms must be invoked to reconcile the promoter decoy model. Moreover, some Drosophila enhancers such as the iab enhancers can activate genes located on different chromosomes through a phenomenon termed transvection (Hopmann et al., 1995). Clearly, these enhancers do not rely solely on tracking to function.

Alternative to the tracking model of enhancer action, the looping model proposes that distant enhancers can activate transcription by physically interacting with promoters through formation of chromatin loops. The use of the Chromatin Conformation Capture (3C) method has provided direct evidence of such chromatin loops between enhancers and promoters. For instance, a single enhancer has been found to interact intra- and inter-chromosomally with only one of the 1300 olfactory receptor genes in a single neuron (Lomvardas et al., 2006). Based on the looping model of enhancer action, the looping model of insulator function proposes that insulators may interfere with chromatin loop formation between an enhancer and a promoter through interactions with like elements or sub-nuclear structures. Interactions between insulators have been documented in several studies. For example, two su(Hw) insulators in tandem mutually abolish enhancer-blocking, allowing the enhancer to bypass the insulators. However, when two su(Hw) insulators flank both sides of either the enhancer or the promoter, their ability to block the enhancer is strengthened (Cai and Shen, 2001; Muravyova et al., 2001). These results suggest that two closely positioned su(Hw) insulators

preferentially interact with each other, precluding them from forming chromatin loop with other insulators or nuclear structures that are required for effective enhancer blocking.

Interactions between insulators are likely to be mediated by insulator-binding proteins. At least two proteins, SUHW and MOD(MDG4), are required for the insulator function of the su(Hw) element. SUHW and MOD(MDG4) have been found to cluster into ~20 loci (termed insulator bodies) at the nuclear periphery. Integrated *gypsy* retrotransposons, which contain the 340 bp SUHW binding site, have also been shown to locate to these peripheral loci. These observations prompted the hypothesis that insulator bodies consist of endogenous su(Hw)-binding sites brought together by MOD(MDG4) through the BTB/POZ (Broad complex, Tramtrack, bric a brac/poxvirus and zinc finger) domain, which mediates protein oligomerization (Gerasimova et al., 2000; Katsani et al., 1999). The consequences of the formation of insulator bodies are two fold: first, it could interfere with enhancer-promoter interactions by creating physical constraints on chromatin; second, it could bring distant genes into the same sub-nuclear compartment to be co-regulated. However, the results presented in Chapter 2 show that the su(Hw) insulator does not exhibit preferential distribution towards nuclear periphery and is functional in the nuclear interior, suggesting mechanisms independent of the insulator body.

What properties of insulators allow them to loop chromatin? Some clues to the answer come from special chromatin structures found within insulators. Many insulators harbor nuclease-hypersensitive sites (HS) or nucleosome-depleted regions (Barges et al., 2000; Karch et al., 1994; Kellum and Schedl, 1991, 1992b; Vazquez and Schedl,

2000). A recent paper reported that nucleosome depletion in the 5'HS4 insulator is dependent on CTCF and is required for enhancer blocking (Zhao et al., 2006). In addition, several insulators are known to contain MARs/SARs (Matrix/Scaffold attachment region)(Antes et al., 2001; Nabirochkin et al., 1998; Stief et al., 1989), which are DNA sequences that remain associated with a fibrous protein network within the nucleus named nuclear matrix. The nuclear matrix has been proposed to provide attachment sites for chromatin loops. The presence of MARs/SARs in insulators suggests that insulators may organize the genome into independent chromatin loop domains by attaching to the nuclear matrix. The attachment of chromatin loops to the matrix could block the communication between the enhancer and the promoter in separate loops. These open and flexible chromatin structures found in insulators may enhance their ability to interaction with like elements or nuclear structures to form chromatin loops.

Mechanism of barrier function

The mechanism of barrier activity is best studied in yeast. The formation of repressive chromatin domain in yeast depends on a linear propagation of silencing complexes. For instance, the spread of the Sir2/3/4 complex from silencing centers generates large domains of hypoacetylated chromatin through a histone deacetylase (HDAC) activity (Grunstein, 1998; Moazed, 2001; Suka et al., 2001). How silencing complexes can spread along the chromatin is illustrated by the study on the *Drosophila* Heterochromatin Protein 1 (HP1). HP1 binds to histone H3 that is methylated at lysine

9 (H3K9me), a hallmark of heterochromatin. A histone methyltrasferase (HMT) is then recruited by the H3K9me-bound HP1 to methylate the next H3K9, starting another cycle of HP1 binding/H3K9 methylation (Rea et al., 2000). It has been proposed that barriers stop the propagation of silencing complexes by breaking such chain reactions, which could occur through multiple mechanisms.

First, chain breaking can be achieved by disrupting the substrate of the chain reaction, such as the ordered nucleosome arrays characteristic of heterochromatin, thus removing the basis of propagation. Consistent with this model, it has been reported that the yeast nucleosome-remodeling complex, Swi/Snf, which mobilize nucleosomes, can function as barrier protein when tethered to DNA (Oki et al., 2004). The authors also showed that the yeast *HMR* $tRNA^{Thr}$ barrier is associated with a nucleosome-free region (Oki and Kamakaka, 2005). Another example of the substrate of the silencing complex is the core histones. A barrier in the *Drosophila white* locus was found to counteract heterochromatin formation by replacing histone H3 with an H3 variant, H3.3, which is a poor substrate for the HMTs of the silencing complex (Nakayama et al., 2007). Second, barriers may actively form a center of active chromatin that counteracts the spreading of silent chromatin. In support of this view, the function of yeast *HMR* $tRNA^{Thr}$ barrier has been shown to require histone acetyltransferases (HATs), which add active marks on chromatin. Moreover, tethering the HATs to DNA can produce robust barriers (Donze and Kamakaka, 2001). Additional evidence comes from the chicken *β-globin* locus. The 5' HS4 insulator of the chicken *β-globin* locus coincides with a constitutive site of histone hyperacetylation, which is critical for protection against long-term silencing in

mammalian cells (Mutskov, Farrell et al. 2002). The histone hyperacetylation is maintained by histone-modifying enzymes that are recruited by the barrier protein USF1. Knockdown of USF1 activity compromises recruitment of histone modifications and causes encroachment of H3K9 methylation (West, Huang et al. 2004).

Chromatin boundaries in *Drosohpila* Hox gene complexes

Hox genes specify segment identity along the animal body axis. The precise spatial and temporal regulation of Hox genes is a prerequisite of the realization of a proper body plan. Hox genes have extensive cis-regulatory regions containing tissue-specific enhancers and silencers that can function over long distances. For example, the downstream region of the *Abd-B* gene of the BX-C contains a series of *infrabdominal* (*iab*) enhancers, each responsible for activating *Abd-B* in one parasegment (Fig. 1.2A). For instance, the *iab-6* and *iab-7* enhancers activate *Abd-B* expression in parasegment 11 and 12 (PS11 and PS12) respectively. Genetic evidence suggested that these enhancers are in independent domains. It has been shown that the deletion of a DNA element, Fab-7, between *iab-6* and *iab-7* leads to an ectopic activation of *iab-7* in PS11 (which is controlled by *iab-6* normally), suggesting that Fab-7 normally acts as a boundary to separate the two *iab* domains (Gyurkovics et al., 1990). Two other boundaries, Mcp and Fab-8, were found to separate the *iab-4* / *iab-5* and *iab-7* / *iab-8* domains, respectively (Barges et al., 2000). The discovery of multiple boundaries in the regulatory region of *Abd-B* poses the question: How do the *iab* enhancers overcome the boundaries and activate the promoter? A possible solution

could be provided by a novel class of regulatory elements, promoter targeting sequences (PTS) (Chen et al., 2005; Zhou and Levine, 1999). In a transgenic context the PTS has been shown to help distal enhancers to overcome the enhancer-blocking function of Fab-8. However, the *in vivo* significance of the PTS element has been called into question as mutations that remove PTS elements produce very mild or no phenotype (Mihaly et al., 2006).

It is unclear whether or not the genes in ANT-C are organized into independent domains by chromatin boundaries. The discovery of the SF-1 chromatin boundary in ANT-C suggests that boundaries may also be important for gene regulation in ANT-C (Belozerov et al., 2003a). SF-1 is located between the homeotic *Sex comb reduced (Scr)* gene and the non-homeotic *fushi tarazu (ftz)* gene, which have distinct expression patterns (Fig. 1.2B). The *ftz* gene has a series of upstream and downstream enhancers that drive a seven-stripe expression pattern from early to late embryogenesis (Dearolf et al., 1989, 1990). The expression of the *Scr* gene is controlled by a complex system of cis-regulatory elements. Its expression in early embryos is established by multiple tissue-specific enhancers, including a distal enhancer that is ~30 kb away, in the *ftz* downstream region. *Scr* expression is subsequently maintained by two distant Polycomb/Trithorax-response elements (PREs/TREs) located ~15 kb downstream and ~ 40 kb upstream of the transcription start site (Gindhart and Kaufman, 1995; Gorman and Kaufman, 1995). The fact that regulatory elements of the two genes are interspersed in common intergenic regions implies that there must be mechanisms to ensure specificity of cis-regulatory interactions. Some enhancers have been shown to be selective in

terms of interaction with promoters, which can be a mechanism to ensure specific enhancer-promoter interaction. However, most enhancers are believed to be promiscuous, including some *ftz* enhancers, which have been shown to be able to activate the *Scr* promoter (Gorman and Kaufman, 1995). The presence of an insulator could provide another mechanism of the independent regulation of the *Scr* and *ftz* genes. The discovery of SF-1 in this region is consistent with this view. The proposed SF-1 functions include restricting the enhancers of the two neighboring genes to appropriate targets and protecting *ftz* from the Polycomb-mediated formation of silent chromatin that spreads from nearby homeotic genes (Belozerov et al., 2003a).

The mechanism of SF-1 function is still unknown due in large part to our limited knowledge of the SF-1 boundary proteins. Chapter Three will be devoted to the identification of novel proteins involved in boundary function of SF-1 as well as other insulators.

Increasing evidence suggests that boundaries function by interacting with like elements and forming chromatin loops (Blanton et al., 2003; Cai and Shen, 2001; Gerasimova et al., 2000; Muravyova et al., 2001; Tolhuis et al., 2002). Accordingly, the enhancer-blocking activity of SF1 requires the GAGA factor, a protein capable of mediating insulator pairing through the BTB/POZ protein-dimerization domain (Melnikova et al., 2004). Based on the looping model, we hypothesize that SF-1 may function by interacting with additional boundaries downstream of *ftz* to form an independent *ftz* chromatin loop domain. Additionally, the formation of such chromatin loop may facilitate the function of the *Scr* distal enhancers located downstream of *ftz*. In

Chapter Four, I will present the search and identification the hypothesized boundaries using the Chromosome Conformation Capture technique.

Figure 1.1 Artistic representation of the organization of the eukaryotic genome

DNA (black lines), nucleosomes (orange circles), genes (black, yellow and blue arrows), enhancers (color boxes), insulators (red ovals) and nuclear envelope (yellow half circle) are depicted. Heterochromatin is drawn as densely packed nucleosomes (orange circles). Open chromatin is drawn as sparsely distributed nucleosomes on DNA. Dotted lines mark the autonomous domains of gene regulation. Green curved and straight arrows represent activation. Red dashed curve represents that the enhancer is blocked by the insulator.

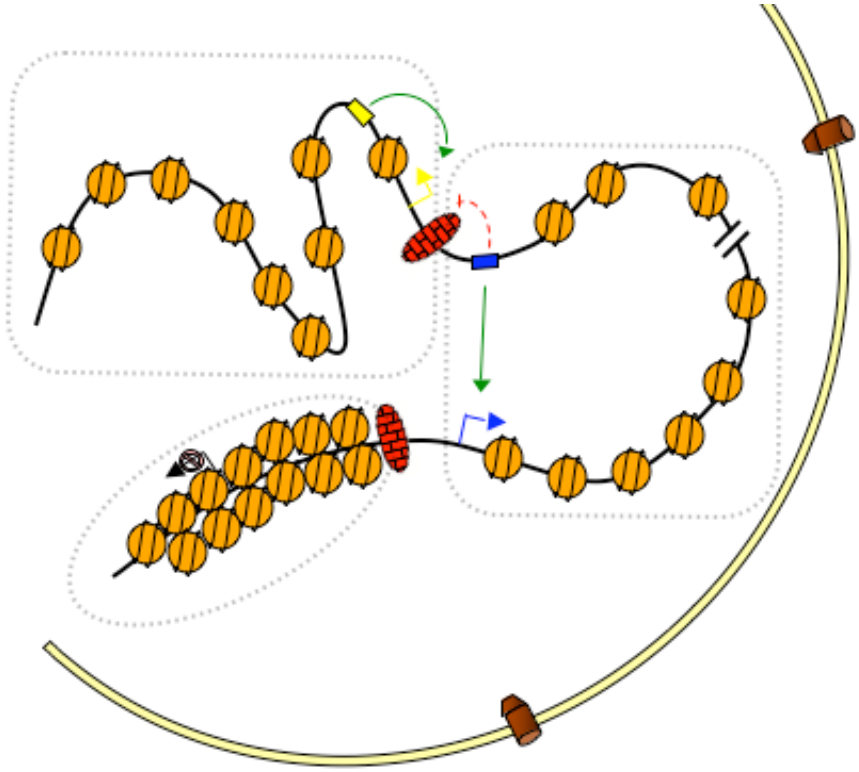

Figure 1.2 Hox gene complexes in *Drosophila*

(A) The Hox genes of the *Bithorax* complex and their regulatory regions are depicted. The three Hox genes of BX-C, *Ubx, abd-A* and *Abd-B* are indicated below the scale bar. Colored boxes represent individual cis-regulatory domains. The orange and red regions control *Ubx* expression. The regions in different shades of blue control *abd-A* expression. Regions in different shades of green control *Abd-B* expression. The names of these regulatory domains are indicated above the multicolor bar. The body segments that are controlled by these cis-regulatory domains are indicated with the same color on the diagram of the adult fly. The location of known chromatin boundaries (red ovals) and Polycomb response elements (checkerboard patterned boxes) of *Abd-B* are indicated on the scale bar. Modified from Maeda and Karch 2006. **(B)** The Hox complexes of *Drosophila* are depicted on top of the graph. The *Scr-Antp* intergenic region in the *Antennapedia* complex in shown in greater details at the bottom. The three genes in this genetic interval, *Scr, ftz* and *Antp* are indicated as colored boxes. Enhancers are depicted as circles using the same color as the genes they regulate. Insulators are depicted as red ovals with a brick wall pattern. Densely packed nucleosomes (orange circles) indicate silent chromatin formation mediated by Polycomb group proteins. The expression of *Scr, ftz* and *Antp* in germ-band extended-stage embryos is shown below the map.

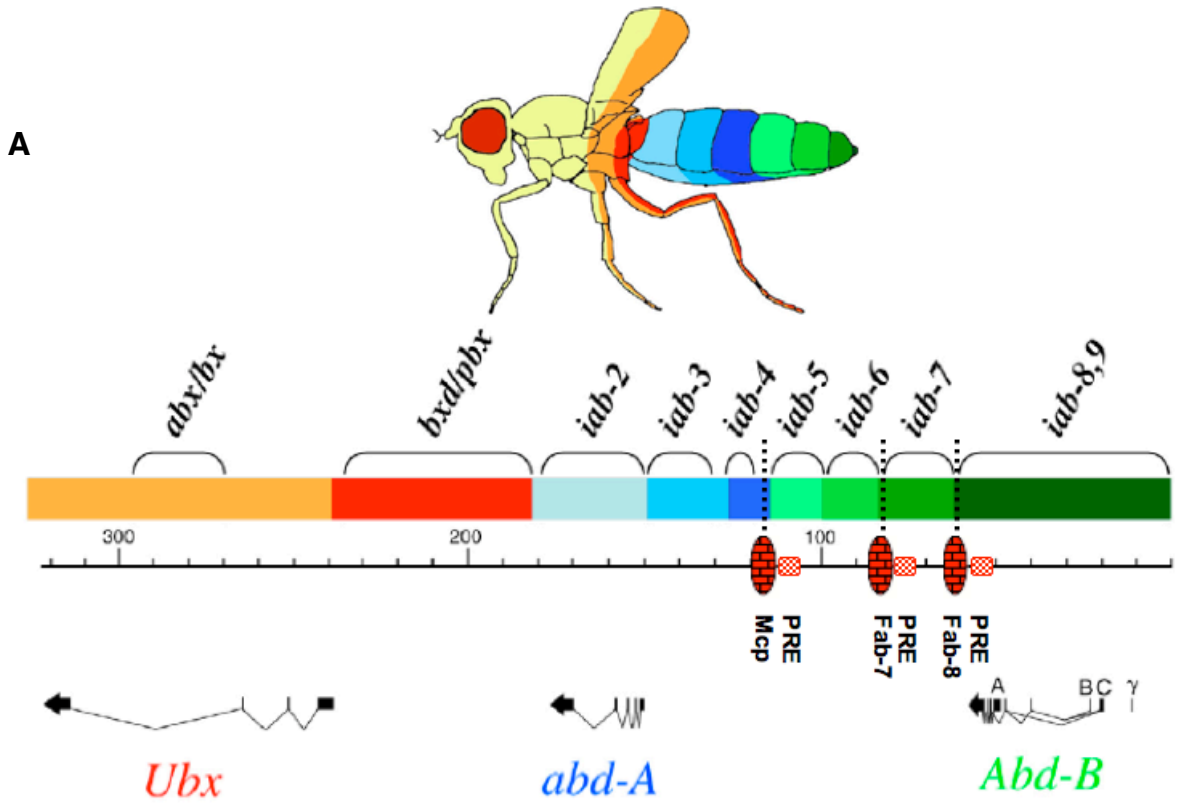

Modified from Maeda and Karch 2006

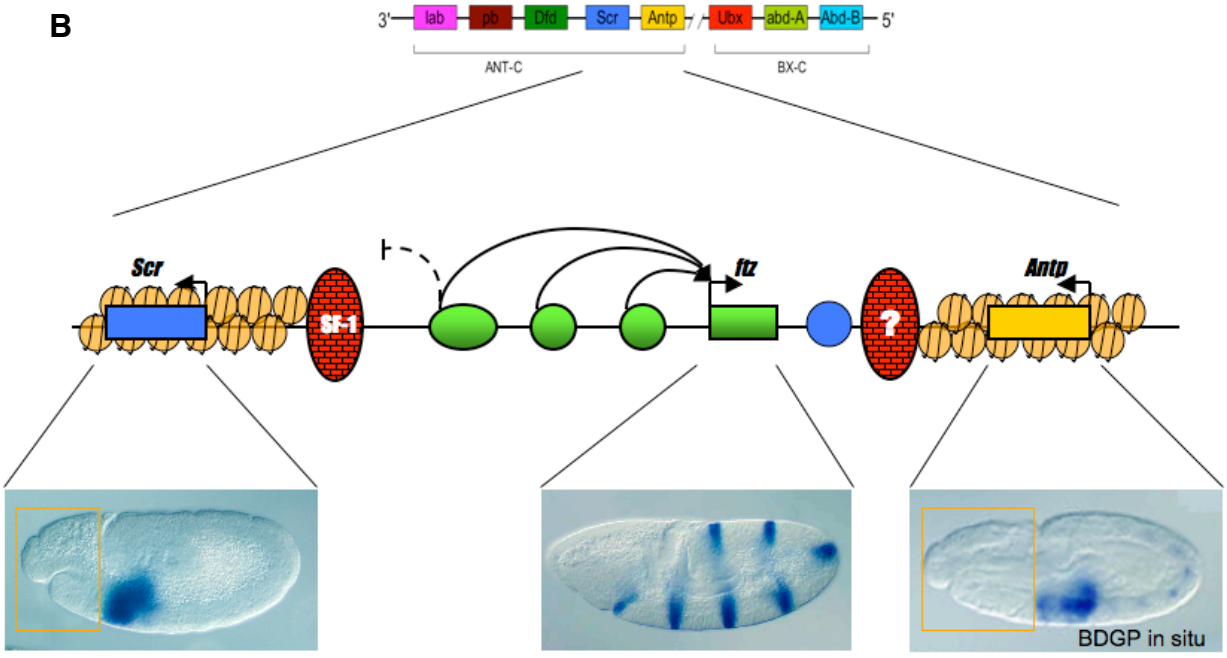

CHAPTER 2

NUCLEAR LOCATION OF A CHROMATIN INSULATOR IN DROSOPHILA[1]

---

[1]Qinghao Xu, Mo Li and Haini N. Cai. 2004. *Journal of Cell Science*. 117, 1025-1032

Summary

Chromatin-related functions are associated with spatial organization in the nucleus. We have investigated the relationship between the enhancer-blocking activity and sub-nuclear localization of the Drosophila suHw insulator. Using fluorescent in situ hybridization (FISH), we observed that genomic loci containing the gypsy retrotransposon were distributed closer to the nuclear periphery than regions without the gypsy retrotransposon. However, transgenes containing a functional 340-bp suHw insulator did not exhibit such biased distribution towards the nuclear periphery, suggesting that the suHw insulator sequence is not responsible for the peripheral localization of the gypsy retrotransposon. Antibody stains showed that the two proteins essential for the suHw insulator activity, SUHW and MOD(MDG4), are not restricted to the nuclear periphery. The enhancer-blocking activity of suHw remained intact under the heat shock conditions which was shown to disrupt the association of gypsy, SUHW and MOD(MDG4) with the nuclear periphery. Our results indicate that the suHw insulator can function in the nuclear interior, possibly through local interactions with chromatin components or other nuclear structures.

INTRODUCTION

Chromatin-related activities are organized at different anatomic levels in the nucleus (Belmont, 2001; Chubb and Bickmore, 2003; Chubb et al., 2002; Cremer and Cremer, 2001; Cremer et al., 2000; Dillon and Festenstein, 2002; Gasser, 2002; Heun et al., 2001; Marshall et al., 2001; Parada and Misteli, 2002; Spector and Gasser, 2003; Vazquez et al., 2001). For example, constitutively silent centromeric and telomeric heterochromatin as well as gene-poor chromosomes are frequently found near the nuclear periphery. In contrast, regulated transcription may be organized at a more local scale. In human interphase nuclei, inactive genes are often found in the interior of chromosomal territories whereas active genes are often positioned near the periphery or in the inter-chromatin space (Chubb et al., 2002; Cremer and Cremer, 2001; Croft et al., 1999; Feuerbach et al., 2002; Galy et al., 2000; Mahy et al., 2002a; Mahy et al., 2002b).

Chromatin boundaries, or insulators, delimit chromatin domains of distinct structures and transcriptional activities (Gerasimova and Corces, 2001; Geyer and Clark, 2002; Labrador and Corces, 2002). They play important roles in regulating gene activity in complex genetic loci in diverse organisms from yeast to humans (Bi and Broach, 2001; Ishii and Laemmli, 2003; Mihaly et al., 1998; Noma et al., 2001; West et al., 2002). Insulators are characterized by two distinct assays for their ability to block enhancer-promoter interactions, and to protect transgenes from influences of neighboring chromatins. Despite extensive studies, molecular mechanisms underlying insulator activity remain controversial (Cai and Shen, 2001; Dorsett, 1999; Gerasimova et al., 2000; Geyer, 1997b).

The Drosophila gypsy retrotransposon insertion disrupts communications between distal enhancers and a downstream gene promoter (Geyer and Corces, 1987). A 340-bp DNA near the 5' LTR of the retrotransposon, which binds to SUHW and interact with MOD(MDG4) indirectly, is necessary and sufficient for the insulator activity (Gerasimova et al., 1995; Spana et al., 1988). We have previously shown that the cis-arrangement of suHw insulator critically affects its activity: a single intervening suHw blocks enhancer-promoter interactions, whereas two tandem suHw elements abolish their insulator activity (Cai and Levine, 1997; Muravyova et al., 2001). These observations suggest that suHw may interact with another insulator and/or unidentified nuclear anchor sites, thereby separating enhancers and promoters into different chromatin loops. The interaction between the tandemly-paired suHw insulators neutralize their ability to mediate formation of such chromatin loops, leading to the loss of insulator activity.

Consistent with the observation, it was recently reported that the gypsy retrotransposon is associated with the nuclear periphery (Gerasimova et al., 2000; Gerasimova and Corces, 1998). Furthermore, SUHW and MOD proteins also localize near the nuclear periphery in large foci. Genetic mutations in *suHw* and *mod(mdg4*) that abolish the insulator function also disrupt these protien foci and the association of gypsy with the nuclear periphery. Based on these observations it was proposed that the enhancer-blocking activity of the suHw DNA depends on its interaction with an insulator complex near the nuclear periphery (Gerasimova et al., 2000).

To test whether association to the nuclear periphery is required for the suHw insulator function, we examined the nuclear localization of suHw in multiple transgenic lines containing either a single or tandemly paired suHw insulators. Using FISH analysis, we show that genomic loci containing the full-length gypsy retrotransposon were present at a higher proportion near the nuclear periphery than loci without the gypsy retrotransposon. However, transgenes containing the functional 340-bp suHw insulator did not exhibit such biased distribution towards the nuclear periphery. Antibody stain showed that the SUHW protein foci are present both at the periphery and the nuclear interior, similar to the distribution of the transgenes containing the suHw DNA. A subset of interior FISH foci also colocalized with the SUHW protein foci. The enhancer-blocking activity of suHw remained intact under the heat shock conditions previously shown to disrupt the association of gypsy with the nuclear periphery. Our results suggest that the insulator activity of suHw is independent of its proximity to the nuclear periphery.

RESULTS AND DISCUSSION

We decided to investigate the correlation between the nuclear location and insulator function of the suHw element. For this purpose, we probed the nuclear localization of reporter genes linked to the suHw DNA in diploid larval cells from a collection of fly lines each harboring an independently inserted suHw- transgene. This collection offers several advantages. First, the transgenes contain the suHw DNA, either as a functional single element or as a tandem pair, allowing us to directly assess the correlation between enhancer-blocking activity and nuclear localization of the

insulator. Second, each of the transgenes is located in a distinct chromosomal position, providing an important control for the possible interference from different chromosomal environments. Finally, the 340-bp suHw insulator was used instead of the full-length gypsy retrotransposon, thus minimizing potential influences from the non-insulator sequence of the gypsy element.

Sub-nuclear localization of transgenes

It has been reported that chromosomes assume stereotypical spatial organization in interphase nuclei in human cells (Chubb et al., 2002; Mahy et al., 2002b; Tanabe et al., 2002; Walter et al., 2003). Genes have also been found to localize non-randomly along the apical-basal axis that corresponds to their relative chromosomal positions in Drosophila embryonic nuclei (Wilkie and Davis, 2001; Wilkie et al., 1999). In order to evaluate how the presence of the suHw insulator might impact the nuclear compartmentalization of its neighboring DNA, we first examined the nuclear distribution of transgenes that harbor no suHw insulator. Since all of the transgenes used here contain a *lacZ* reporter gene, driven by either embryonic or larval enhancers, we used a lacZ-specific DNA probe for FISH analysis.

Larval imaginal disc cells from different fly lines containing non-suHw (NS) transgenes were fixed with 2% paraformaldehyde, hybridized to a Cy-3 labeled lacZ probe (red) and counter stained with a polyclonal antibody against nuclear lamin (Green). Using confocal microscopy we detected fluorescent foci at various positions along the radial axes of these nuclei (NS-Cy3, Fig. 2.1A). The control experiment with

nuclei from non-transgenic imaginal disc showed no such fluorescence foci (yw-Cy3, Fig. 2.1B).

We collected confocal images of imaginal disc tissues from four NS transgenic line (61-90 each). The shortest distance between the FISH foci and the ring of the lamin stain was measured and expressed as a function of the radius (% Radius). The histogram of foci distribution indicates that these NS transgenes are present throughout the nuclear volume (Fig. 2.1D).

To assess the distribution of NS transgenes in a three-dimensional space, a mathematical model was used to simulate spherical space with randomly distributed foci (Figs. 2.1F, G; also see Methods). The model contains correction for the under representation of peripheral foci when viewed from a fixed angle (an example is shown in Panel A and C, arrowheads). The distribution pattern of a total of 325 Cy3-labeled foci from four independent lines of transgenes was plotted against the random distribution model (Figs. 2.1F, G). The median distance between the NS transgene foci and the nuclear lamin is 31% of radius (Fig. 2.1F, blue bar), significantly different from that for the random model of 25% of the radius (Fig. 2.1F, grey bar, $P<10^{-8}$). Comparison of the NS-Cy3 foci histograms with the random distribution model (Fig. 2.1G, blue and gray profiles) shows that this difference is mainly the result of a reduced presence of transgenes in the most peripheral 0-15% of the radius (perinuclear zone, blue shaded area, Fig. 2.1G). Interestingly, transgene foci were found at a higher than expected frequency in the nuclear volume immediately interior to the perinuclear zone, in a region that spans the next 25% of the radius, which we termed sub-perinuclear zone (orange

shaded area, Fig. 2.1G). Such non-random distribution is also seen with the histograms of the individual NS transgenes (colored lines, Fig. 2.1D). In addition to projected distance measured from top view panels (2-D measurements), we further calculated the real foci-lamin distance using measurements from all three views (top and two side view panels, 3-D measurements). The 3-D measurements from 27 NS nuclei also showed a reduced presence of transgenes in the perinuclear region (see black line in Fig. 2.1D). To probe the reason for the under-representation of the transgenes, we performed counter-stain of these nuclei with DAPI and quantitated fluorescent intensity across the nucleus with high-resolution confocal microcopy. Our results indicated that DNA concentration is uneven throughout the nuclear interior, and appears to be reduced near the periphery (data not shown). Therefore, the low perinuclear concentration of transgenes may reflect the property of the bulk DNA. Taken together, our results indicate that the NS transgenes are not preferentially associated with the nuclear periphery.

The effect of full-length gypsy insertion on the sub-nuclear localization of neighboring DNA

It was previously reported that the gypsy retrotransposon preferentially localizes near the nuclear periphery (Gerasimova et al., 2000). Furthermore, this peripheral association was abolished by mutations in the SUHW and MOD(MDG4) genes that abolished the insulator function (Gerasimova et al., 2000). We probed the distribution of the gypsy retrotransposon in three independent insertion lines using FISH with Cy3-

labeled probes against the *yellow* and *cut* sequences near the insertion sites. We found a higher proportion of gypsy foci near the nuclear periphery compared to NS transgenes (Fig. 2.1C). The median distance between the gypsy foci and the lamin stain from 254 measurements was 26% of the radius, significantly smaller than the 33% radius for the NS transgenes (Fig. 2.1F, $P<10^{-7}$). Although the gypsy foci are still underrepresented in the perinuclear zone when compared with the random model (Figs. 2.1F, G), they are more narrowly concentrated in the sub-perinuclear region at the expense of the nuclear interior: 75% of the foci were within 33% of the radius from the lamin stain, compared to 45% of the radius for the random model and average of 41% of the radius for the NS transgenes (see Figs. 2.1F, G). Every gypsy line showed a single narrow peak of foci distribution that centered around 26% radius, whereas majority of NS lines exhibited broader foci distribution centered around 35-40% radius (Figs. 2.1D, E). We also measured the 3-D distance between lamin and gypsy foci in a small number of nuclei. The result confirmed the closer association between gypsy and the nuclear periphery (black line, Fig. 2.1E).

The above results showed that the gypsy and surrounding DNA assume a more peripheral distribution than the NS transgenes. However, the median distance between the gypsy DNA and lamin stain in this study appears to be greater than that reported previously (Gerasimova et al., 2000). One possible explanation for this apparent discrepancy might be the different genomic DNA used as probes. We used probes against a 6-8 kb region, whereas a much larger region was used in the previous study. A larger probe could increase the size of the fluorescent foci, which may change the

apparent nuclear localization. To verify this, we tested the same gypsy lines used in the previous study (courtesy of T. Gerasimova and V. Corces), using the shorter probes. We did not observe closer periphery association in these gypsy lines (data not shown).

Transgenes containing the suHw insulator do not associate with the nuclear periphery

We next examined the sub-nuclear localization of transgenes containing the 340 bp suHw insulator. We first tested transgenes containing a single functional suHw (SS) using Cy3-labeled lacZ probe. The transgene foci do not appear to preferentially associate with the nuclear periphery (Fig. 2.2A). The median distance between the lamin and SS transgene foci from 333 measurements is 34% of radius (Fig. 2.2E, red bar), comparable to that of the NS transgenes (32.5% radius, Fig. 2.1F), and significantly different from that of the gypsy transposon (26% radius, $P<10^{-9}$, Fig. 2.1F). Combined foci histogram of the SS transgenes is also more similar to that of NS transgenes than to gypsy lines (Fig. 2.2F, compared to Fig. 2.1G). As seen before, the 2-D foci histograms from individual lines (Fig. 2.2C) are in good agreement with the 3-D and combined 2-D histogram for the group (black line, Figs. 2.2C, F).

To further test if changes in the suHw insulator function is accompanied by changes in its nuclear localization, we probed the nuclear localization of transgenes containing tandemly paired suHw (DS), which neutralized its enhancer-blocking activity. The DS transgene foci labeled with the Cy3-lacZ probe are found within the same range along the nuclear radius as the single insulator transgenes (Figs. 2.2B, D). Median

distance between transgene and nuclear lamin from 307 measurements is 35% radius, similar to the SS transgenes (35.5% radius, Fig. 2.2E), and different from that of gypsy (26% radius, $P<10^{-9}$, Fig. 2.1F, Fig. 2.2E). Again, the foci distribution histograms of individual DS transgenes, the combined histogram of the DS group, and the 3-D foci distribution histogram of the group were in good agreement, and showed little difference from those of the NS and the SS groups (see Figs. 2.2D, F). These results indicate that unlike the full-length gypsy retrotransposon, the suHw insulator does not appear to be closely associated with the nuclear periphery.

We were surprised by this difference between the suHw insulator and the full-length gypsy retrotransposon. To exclude the possibility that clustering of a transgene group in unusual chromosomal locations influenced their nuclear localization, we mapped the chromosomal sites of selected lines from all groups by in situ hybridization. Our results showed that the insertion sites for all groups appear to be random in the euchromatic regions, and no clustering was seen (Fig. 2.2G).

Our results showed that, unlike the full-length gypsy retrotransposon, the functional suHw insulator does not tether DNA to the nuclear periphery. These results suggest that the suHw insulator is functional in the nuclear interior. Gypsy sequences unrelated to the suHw insulator may be responsible for the periphery localization of the transposon. Consistent with our findings, it was recently reported that the boundary activity of suHw does not require its association with the nuclear periphery (Calvi and Spradling, 2001).

Enhancer-blocking activity of the suHw insulator is permitted at the nuclear interior.

Previous studies showed that the gypsy retrotransposon and two insulator proteins, SUHW and MOD(MDG4) co-localized to the nuclear periphery in larval imaginal disc cells (Gerasimova et al., 2000). Mutations in *suHw* and *mod(mdg4)* that disrupt insulator function abolished the gypsy association with the nuclear periphery (Gerasimova et al., 2000; Gerasimova and Corces, 1998). Based on these observations, it has been suggested that the insulator activity of the gypsy element is mediated by the interaction between these two proteins with anchor sites at or near the nuclear envelope (Gerasimova et al., 2000). Our observation that suHw insulators are localized both in the sub-perinuclear and more interior region of cell nuclei (Fig. 2.2) raised the possibility that insulator proteins may be localized in the nuclear interior as well.

To test this, we analyzed the nuclear localization of the SUHW protein by immunofluorescence staining using an anti-SUHW antibody (courtesy of T. Gerasimova and V. Corces, (Gerasimova et al., 2000; Gerasimova and Corces, 1998). Confocal images showed a punctated pattern of SUHW distribution, with large foci both at the periphery and interior of the nuclei (Figs. 2.3A-D). In addition, smaller foci and more diffused stain were observed throughout the nuclei. The 2-D distance between 68 SUHW protein foci and the nuclear periphery showed that the SUHW foci distribution resembles those of the transgene DNAs, with a substantial portion within the sub-perinuclear zone and further interior (Fig. 2.3E). This result indicates that the SUHW

protein, which is essential for suHw insulator function, could co-localize with the suHw DNA at both periphery and interior. We also conducted triple stains of suHw DNA, SUHW protein and lamin. The triple stain efficiency was lower due to the different optimal fixation condition for SUHW and that for FISH with the short probe. However, these stains showed that at least 50% ($n > 25$) of the suHw DNA foci at the internal sites are co-localized with the SUHW protein (Fig. 2.3F-H). In summary, our results support the suHw insulator functional in the nuclear interior.

It has been reported that heat shock of larvae at 37 ºC for 20 minutes is sufficient to disrupt gypsy association with the nuclear periphery (Gerasimova et al., 2000). We reasoned that if the anchoring of suHw insulator to the nuclear periphery is necessary for its enhancer-blocking activity, heat-induced disassociation of the SUHW, and the insulator DNA, might disrupt its insulator activity. To test this, we examined the enhancer-blocking activity of the suHw insulator in heat-shocked transgenic embryos. In 3T2 transgenic embryos, which contain the *evenskipped* stripe 2 (E2) and stripe 3 (E3) enhancers separated by a neutral spacer (T), both stripe enhancers activated the downstream *eve-lacZ* reporter gene, shown by the lacZ expression (Fig. 2.3I). In 3S2 embryos, the suHw insulator DNA in place of the neutral spacer blocked the distal E3 enhancer from the eve-lacZ promoter, resulting in the loss of the E3 stripe (Fig. 2.3J). The function of the proximal E2 enhancer was unaffected as seen in the single E2 stripe (Fig. 2.3J). The nuclear location of the transgenes containing the neutral spacer (3T2, C196) and suHw (3S2, C36) are similar to other transgenes in the same group (blue line, Fig. 2.1D; red line, Fig. 2.2C). We next tested the enhancer-blocking function of

suHw in 3S2 embryos that had been heat shocked for 30 minutes at 37 ºC. The suHw-mediated block of the distal E3 enhancer remained intact (Fig. 2.3K). This result indicates that the peripheral association of the SUHW protein is not essential for enhancer-blocking activity of the suHw insulator.

In conclusion, we showed that unlike the full length Gypsy retrotransposon, the functional suHw insulator DNA is not preferentially associated with the nuclear periphery. Rather, it is positioned throughout the nuclear volume. We showed that SUHW protein is also present both at the nuclear periphery and in the nuclear interior, in a similar distribution as the suHw DNA. We showed that the 340 bp suHw insulator DNA and the SUHW protein are co-localized in some of the interior sites. We further showed that heat shock condition which resulted in the disassociation of the SUHW and MOD(MDG4) from the nuclear periphery does not disrupt the enhancer-blocking function of the suHw insulator in transgenic embryos. These results provided structural and functional evidence that the suHw insulator activity does not require its association with the nuclear periphery, and that components in the nuclear interior can support the insulator function of suHw, such as providing anchor sites for insulator interactions. Identification of these components should provide insights into the mechanisms of insulator activity. A recent study linking the chromatin barrier activity in the yeast HML silent loci with nuclear pore components at the nuclear periphery (Ishii et al., 2002) suggests that diverse mechanisms may underlie the function of different insulators or boundaries from different organisms.

MATERIALS AND METHODS

Fly strains

All flies were maintained in standard culture media at 23ºC. The strains of $y^1 w^{67c23}$ and w^{1118} were used as non-transgenic controls. All transgenic fly strains used in the study have been described previously ((Belozerov et al., 2003b; Cai and Levine, 1995; Cai and Levine, 1997; Cai and Shen, 2001; Cai et al., 2001). Briefly, the majority of the transgenes are pCaSPeR derivatives that contain the suHw insulators in various arrangements as well as embryonic or larval enhancers. Embryonic enhancers are inserted upstream of the *eve* basal promoter (–42 to +200) fused in frame with lacZ coding region (Cai and Levine, 1997; Small et al., 1992). Larval enhancers such as the *glass* GMR enhancer and the bristle specific enhancers of the *yellow* gene were cloned, along with suHw, into the first intron in transgenic mini-yellow gene (Belozerov et al., 2003b). The following gypsy strains were provided by the Bloomington stock center: #189 y^2, w^a and #1355 y^2; *In(3LR)208/TM3,* Sb^1; #171 y^1 ct^K; bw^1 and #1502 z^{a694} ct^6. The following gypsy strains were generously provided by T. Gerasimova and V. Corces: y^2 w^{a4} ct^6 sn^w /Y *x* X^X/Y (TG1) and y^2 w^{a4} ct^6 sn^w /Y *x* X^X v y^f /Y (TG2).

In situ hybridizations

Probe preparation: LacZ and cut genome DNA that were used to prepared FISH probe were cloned by PCR into the pTOPO vector (Invitrogen, CA) with the following primers:

LacZ/N: GGGCGTTACCCAACTTAATCG

LacZ/C1: GACACCAGACCAACTGGT

LacZ/C2: GCGTGAGCGGTCGTAATC

Ct3'6462: GTTGCTGCTACTACTGCTGCTGG

Ct5'154: ACACTCAAAGAGCAGCTATCCAC

Ct+6k-5': GCAAGCACATGTCGAATCAGCCAAC

Ct+6k-3' GCCTGGCATTATTCTGTTCTGTTGTC

FISH analysis was performed following a published protocol (Dernburg, 2000). The fluorescence probes were prepared as follows. Plasmid or fragment of template DNA was digested to average 100-150 bp with six 4-base cutter restriction enzymes. TdT (terminal transferase) labeling of probe with Cy3-dUTP was according to manufacture's instruction (TdT labeling Kit, Roche). Probe was resuspended in 0.8 x prehybridization buffer (1x prehybridization buffer: 10% dextran sulfate, 50% formamide, 3x SSC) Imaginal discs from third instar larvae were dissected in 1X Buffer B (10mM KPO4, pH 6.8, 15mM NaCl 45mM KCl, 2mM $MgCl_2$). Several discs were then transferred into 2% formaldehyde/1XPBS and fixed for 25min. The discs were then treated with 45% acetic acid for 6 min on Denhardt-gelatin treated slides, covered with siliconized cover slip without pressure. Slides are frozen in liquid N_2 or at -80º C until solid. Cover slip of the frozen slide was quickly flipped off and the slide was dunked in 100% methanol and dehydrated for 2 hours at room temperature to overnight at –20ºC. Slides were then washed in 2X SSCT (0.2% Tween 80), followed by a series of washes that change to 50% Formamide/4x SSCT. Prehybridization was in 50% formamide

/4xSSCT for one hour at 37 °C. After the probe is applied to the disc tissues and covered with a cover slip, the slide was denatured on the back of heat block preset at 94ºC for 2 minutes under a humidifier chamber and hybridized at 37ºC overnight in a humidifier chamber. Post hybridization washes were for a total o for 1 hour at 37 °C. Slides were blocked with 10% BSA/1x PBS for 30 minutes and incubated with primary antibody in PNBTx (anti-lamin B-Dm, Rabbit 836, Paul Fisher) at room temperature for 3 hr, washed and incubated with secondary antibody (e.g., Alexa488 anti-rabbit) for 3 hr or overnight at 4°C. The optional fixation condition for the SUHW protein requires more extended fixation (25-40 minutes, for detail see Gerasimova et. al. 2001). Samples were counter stained with DAPI and mounted in Citifluor, an antifading mounting medium.

Polytene chromosomal in situ hybridization were done as described previously (Cai et al., 1994) with the following modifications: after the probe was added, squashed chromosomes were heat-denatured by heating the slides on the heat block at 94ºC for 2 minutes.

Whole mount embryo RNA in situ hybridization was performed with the digoxigenin-UTP labeled antisense RNA probes. Expression patterns were visualized by colorimetric reaction following incubation with anti-digoxigenin antibody conjugated to alkaline phosphotase (Genius Kit, Boehringer, (Cai et al., 2001; Tautz and Pfeifle, 1989).

Data analysis and statistical modeling

Confocal microscopy was done using a Leica TCS SP2 spectral multiphoton confocal microscope. Images were collected from 0.3 mm serial optical sections at a 2x zoom. The distance between hybridization foci and nuclear lamin stain were measured either with the Leica software package or manually on projected images, and expressed as a percentage of the nuclear radius (longest radius when ovoid shaped nuclei were used). The shortest distance between transgene foci and the lamin stain from three viewing angle of a single nucleus were selected and used for 3-D distance measurements. Data for transgene groups (e.g., NS, SS, DS or gypsy) were averaged using multiple fly lines. Statistical analyses of data from paired groups were done using t-test and a Chi square analysis (Kruskal-Wallis test). Significance level of 0.05 was used for all tests. The random sample model is:

$$(U) = -(3/2) \times U \times SQRT(1-U^2) + (3U/2 \times SIN(SQRT(1-U^2))),$$

where U describes the shortest distance between a random point inside a ideal spherical space and the exterior of the sphere within a plane that is perpendicular to a fixed axis of the sphere (light path).

ACKNOWLEDGMENT

We thank T. Gerasimova and V. Corces and for the gypsy strain, the anti-SUHW antibody and for sharing experimental protocols; Paul Fisher for the anti-lamin antibody, Linyun Ma for helpful discussions on statistics modeling; John Shield and Mark Farmer for technical assistant with confocal microscopy; Ping Shen and Edward Kipreos for critical reading of the manuscript. Most of the work presented in this chapter was published in *Journal of Cell Science* (Xu et al., 2004). I thank the editors of *Journal of Cell Science* for allowing me to use the manuscript in this thesis. This work was supported by a grant from the NIH.

Figure 2.1. The effect of the gypsy sequence on the nuclear localization of neighboring chromosomal DNA. A-C: Confocal images of Drosophila imaginal disc nuclei containing LacZ transgenes, no transgene, or gypsy retrotransposons, Disc tissue was visualized with FISH using Cy3-labeled probes (red) and an antibody against the nuclear lamin (green). The main view panel and the side view bars are separated by white lines. The positions of focal planes are indicated by thin yellow lines. Nuclei from a NS transgenic (**A**), or a non-transgenic (**B**) larva were hybridized with Cy3-labeled lacZ probe. FISH foci were visible within nuclei from transgenic larva. No stained foci above background were observed in majority of the nuclei from the non-transgenic larva. Single or sometimes two fluorescence foci per nucleus were detected at various focal planes in virtually all nuclei, depending on transgene copy number and states of homolog synapse. A small number of Cy3 foci appear outside of the lamin ring due to weak or incomplete lamin stain of the nearby nuclei. The arrowheads in Panel A and C indicate Cy3 foci appearing in the center of the nucleus in the top view but are more peripheral from the side view. **C.** Nuclei from a gypsy line were hybridized with a Cy3 probe from an 8 kb-genomic region in the *cut* locus near the retrotransposon (gypsy-Cy3). The gypsy foci (red) are present frequently near the nuclear periphery (green). **D.** Histograms of 2-D foci distribution for individual NS transgenes (colored lines) and 3-D foci distribution for pooled NS transgenes (black lines). Relative frequency of the sample are plotted against the FISH-lamin distance (% radius) of the sample. **E**. Histograms of 2-D foci distribution for individual gypsy lines (colored lines) and histogram of 3-D foci distribution for all gypsy lines (black lines). **F.** Summary of foci

distribution in a quartile diagram. Relative FISH-lamin distance for each sample group (represented by the colored bars) is compared with a model of randomly distributed samples (represented by the grey bar, see Methods for details). **G.** Foci histograms along the nuclear radius for selected sample groups (colored lines) and density of probability along the nuclear radius for the random distribution model (grey dashed line, see methods).

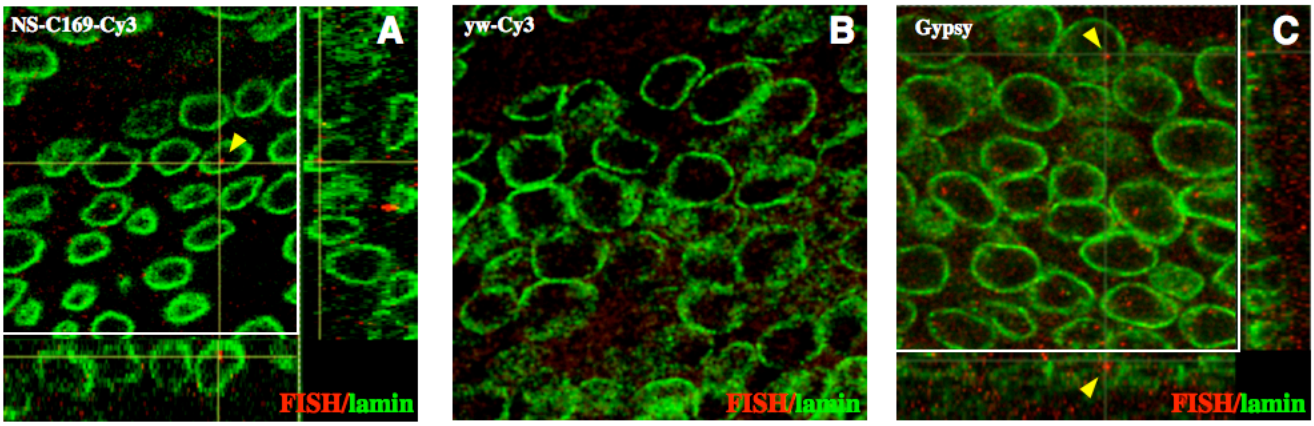
NS-C169-Cy3
A
FISH/lamin
yw-Cy3
B
FISH/lamin
Gypsy
C
FISH/lamin

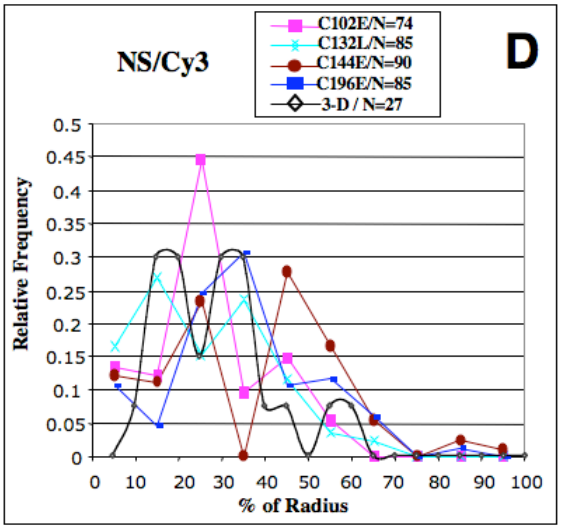
NS/Cy3
D
C102E/N=74
C132L/N=85
C144E/N=90
C196E/N=85
3-D / N=27
Relative Frequency
% of Radius

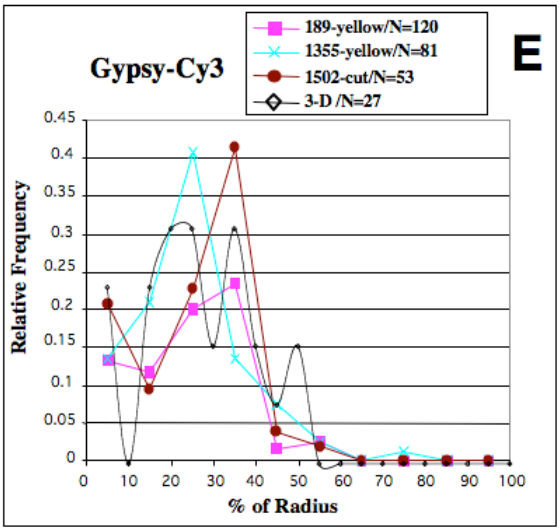
Gypsy-Cy3
E
189-yellow/N=120
1355-yellow/N=81
1502-cut/N=53
3-D /N=27
Relative Frequency
% of Radius

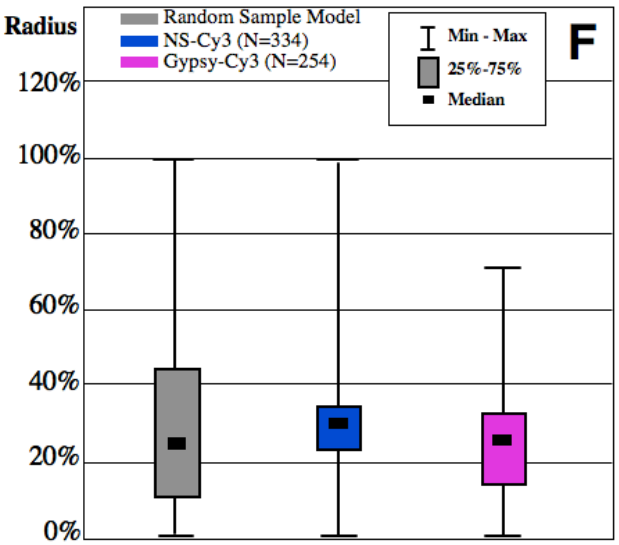
Radius
Random Sample Model
NS-Cy3 (N=334)
Gypsy-Cy3 (N=254)
Min - Max
25%-75%
Median
F

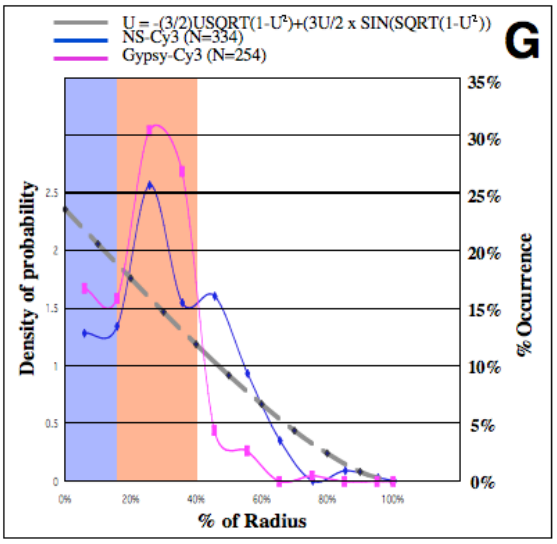
U = -(3/2)USQRT(1-U²)+(3U/2 x SIN(SQRT(1-U²))
NS-Cy3 (N=334)
Gypsy-Cy3 (N=254)
G
Density of probability
% Occurrence
% of Radius

Figure 2.2. The nuclear localization of transgenes containing the suHw insulator in functional or non-functional arrangements. **A.** A confocal image of imaginal disc nuclei from a single-suHw (SS) transgenic larva hybridized with Cy3-labeled lacZ DNA probes (red) and an anti-lamin antibody (green). **B.** A confocal image from a transgenic line with paired-suHw (DS). **C-D.** Histogram of foci distribution along the radius for the SS-Cy3 group (C) and the DS-Cy3 group (D) in independent transgene lines (colored lines). The 3-D foci histograms from pooled samples are represented by the black lines. **E.** Summary of foci distribution in a quartile diagram. Distance between FISH foci and lamin stain as a fraction of the nuclear radius for each sample group (represented by the colored bars) is compared with a model of randomly distributed samples (grey bar). **F.** Foci histograms along the nuclear radius for each sample groups (colored lines) and density of probability along the nuclear radius for the random distribution model (grey dashed line). **G.** Diagram of cytological locations of insertion sites of selected transgenes. Small vertical lines represent transgene insertions at various locations of the three major chromosomes (black, gypsy lines; blue, NS lines; red, SS lines and green, DS lines). The insertion sites for the individual lines are also listed in a table below.

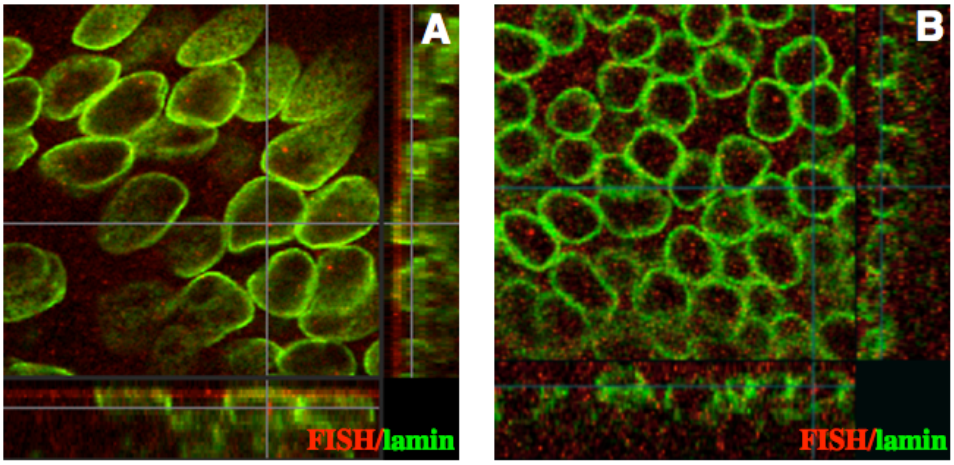

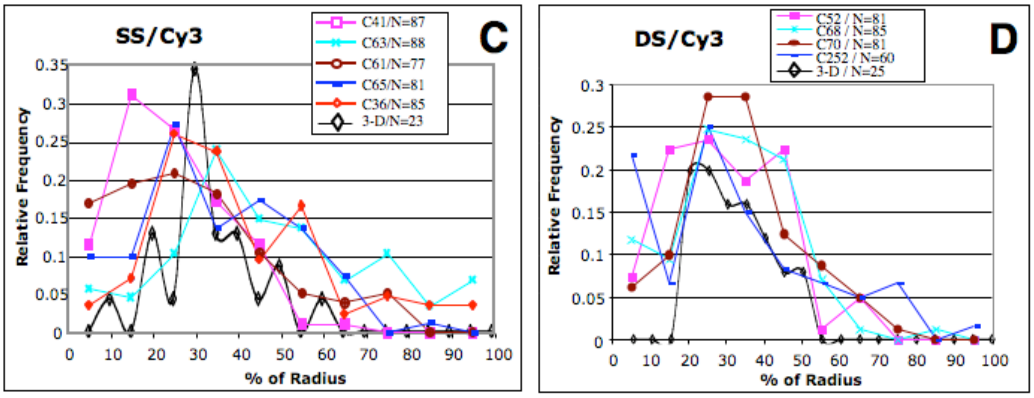

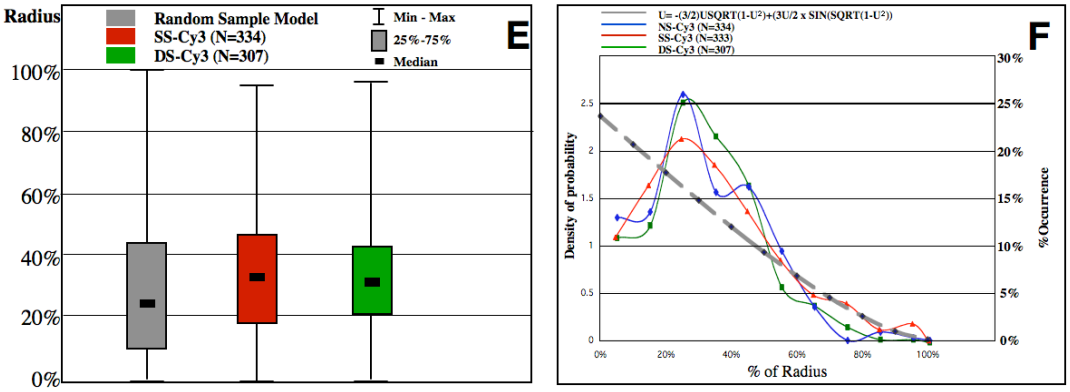

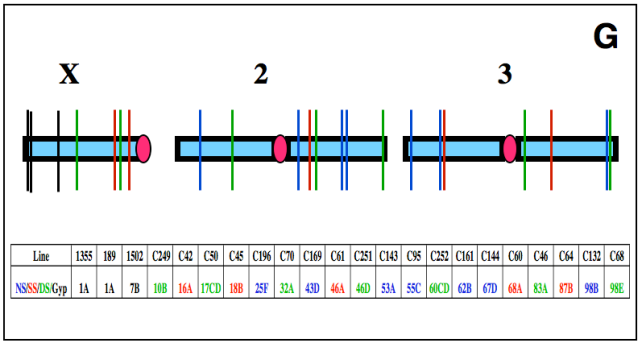

Line	1355	189	1502	C249	C42	C50	C45	C196	C70	C169	C61	C251	C143	C95	C252	C161	C144	C60	C46	C64	C132	C68
NS/SS/DS/Cyp	1A	1A	7B	10B	16A	17CD	18B	25F	32A	43D	46A	46D	53A	55C	60CD	62B	67D	68A	83A	87B	98B	98E

Figure 2.3. The nuclear interior is permissive for the insulator function of suHw. **A-D:** Serial confocal sections (0.3μ apart) of larval imaginal disc cells stained with anti-SUHW (red) and anti-lamin (blue) antibodies. The SUHW protein foci are detected at both nuclear periphery and interior region. **E.** SUHW protein foci histograms along the nuclear radius. **F-H:** A confocal section of a imaginal disc containing the 3S2 transgene, triple stained for the transgene (FISH, red), SUHW (green) and lamin (blue). **I-K.** Enhancer-blocking activity of the suHw insulator is not disrupted by heat shock. Whole mount RNA in situ hybridizations were performed with transgenic embryos containing 3T2 (**I**), and 3S2 transgenes (**J** and **K**). The transgene constructs are diagramed below the embryos with the colored bars representing the *evenskipped* stripe enhancers (E2 and E3) and the neutral spacer (T); and the black oval representing the 340 bp suHw element (S). Enhancers that directed the lacZ stripe expression are indicated above the embryos. The embryos were incubated at 25ºC (D, E) or 37ºC (F) for 30 minutes before fixation and staining.

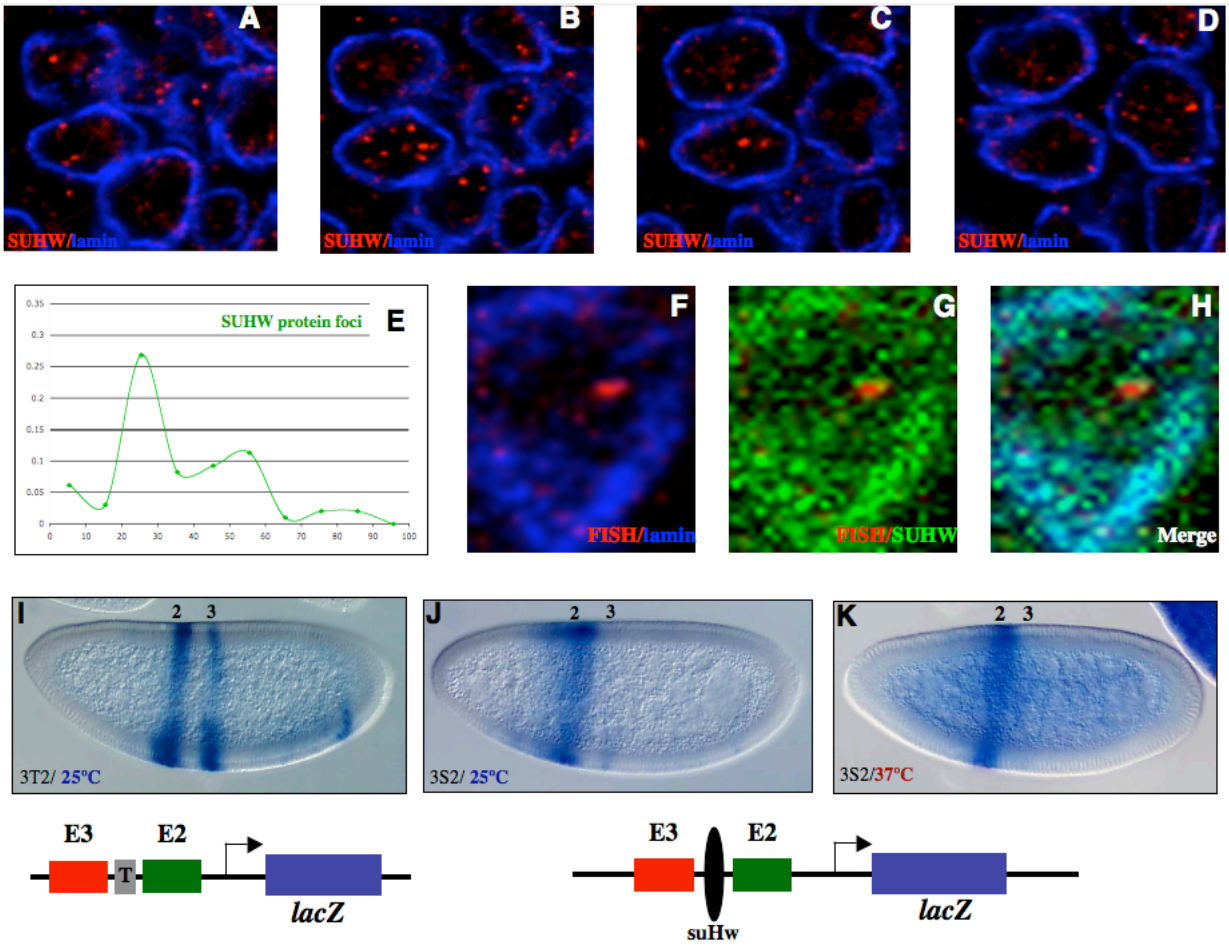
A
SUHW/lamin
B
SUHW/lamin
C
SUHW/lamin
D
SUHW/lamin
SUHW protein foci
E
F
FISH/lamin
G
FISH/SUHW
H
Merge
I
2 3
3T2/ 25°C
J
2 3
3S2/ 25°C
K
2 3
3S2/37°C
E3
E2
T
lacZ
E3
E2
suHw
lacZ

CHAPTER 3

NUCLEOSOME-REMODELING FACTORS ARE REQUIRED FOR THE ENHANCER-BLOCKING ACTIVITY OF CHROMATIN BOUNDARIES IN *DROSOPHILA*[1]

---

[1]Mo Li, Vladimir E. Belozerov and Haini N. Cai*. Submitted to *The EMBO Journal*, 6/10/2007

ABSTRACT

Chromatin boundaries, also called insulators, separate neighboring chromatin domains and regulate enhancer-promoter interactions in diverse species. However, the mechanisms of insulator action remain poorly understood. Here we report that Ebx/NURF301, a component of the NURF nucleosome-remodeling complex, mediates enhancer-blocking activity in *Drosophila*. Using a novel cell-based insulator assay, we show that Ebx/NURF301 and Iswi, the ATPase component of NURF, modulate the activity of multiple *Drosophila* insulators including SF1, suHw, Fab-7 and Fab-8. Reduced level of Ebx/NURF301 or Iswi also disrupts the enhancer-blocking activity of SF1 and suHw in transgenic embryos. Our findings provide the first evidence that a nucleosome-remodeling complex directly participates in the enhancer-blocking mechanism of chromatin boundaries. They also suggest that diverse types of *Drosophila* insulators, previously known to depend on distinct cis and trans components, share a common mechanism that can mobilize nucleosomes and create open and flexible chromatin.

INTRODUCTION

The eukaryotic genome is believed to be organized into distinct structural and functional domains. Increasing evidence suggests that DNA sequences at the boundary between chromatin domains affect the expression of neighboring genes in a wide variety of organisms. The best characterized examples of chromatin boundary elements include scs and scs', which delimit the active chromatin domain of the *Drosophila hsp 70* genes during heatshock (Kellum and Schedl, 1991, 1992a); the yeast telomeric and silent mating type loci boundaries, which restrict the spread of the repressive chromatin (Bi and Broach, 2001; Donze et al., 1999; Donze and Kamakaka, 2001; Ferrari et al., 2004), the mammalian ICR boundary, which modulates enhancer access to the imprinted H19 and Igf2 genes (Bell and Felsenfeld, 2000; Hark et al., 2000), and the compound boundary 5'HS4 in the *β-globin* locus (Bell et al., 1999; Chung et al., 1993; West et al., 2004). Chromatin boundaries from diverse genetic loci and organismal origins exhibit two essential functional characteristics: they block interactions between an enhancer and a promoter, and they insulate integrated reporter genes against transcriptional influences of the surrounding genome (for recent reviews, see (Cai, 2006; Celniker and Drewell, 2007; Gaszner and Felsenfeld, 2006; Lanctot et al., 2007; Sipos and Gyurkovics, 2005; Wei et al., 2005; West and Fraser, 2005).

The mechanism(s) underlying insulator activity is not understood. A "decoy" model suggests that insulators may mimic promoters to trap enhancers or intercept protein factors required for enhancer activities (Geyer and Clark, 2002; Rollins et al., 2004; Torigoi et al., 2000). Consistent with this model, several insulators contain

promoter sequence motifs and interact with known transcription activators, such as *Drosophila* SuHw and GAGA factors and mammalian CTCF protein. An alternative "looping" model proposes that a boundary element may interact with a like-element or nuclear structure, possibly through dimerization of bound proteins, to restrict potentially interacting enhancers and promoters into topologically separate chromatin loop domains. This model is consistent with the finding that boundary proteins Mod(mdg4) and GAGA contain protein dimerization domains and can mediate interactions between distant DNA elements.(Ameres et al., 2005; Cai and Shen, 2001; Dunn et al., 2003; Gerasimova et al., 2000; Gruzdeva et al., 2005; Kyrchanova et al., 2007; Mahmoudi et al., 2002; Mlynarova et al., 2002). A third model, based on studies of the boundaries in yeast telomeric and silent mating type loci and the vertebrate *β-globin* locus, proposes that boundaries recruit histone modification enzymes to establish a local center of active chromatin that counters the spread of silent chromatin (Donze and Kamakaka, 2001; Nakayama et al., 2007; West et al., 2004).

Ebx/NURF301 is the largest subunit of the *Drosophila* NURF, an Iswi ATPase-containing nucleosome-remodeling complex. It has been shown to disrupt ordered nucleosomes and increase DNA accessibility by "sliding" nucleosomes (Tsukiyama et al., 1995; Tsukiyama and Wu, 1995). Ebx/NURF is also required for activation of numerous genes including the heatshock and homeotic genes (Babu et al., 1987; Badenhorst et al., 2002; Elfring et al., 1994; Xiao et al., 2001). Here we report the identification of Ebx/NURF301 by its ability to bind to the *Drosophila* boundary SF1. Using a novel cell-based insulator assay we probed the role of Ebx/NURF301and Iswi in

enhancer-blocking function of boundary elements. We show that RNAi-mediated knockdown of Ebx/NURF301 and Iswi affect the activity of multiple *Drosophila* boundaries, including SF1, suHw, Fab-7 and Fab-8. Mutations in *Ebx/*Nurf301 and *Iswi* genes also disrupt the enhancer-blocking activity of suHw and SF1 in transgenic embryos. Our results provide the first evidence that a nucleosome-remodeling complex participates in the enhancer-blocking function. It also reveals that diverse classes of insulators, which have been known to be distinct in cis-sequences or trans-factors, depend on the same NURF components and possibly a common mechanism for their activity.

RESULTS

Identification of SF-1 interacting factors by yeast-one-hybrid screen

We previously reported the identification of the *Drosophila* SF1 boundary between the *Sex comb reduced (Scr)* and *fushi tarazu (ftz)* genes in the Antennapedia homeotic gene complex (Belozerov, 2003). We propose that SF1 could ensure independent gene regulation in this genomic interval (see map in Fig. 3.1A). In order to identify novel proteins that facilitate boundary function, we conducted a Yeast One Hybrid (YOH) screen using the *Drosophila* embryonic cDNA-Gal4 AD fusion library and the minimal insulator element from SF1 (Wang and Reed, 1993), Clontech/BD Biosciences). For bait DNA, we used the 275 bp SF1b3 minimal boundary element, which contains multiple GAGA factor binding sites and was previously shown to block enhancers in transgenic embryos (Belozerov et al., 2003b). We also used concatenated

copies of a 9-bp repeat sequence within SF1b3 that facilitates the insulator activity in our previous transgenic analysis as bait DNA (data not shown). These sequences were cloned upstream of the HIS-3 and Lac-Z reporter genes (Fig. 3.1B, see Methods for details). Three million independent yeast colonies containing the bait DNA/His-3 reporter and Gal4-AD-Drosophila protein fusions were screened (Fig. 3.1B). The cDNA sequences of 31 strong HIS-3 positive clones from the screens were determined. Based on sequence and expression data, selected clones were retested with a second bait construct containing the LacZ reporter to eliminate false positive clones and non-specific activator clones. The CG7022 cDNA-Gal4, which corresponds to enhancer of bithorax [*Ebx*], also known as NURF301, specifically activated the lacZ reporter gene in an SF1b3–dependent fashion (Fig. 3.1B).

Ebx/NURF301 is the largest subunit of *Drosophila* NURF, an Iswi ATPase-containing nucleosome-remodeling complex (Xiao et al., 2001). It was of particular interest to us among other YOH candidates because it has been shown to collaborate with GAF, a protein required for SF1 boundary activity (Belozerov et al., 2003b; Okada and Hirose, 1998; Tsukiyama et al., 1994). The Ebx/NURF301 protein shares similarity with ACF1, the major subunit of two other Iswi-containing nucleosome-remodeling complexes ACF and CHRAC (Ito et al., 1997), and can mediate nucleosome destabilization. NURF301 contains an HGMA/AT-hook/HMGI(Y)-like domain that facilitates minor groove contact to DNA with low sequence specificity (Xiao et al., 2001). Its recruitment to specific target genes in vivo was thought to be mediated by binding to nucleosomes and by interactions with other sequence-specific transcription factors such

as GAGA (Xiao et al., 2001). However, the recovery of Ebx/NURF301 in our YOH screen suggests that sequence-specific interaction between the SF1b3 element and Ebx/NURF301 also contributes to its recruitment to chromatin.

A cell based enhancer-blocking assay

To quickly test the functional significance of the multiple YOH candidates including NURF301, we decided to establish a *Drosophila* cell culture system. Compared to the traditional genetic and transgenic systems, a cell-based enhancer-blocking assay provides a faster, easier and more quantitative platform to study boundary activity. In addition, P-element-based transgenes have been known to insert as single copy into the genome upon stable transfection thus creating an authentic genomic environment for studying the regulatory aspects of chromatin boundaries (Segal et al., 1996). More importantly, the cell-based boundary assay can be used in combination with RNAi-mediated knockdown to quickly verify large numbers of candidate genes (Caplen et al., 2000; Cheng et al., 2005).

An important consideration in designing transgenes for an enhancer-blocking assay is selecting a pair of clearly delineated and well-matched enhancer-promoter combination. We chose the basal promoter from the evenskipped gene, which contains a 42-bp upstream sequence and a canonical TATA box (Small et al., 1992). It exhibits low basal activity with several reporter genes but responds robustly to a variety of enhancers in transgenic *Drosophila* (Cai and Levine, 1997; Ohtsuki and Levine, 1998a). The Cu^{2+} inducible metallothionein enhancer (MT) was inserted upstream of the eve-

GFP fusion reporter in a P-element backbone (MT-eve-GFP, Fig. 3.2A, top (Bunch et al., 1988), and introduced into *Drosophila* S2 cells via transient transfection. The MT enhancer mediates a 10-fold induction of the GFP reporter by Cu^{2+} (see micrograph and FACS plot, Fig. 3.2A). We found that a 2.2-kb neutral spacer between the enhancer and the promoter did not significantly attenuate the GFP activation (MT-sp-GFP, Fig. 3.2B). Next, we tested if suHw, a well-characterized *Drosophila* boundary element, could block the MT enhancer (MT-suHw-GFP, Fig. 3.2C, top). FACS analysis showed that the suHw element inserted between MT and the eve-GFP fusion gene almost completely blocked the effect of the enhancer (Fig. 3.2C, bottom). These results indicate that the suHw chromatin boundary functions as a strong enhancer blocker in the S2 cells. We have also obtained similar results in *Drosophila* Kc cells (data not shown).

To provide a reference reporter within the same cell that controls for factors other than the boundary element, we constructed a transgene with the ds-Red fluorescent protein (RFP) driven from the basal promoter of the heatshock (*hsp 70*) gene and the MT enhancer (MT-RFP, see diagrams in Fig. 3.2D (Barolo et al., 2004; Bevis and Glick, 2002). Cells cotransfected with MT-GFP and MT-RFP plasmids are double positive for GFP and RFP upon induction (upper right quadrant, Fig. 3.2D, also see relative induction ratio [R:G] in Fig. 3.2G). Again, a spacer between MT and GFP does not significantly attenuate the ratio between GFP and RFP induction (Fig. 3.2E, [R:G-spacer] in Fig. 3.2G). However, a suHw element between the MT and the eve-GFP reporter dramatically reduced GFP induction by MT relative to the control RFP (Fig.

3.2F, [R:G-suHw] in Fig. 3.2G). We also tested the enhancer-blocking assay in stably transfected cells, which contain integrated transgenes in a more native genomic and chromosomal environment. It has been reported that *Drosophila* P transposase can mediate single-copy or low-copy integration of P transgenes, resulting in a more authentic regulatory environment than the tandem array integration in conventional stable transfection (Segal et al., 1996). We tested this by transfecting S2 cells with the MT-GFP transgene in the presence or absence of pTurbo, a P transposase encoding plasmid. We found that the rate of transgene integration, as indicated by the GFP-positive frequency 30 days post-transfection, increased by 20-200 fold in the presence of pTurbo (from 0.02-0.1% to 2-4%). More importantly, reporter gene induction and insulator function in the stably transfected S2 cells are comparable to those in transient transfection (data not shown).

To control for chromosomal position effect on the integrated enhancer-blocking transgene, we created a dual-reporter construct that contains within the same transgene divergently transcribed GFP and RFP with a shared intergenic MT enhancer (2xR, Fig. 3.3A, top). This transgene allows both the GFP and RFP reporters to be present at the same copy number and the same genomic location in stably transfected cells, minimizing position effect. Cells transfected with the dual reporter construct with no insulator showed strong induction of both GFP and RFP although GFP induction appeared to be stronger than that of RFP (Fig. 3.3A, see GFP/RFP ratio in Fig. 3.3C, leftmost bar). However, when the suHw insulator element was inserted between MT and GFP, the GFP induction was dramatically reduced (2xR-suHw, Fig. 3.3B, C). We

next tested additional boundary elements including SF1, SF1b, a sub-fragment of SF1, and two boundary elements from the Bithorax complex, Fab-7 and Fab-8 (Fig. 3.3C, (Belozerov, 2003; Galloni et al., 1993; Hagstrom et al., 1996; Moon et al., 2005; Schweinsberg et al., 2004; Zhou et al., 1996). All four elements effectively reduced the MT-induced GFP expression in transiently transfected S2 cells similar to suHw (Fig. 3.3C). The enhancer-blocking activity of the 2xR-suHw transgene was also found to be comparable in transient and stably transfected S2 cells as well as in Kc cells (data not shown). The dual-reporter transgene provided a convenient, versatile and sensitive assay for enhancer-blocking activity and was therefore adopted for further studies.

Probing boundary function using RNAi-mediated interference

A major advantage of a cell-based boundary assay is the possibility of using RNA interference to probe boundary function and screen for boundary components. The effectiveness of dsRNA in posttranscriptional silencing of gene activity is well established in invertebrate species like *C. elegans* and *Drosophila* (Hammond et al., 2000). We tested the effect of RNAi knockdown on the activity of suHw, which depends on at least two known proteins, SuHw and Mod(mdg4) (Gerasimova et al., 1995; Parkhurst et al., 1988; Spana et al., 1988). S2 cells were transiently transfected with 2xR-suHw and incubated with dsRNAs against SuHw, Mod(mdg4), and dCTCF, the latter being a boundary protein unrelated to suHw function (Moon et al., 2005; Schweinsberg et al., 2004). The cells were then induced for reporter activation, followed by FACS analysis and multiplex RT-PCR quantitation of target mRNA. As

shown in Fig. 3.3D, incubation with dsRNA-SuHw resulted in a reduced level of SuHw mRNA compared to the internal control actin mRNA (average mRNA reduction 30%, replicate n=4, Fig. 3.3D, top left). This coincided with a dramatic 400% increase in the GFP/RFP ratio when normalized against the no-RNA control (Fig. 3.3D, bottom left). The response reflects the key role SuHw plays in the activity of the suHw insulator. The presence of multiple-copied transgenes could further sensitize the RNAi assay for proteins that are in relative low abundance in S2 cells. To test the specificity of the knockdown, we examined the effect of dsRNA against dCTCF, a protein required for enhancer-blocking activity of the *Drosophila* Fab-8 insulator (Moon et al., 2005). The dsRNA treatment reduced the dCTCF mRNA level by 80% in the cell, but caused no change in GFP/RFP ratio (Fig. 3.3D). We also tested the effect of knocking down Mod(mdg4)-67.2, another protein involved in the suHw insulator function. To our surprise, an average of 43% reduction in Mod(mdg4) mRNA level coincided with only a mild 8% increase in the GFP/RFP ratio (Fig. 3.3D, right). This weak response could be due to several reasons. First, the reduction in Mod(mdg4) caused by RNAi may not be sufficient to disrupt the suHw insulator function. Second, the mod(mdg4) gene encodes no less than 26 alternatively-spliced isoforms involved in many aspects of cell and chromosomal biology. The dsRNA we used to target Mod(mdg4) 67.2 did not include the common BTB domain. It is possible that other isoforms could escape the knockdown and compensate for the loss of Mod(mdg4)-67.2. We next tested the effect of RNAi-mediated knockdown on the Fab-8 insulator, whose function depends on the dCTCF protein. Treatment of S2 cells containing 2xR-Fab-8 with dsRNA-dCTCF

caused a strong reduction in the dCTCF mRNA level, which coincided with a 338% increase in the GFP/RFP ratio (replicate n=3), indicating a disruption of the Fab-8 insulator activity (Fig. 3.3D, right). In contrast, a strong knockdown of SuHw resulted in no change in the Fab-8 insulator activity (Fig. 3.3D, right). These results indicate that dsRNA-mediated knockdown of boundary components elicits specific responses in the cell-based enhancer-blocking assay.

NURF components modulate enhancer-blocking activity of multiple *Drosophila* boundaries

We conducted functional screening of the YOH candidates using RNAi-mediated knockdown in the S2 cell insulator assay. Cells containing 2xR-SF1b were treated with dsRNA against the YOH candidates followed by reporter induction, FACS and RT-PCR. Among the candidates we tested, only NURF301 knockdown showed a consistent effect on the SF1b insulator activity. A 30-35% reduction in the level of Ebx/NURF301 mRNA coincided with a significant increase in the GFP/RFP ratio (20%, P=0.01), suggesting that Ebx/NURF301 plays a role in the SF1b insulator activity (Fig. 3.4A). We next tested whether other *Drosophila* insulators are also dependent on NURF301. We found that a reduced level of NURF301 also disrupted the function of suHw and Fab-7 insulators, shown by the 40% ($P<0.0001$) and 50% (P=0.015) increases in GFP/RFP ratio, respectively (Fig. 3.4B-C). Interestingly, a similar knockdown of NURF301 did not significantly disrupt the activity of Fab-8 insulator (P=0.09, Fig. 3.4D). *Ebx* is a key component of NURF, an Iswi ATPase-containing nucleosome-remodeling complex,

which has been shown to disrupt ordered nucleosome arrays and “slide” nucleosomes (Tsukiyama et al., 1994; Tsukiyama et al., 1995; Varga-Weisz et al., 1995; Xiao et al., 2001). To probe whether the NURF complex mediates the effect of Ebx/NURF301 on insulator function, we tested if the Iswi ATPase, another key component of NURF, is also involved in the function of these insulators. We found that the *Iswi* knockdown significantly disrupted the enhancer-blocking activity of suHw ($P<0.0016$) and Fab-7 ($P=0.024$), as seen with the NURF301 knockdowns (Fig. 3.4B-C), but did not cause in a significant change in the SF1b insulator activity ($P=0.15$, Fig. 3.4A). The *Iswi* knockdown also resulted in a significant enhancement (40%, $P=6x10^{-8}$) in Fab-8 insulator activity, similar to that seen in the Ebx/NURF301 knockdown (Fig. 3.4D). Our results indicate that the effect of *Iswi* knockdown is qualitatively consistent with the effect of Ebx/NURF301 reduction, although they may differ in magnitude. The subtle differences between the effects of NURF301 and *Iswi* knockdowns might be due to the fact that Iswi participates in two additional nucleosome-remodeling complexes ACF and CHRAC, which could organize ordered nucleosome array and antagonize the effect of NURF (Deuring et al., 2000; Fyodorov et al., 2004; Ito et al., 1997; Varga-Weisz et al., 1997; Xiao et al., 2001). Unlike knockdown of Ebx/NURF301, change in Iswi level may upset the balance among multiple Iswi–containing complexes and counter the effect of Ebx/NURF301 knockdown. We also noticed that the effect of Ebx/NURF301 and *Iswi* knockdowns on the activity of suHw and Fab-8 appears to be less severe when compared to the SuHw and dCTCF knockdowns. It is possible that these insulators have different functional thresholds for different protein components. It may also

suggest that these NURF components function in a redundant fashion with other proteins to modulate the function of these insulators.

NURF mutations disrupt insulator function in transgenic *Drosophila* embryos

To validate the relevance of the NURF components in insulator function in vivo, we tested whether reducing the maternal input of Ebx/NURF301 and Iswi affects the enhancer-blocking activity of suHw and SF1b by examining embryos containing enhancer-blocking transgenes (Badenhorst et al., 2002; Cai and Levine, 1997; Deuring et al., 2000). The suHw-containing transgene PS3 has a distal enhancer from the twist gene (P, see map in Fig. 3.5A), which is active in the ventral region of early embryos, and a proximal Stripe-3 enhancer from the evenskipped gene (3) that is active in a stripe in the middle of embryo (Fig. 3.5A). A suHw insulator inserted between the two enhancers largely blocks the ventral expression of the lacZ reporter driven by the distal P enhancer (67% strong block, 8% no block), without affecting the downstream stripe 3 enhancer (see photo of wild type embryo, Fig. 3.5A). Embryos produced by female heterozygous for the *Ebx*^{ry122} null mutation contain reduced maternal Ebx/NURF301 and showed a significant increase of the PE-directed lacZ expression in the ventral region (45% strong block, 12% no block, P=0.0015), indicating compromised insulator activity (Fig. 3.5A). A derepression of the distal enhancer is seen in embryos produced by female heterozygous for the *Iswi*^{1} null mutation (58% strong block, 17% no block, P=0.2, Fig. 3.5A). Next, we tested the ability of SF1b to block embryonic tissue-specific enhancers in wild-type and NURF mutant embryos. We used a NFbFbH transgene

containing a distal enhancer from the rhomboid gene (N), active in a pair of ventral lateral stripes, and a proximal Stripe-1 enhancer from the hairy gene (H) that activates lacZ in a head stripe (Cai and Levine, 1997). Two tandem SF1b insulators (Fb) inserted between the enhancers completely blocked lacZ expression in the lateral region of the wild type embryo (78% strong block, 1% no block, Fig. 3.5B). In embryos produced by female heterozygous for the *Ebx*^{ry122} null mutation, the lacZ expression is significantly derepressed in the lateral region (58% strong block, 9% no block, P=0.0015,), indicating a reduced SF1b insulator activity (Fig. 3.5B). A significant derepression of the distal N enhancer is also seen in embryos produced by females heterozygous for the *Iswi*^{1} null mutation (53% strong block, 11% no block, P=0.0001, Fig. 3.5B). Our results indicate that the Ebx/NURF301 and Iswi proteins indeed play an important role in facilitating insulator function in vivo. Taken together, we have shown that Ebx/NURF301 and Iswi modulate enhancer-blocking function by chromatin boundaries, possibly as part of the NURF nucleosome-remodeling complex.

DISCUSSION

Ebx and Iswi modulate the function of multiple Drosophila insulators

Drosophila has one of the most diverse collection of boundary/insulator elements. While most characterized enhancer-blocking activities in vertebrates depend on the CTCF protein, the insulators of *Drosophila* involve a wide variety of cis- and trans-factors. In this study, we provide the first evidence that a common NURF-mediated mechanism facilitates the enhancer-blocking activity of multiple fly insulators, including

suHw, SF1 and Fab7. Intriguingly, Ebx or Iswi downregulation does not disrupt, but rather enhanced the activity of Fab-8, which depends on the *Drosophila* ortholog of CTCF. The reason for such different response is unclear. It is possible that Fab-8, and possibly other CTCF-dependent insulators in vertebrates require a different mechanism that competes or is repressed by nucleosome remodeling activities.

Nucleosome-remodeling and insulator function

Our results also provide the first evidence that a nucleosome-remodeling complex directly participates in the enhancer-blocking mechanism of insulators. The SF1, Fab-7 and Mcp-1 insulators have been shown previously shown to depend on GAF, a protein known to partner with NURF during chromatin remodeling and transcription activation (Belozerov et al., 2003b; Deuring et al., 2000; Okada and Hirose, 1998; Schweinsberg et al., 2004; Tsukiyama et al., 1995; Xiao et al., 2001). The requirement of GAF and NURF factors in both transcription activation and enhancer-block suggests that the two activities may be related in mechanism. It is possible that open chromatin and transcription initiation, facilitated by GAF and NURF, functionally mimics aspects of a promoter and “traps” enhancers or activators (promoter decoy model, Fig. 3.6A, (Geyer and Clark, 2002). This is consistent with the observation that certain insulator DNAs contain promoter-like sequences and coincide with transcription origin of non-coding RNAs (Avramova and Tikhonov, 1999; Bi and Broach, 1999; Hogga and Karch, 2002; Kellum and Schedl, 1991; Ohtsuki and Levine, 1998a; Spana et al., 1988).

An alternative model proposes that boundary elements may interact with each other or with “nuclear anchor sites” to organize genome into loop domains that physically restrict enhancer-promoter interactions (chromatin looping model, Fig. 3.6B, (Cai and Shen, 2001; Muravyova et al., 2001). Consistent with this model, boundary proteins such as GAF and Mod(mdg4) contain the BTB domain, which mediates protein dimerization or oligomerization (Gerasimova et al., 1995; Gruzdeva et al., 2005; Kyrchanova et al., 2007; Mahmoudi et al., 2002; Melnikova et al., 2004; Yoshida et al., 1999). This model is supported by recent reports that distant boundary elements are found in close physical proximity (Blanton et al., 2003; Dekker et al., 2002; Splinter et al., 2006; Tolhuis et al., 2002; Yoon et al., 2007). The ability of NURF to create open and flexible chromatin fiber or even naked DNA regions may enhance interactions between neighboring boundaries. NURF may also promote chromatin looping by simultaneously contacting multiple genomic regions (Fig. 3.6B). It has been reported that ACF, another Iswi-containing nucleosome-remodeling complex related to NURF, can interact with multiple segments of DNA on the surface of nucleosomes, providing a mechanism for DNA looping (Strohner et al., 2005; Varga-Weisz and Becker, 2006). Nucleosome-remodeling complexes ACF/CHRAC and NURD were also reported to interact with SATB1, a mammalian protein that binds to MAR/SAR-like sequences at the base of chromatin loops (Yasui et al., 2002).

A novel *Drosophila* cell-based insulator assay

The only previously reported *Drosophila* cell culture insulator assay used the hsp27 promoter fused to the chloramphenicol acetyl-transferase (CAT) reporter gene (Zhao et al., 1995). The drawbacks of this assay include the use of an extended promoter region, which may contain additional enhancers downstream of the insulator; the inconvenient assay readout of the CAT reporter; and tandem arrays integration of assay transgenes in stably transfected cells. We have developed a new *Drosophila* cell-based insulator assay that recapitulates the key aspects of our P-element-based enhancer-blocking assay in transgenic flies (Cai and Levine, 1995; Cai and Levine, 1997; Cai and Shen, 2001). It employs separate and clearly delineated enhancer and basal promoter modules for insulator tests, and uses dual GFP and RFP reporters for rapid and quantitative FACS readout. The P-element transgene is compatible with transient assay or stable integration, possibly as single copy insertions, providing a more authentic genomic and regulatory environment for studying chromatin boundary function. Selected lines of stably integrated enhancer-blocking transgenes could provide homogenous cell populations both for biochemical analysis of boundary mechanisms and for genome-wide RNAi screens for novel boundary components (Boutros et al., 2004).

MATERIALS AND METHODS

Yeast one-hybrid screen of *Drosophila* embryonic cDNA library

The MATCHMAKER Yeast One-Hybrid System was purchased from (Clontech/BD Biosciences). The SF1b3 element was inserted in the EcoRI and XbaI sites of the pHISi and the EcoRI and XhoI sites of the pLacZi reporter plasmids. The control plasmid containing p53 sites was obtained from BD Biosciences. Linearized "bait"-plasmid containing SF1b3/HIS3 was used to transform the YM4271 yeast strain per manufacture protocol. Stably integrated transformants were selected by HIS3 expression and non-specific activation of HIS3 by the "bait" sequences were modulated by the addition of 45mM 3-AT. The yeast strain containing stably integrated "bait"/His-3 were transformed with pACT2 plasmids containing Gal4-AD fusion cDNA library from 0-20h *Drosophila* embryos (BD Biosciences). Approximately $3x10^6$ colonies were selected for 84 hours on SD/-His plates. Positive colonies were re-tested on SD/-His-Leu, +45mM 3-AT plates to select strong activator of the HIS3 reporter. Plasmids containing candidate cDNAs were isolated from positive colonies, amplified and used for sequencing or for transformation with the pLacZ reporter gene. The colorimetric colony assay for lacZ expression was performed according to the manufacture's protocol.

Cell culture insulator assay transgenes

EGFP and RFP open reading frames were amplified by PCR using pEGFP-N3 (Clonetech) and pRed-Stinger (kindly provided by S. Barolo) as templates, and subsequently inserted between BamHI and PstI sites replacing the lacZ ORF in the

pCAeb-lacZ construct (Cai and Levine, 1997; Small et al., 1992). To make the double reporter construct (pCA2xR), an *hsp 70*-RFP fusion was assembled in pCRII TOPO vector and then inserted between the NsiI and EcoRV sites replacing the mini-white gene (Invitrogen). The Metallothionein (MT) enhancer was cloned using the TOPO TA cloning kit (Invitrogen). The primers used were 5'GTTGCAGGACAGGATGTGG3' and 5' AACGCGGCTTTACACACGG3'. The MT enhancer was placed into pCAeve-GFP upstream from the promoter or between the divergently transcribed reporters in pCA2xR. The 2.2 kb SmaI fragment from the mini-white gene, SF-1, SF-1/b, Su(Hw), Fab-7 and Fab-8 were cut out from respective clones as NotI fragments and inserted into an engineered NotI site between the MT enhancer and eve-GFP of the single- and double-reporter constructs.

S2 cell culture and transfection

Drosophila S2 cells were maintained in HyQ SFX-Insect serum-free medium (HyClone) at 25°C. Transfection DNA plasmids were prepared using the Qiagen Plasmid Mini Kit. Half million cells were allowed to attach to the bottom of 12-well plate wells and incubated for 5 hours with 0.5 ml media containing 1 μg transfection DNA and 2.5 μl of Cellfectin (Invitrogen), followed by incubation with fresh media for at least 24 hour before induction. For stable transfection, 0.1μg pTurbo plasmid encoding the P-element transposase was also included in the transfection cocktail.

Imaging and flow cytometry

Fluorescence microscopy was performed using a Zeiss Axioplan 2 inverted microscope and images were captured with an Olympus DP10 digital camera. Fluorescence Activated Cell Sorting (FACS) analyses were done using FACSCalibur flow cytometer (Becton Dickinson). For each FACS analysis, 2-5x10^4 cells were used. Fluorescence was excited at 488 nm. The photomultiplier detection voltages were set at 400 V for FL1 and 375 V for FL2. Data analysis was done using FloJo software. Green fluorescence was detected with FL1 530/30 BP filter; red fluorescence was detected with FL2 585/42 BP filter. The relative level of induction (I) of the reporter genes in cotransfection experiments is calculated as below: $I = (i/i_{max}) \times 100\%$, (i = positive cells % x positive cells mean fluorescence]$_{induced}$ / [positive cells % x positive cells mean fluorescence]$_{uninduced}$; and $i_{max.}$ is the nearest high integer of the highest i value of all cotransfection experiments. The GFP/RFP ratio (R) in the dual reporter experiments in is [GFP cells % x GFP cells mean fluorescence]$_{induced}$ /[RFP cells % x RFP cells mean fluorescence]$_{induced}$. Change in GFP/RFP ratio (C) in Fig. 3.3D and Fig. 3.4 is calculated as below: $C=R_{RNAi}/ R_{no\ RNAi} \times 100\%$. Standard error of the mean (SEM) is calculated as +/- SD/N^{-2}. Test of significance in the change of GFP/RFP ratio were done using Student's T-test.

RNAi and RT-PCR

For dsRNA synthesis, plasmids containing cDNAs of the target proteins were linearized and used as templates for in vitro transcription using the MEGAscript kit

(Ambion). The sense and antisense RNAs were then annealed. A 1.2Kb Pst I fragment was cloned from full-length Mod(mdg4) cDNA (kindly provided by James Kadonaga). The dCTCF cDNA was obtained from ATCC. An 800 bp fragment of the Su(Hw) cDNA was generated by PCR with the primers: 5'AGGAAAAGAAGGGCAAGCTGC3' and 5'AGCATATGTCCTTCTTCTCC3'. DNA fragments containing Ebx and Iswi exons were generated by PCR using primers 5'CGAGTCGGAGTATCACTACG3' and 5'ACCAGCATGTAAAGTTCTCC3' (for Ebx); 5'CGCTCAATATCCTGCAACTCAG and 5'CATCGTCATCGTGCCAAAGT3' (for Iswi). For RNAi experiment, dsRNA was delivered to the cells either by transfection using Cellfectin reagent or by soaking the cells in ds-RNA containing medium 24 hours after transfection. Cells were induced by addition of 1mM Cu^{2+} 72 hours after RNAi treatment and harvested for FACS analysis 96 hours after addition of dsRNA. Total RNA was extracted using the TRIZOL method according to manufacture's protocol (Invitrogen). RT-PCR was performed using the OneStep RT-PCR kit according to manufacture's protocol (Qiagen). The following primers were used in RT-PCR reactions: for Mod(mdg4) 67.2 isoform 5'TTATTAGCACCGCGGAATCG3' and 5'AGAGCGTTTGTTTGTCGACAC3'; for Su(Hw) 5'GGAAAACACAGCCCGAAACA3' and 5'CCTCATCCGTCAGCTGCTCT3'; for dCTCF 5'AGTACAGCCACCAATAAATCCATC3' and 5'CTTCGTCTACGGTATAGTCCGACA3'; for Ebx 5'ATAAGCGACGCCATCTGTCC3' and 5'TTACGTTCTTCCTCATCATCC3'; for Iswi

5'TTAAGACCGCGAATCTGGTAGTC3' and 5' AAGAGAACTCGAACGAGACGACT3'; and for actin 88F

5'GATGGTGTCTCCCACACCGT3' and 5'CGATCGGCAATACCAGGGT3'. The expected product size for the actin control is 467 bp. The ratio of target gene primers to the actin 88F primers was determined empirically. Equal amount of total RNA was used RT-PCR reactions of untreated and treated samples.

Enhancer-blocking assay in wild type and *Ebx*^{ry122} and *Iswi*^{1} transgenic *Drosophila* embryos

The construction of the enhancer-blocking transgenes containing the suHw and the SF1b insulators was previously described previously (Belozerov, 2003; Cai and Levine, 1997). The *Ebx*^{ry122} and *Iswi*^{1} mutant strains were kindly provided by the Bloomington *Drosophila* Stock Center (Bloomington, Indiana) and Dr. John Tamkun (University of California, Santa Cruz), respectively. Males homozygous for the enhancer-blocking transgenes were mated with virgin females of wild type or those heterozygous for the *Ebx*^{ry122} and *Iswi*^{1} null mutations, respectively. Reporter expression in F1 embryos from all crosses were examined under the same staining condition by whole mount in situ hybridization using anti-lacZ RNA probes according to previously described protocol (Tautz and Pfeifle, 1989). The extent of enhancer-block was evaluated by at least two authors and categorized into no block, weak, medium, and strong block groups under double-blind condition. Test of significance in the change of GFP/RFP ratio were done using Chi-square difference test.

ACKNOWLEDGEMENT

We thank Scott Barolo for the RFP plasmid; Jim Kadonaga for the SuHw and Mod(mdg4) cDNAs; Sally Elgin for the GAF cDNA; John Tamkun for the *Iswi*^{1} stock and the Bloomington Stock Center for the *Ebx*^{py122} stock. I thank Diana Houng for technical assistance with *Iswi* RNAi. We also thank Edward Kipreos, Ping Shen, Sapna Patel, Sharmila Roy and Kevin Liu for critical reading of the manuscript. This work is supported by the NIH.

Fig. 3.1. Yeast-One-Hybrid screen of SF1-interacting proteins

A. SF1 chromatin boundary may ensure independent regulation of the neighboring *Scr* and *ftz* genes. Top: Schematic diagram of the *ftz-Scr* region. Arrows indicate the location and orientation of the *Scr* and *ftz* promoters. Open boxes and circles represent exons and tissue-specific enhancers, respectively, for the *Scr* (green) and *ftz* (red) genes. V, visceral mesoderm enhancer, PS2, parasegment 2 enhancer; D, *ftz* distal enhancer, A, AE1 enhancer, N, neurogenic enhancer, and Z, zebra enhancer. Brown and yellow boxes represent the SF1 and SF1b3 sub-region, respectively. Size and distance of the DNA elements are not drawn to scale. Bottom: Distinct expression patterns of the *Scr* (green) and *ftz* (red) genes in the early *Drosophila* embryo revealed by whole mount fluorescence in situ hybridization using anti-sense probes. B. Top, schematic of the Yeast-One-Hybrid screen. An SF1b3 binding protein (green oval) fused to Gal4-AD (pink oval) activates the integrated SF1b3-His 3 or SF1b3-lacZ selectable markers (see Methods for details). Bottom, SF1b-dependent activation of the lacZ reporter by CG7022. p53 and Trp C, Control proteins that activate the lacZ reporter expression in a sequence-dependent (p53) and sequence-independent (Trp C) fashion.

A

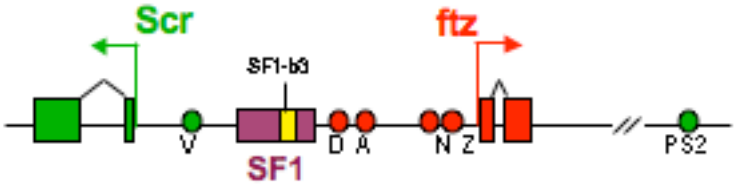

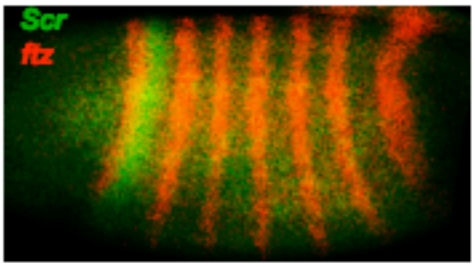

B

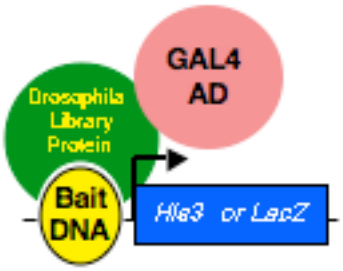

		PREY		
		p53	CG 7022	Trp C
BAIT	SF1 b3			
	p53 site			

Fig. 3.2. Enhancer-blocking assay in *Drosophila* S2 cells.

A. Cu^{++}-mediated induction of GFP reporter in S2 cell transfected with MT-GFP. Top: transgene diagram (not drawn to scale, below same): boxes represent key components of the transgene: the MT enhancer (yellow), the evenskipped basal promoter (light blue) and the GFP reporter gene (green). Middle: fluorescence microscopic images of S2 cell transfected with the MT-GFP transgene before (left) and after (right) induction. Bottom: FACS histogram of uninduced (left) and induced (right) S2 cells. X-axis, log scale of GFP level; Y-axis, number of cells at given GFP level. Red bar at lower right represents percentage of total cells with GFP level above 10^2. B. A spacer DNA does not interfere with the GFP induction. Top: MT-sp-GFP transgene: grey open box, 2.2 kb neutral spacer from white coding region. Bottom: FACS histogram of MT-sp-GFP transgene before (left) and after (right) induction. C. The suHw insulator blocks MT-mediated GFP induction. Top: MT-suHw-GFP transgene: red oval, 340-bp suHw element. Bottom: FACS histogram of MT-suHw-GFP transgene before (left) and after (right) induction. D-G: Reporter induction in S2 cells cotransfected with RFP and GFP transgenes. D. Induction of reporter expression in MT-GFP and MT-RFP co-transfected cells (diagramed on left). Right: FACS flow chart of induced S2 cells cotransfected with both transgenes. X and Y axes, log scale of GFP and RFP level, respectively. The lower-left quadrant contains mostly double negative ($<10^2$), including untransfected and uninduced cells, and the top-right quadrant contains mostly double positive ($>10^2$) cells. Percentage of total cells in each quadrant is indicated at the corner. Ratio of RFP/GFP induction is shown in chart in 2G (R:G). E. Induction of

S2 cells cotransfected with MT-RFP and the MT-sp-GFP (diagramed on left). The 2.2 kb spacer is shown by the grey open box. Right: FACS flow chart of induced S2 cells cotransfected with both transgenes. Ratio of RFP/GFP induction is also shown in 2G (R:G-spacer). F. Induction of S2 cells cotransfected with MT-RFP and MT-suHw-GFP (diagramed on left). The 340 bp suHw element is shown by the red oval. Right: FACS flow chart of induced S2 cells cotransfected with both transgenes. Ratio of RFP/GFP induction is shown in 2G (R:G-suHw). G. Relative level of the RFP (red bars) and GFP (green bars) induction in cotransfection experiments (2D-F, see Methods for detail).

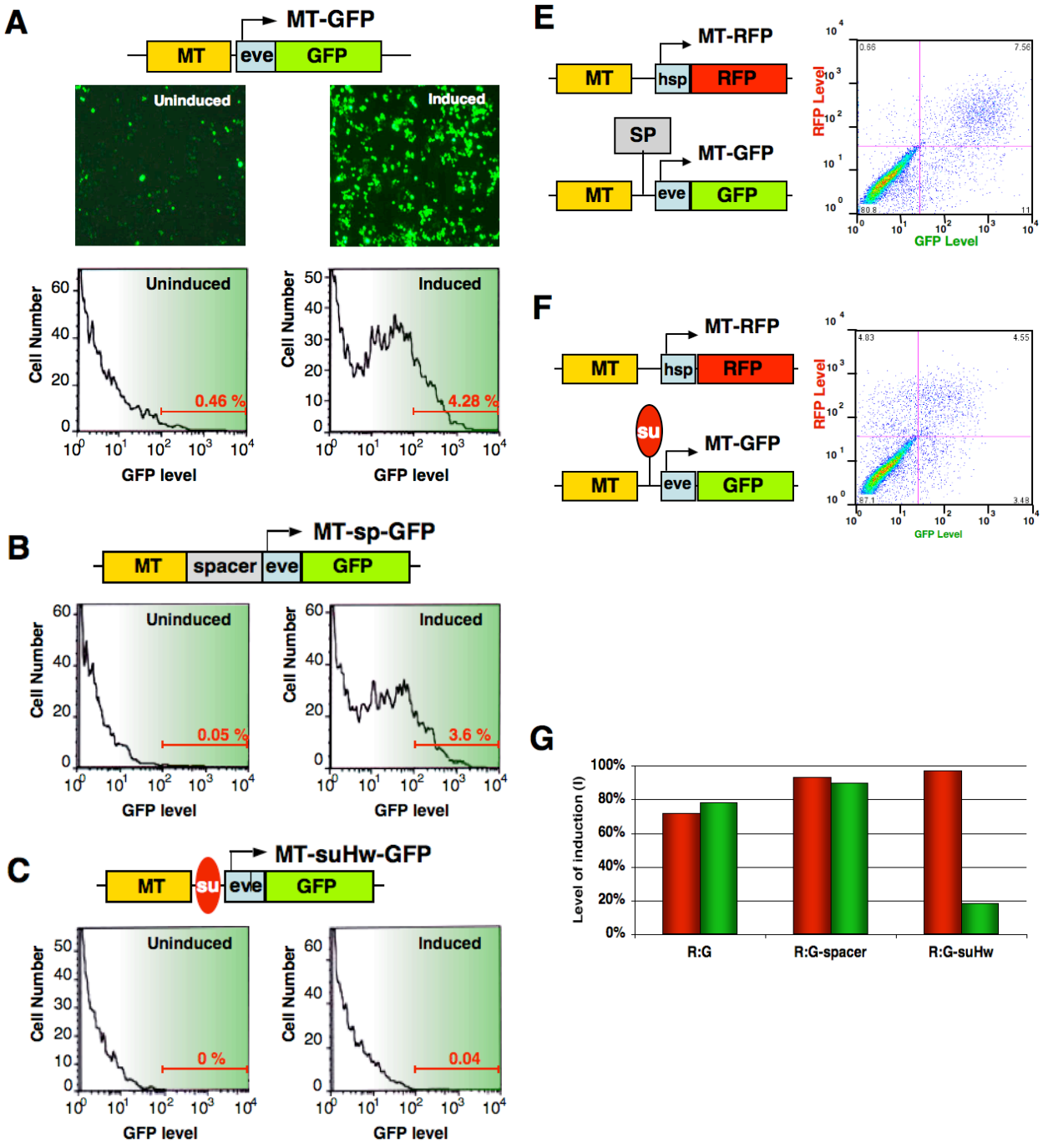
A
MT-GFP
MT
eve
GFP
Uninduced
Induced
Cell Number
GFP level
0.46 %
4.28 %
B
MT-sp-GFP
MT
spacer
eve
GFP
0.05 %
3.6 %
C
MT-suHw-GFP
MT
su
eve
GFP
0 %
0.04
E
MT-RFP
hsp
RFP
SP
MT-GFP
RFP Level
GFP Level
F
MT-RFP
MT-GFP
G
Level of induction (I)
100%
80%
60%
40%
20%
0%
R:G
R:G-spacer
R:G-suHw

Fig. 3.3. Study of insulator function using 2xR dual reporter transgenes and RNAi-mediated gene knockdown.

A. Dual reporter expression in S2 cells. Top: diagram of the 2xR dual reporter transgene: Middle: fluorescence microscopic images of the dual reporter-containing cells before (top) and after (bottom) induction. Bottom: FACS flow chart of dual reporter-containing cells before (left) and after (right) induction. GFP/RFP ratio is shown in chart in 3C (no ins). B: Dual reporter containing suHw. Top: Diagram of 2xR-suHw transgene. The suHw insulator is inserted between MT and eve-GFP. Bottom: FACS flow chart of 2xR-suHw containing cells before (left) and after (right) induction. GFP/RFP ratio is shown in 3C (2xR-suHw). C. Enhancer-blocking activity of suHw, SF1b, Fab7 and Fab8 in S2 cell insulator assay. Top: Diagram of dual reporter transgene with no insulator or testing insulators inserted between MT and eve-GFP. Bottom: Enhancer-blocking test of *Drosophila* insulators. The GFP/RFP ratio for the no insulator control (no ins., left-most column) and various insulator-containing transgenes are shown. Error bars are calculated as SEM = +/- x SD/N^{-2}. Replica number is shown in parentheses (see Methods for details). D. Effect of RNAi-mediated knockdown on suHw and Fab-8 insulator activity. Left top: RT-PCR quantitation of SuHw, Mod(mdg4) and dCTCF mRNA in 2xR suHw-containing cells before (left lanes) and after (right lanes) RNAi treatment. Multiplex RT-PCR was done using knockdown target-specific and Actin 88f control primers (the 467 bp actin product is marked by an asterisk, also see Methods for details). Left bottom: insulator activity (GFP/RFP, untreated cell = 100%) in 2xR-suHw cells with no RNAi, SuHw, Mod(mdg4) and dCTCF RNAi

knockdown (see Methods for more details). Right top: RT-PCR quantitation of SuHw and dCTCF mRNA in 2xR Fab-8-containing cells before (left lanes) and after (right lanes) RNAi treatment. Right bottom: Insulator activity in 2xR-Fab-8 cells with no RNAi, SuHw and dCTCF RNAi knockdown.

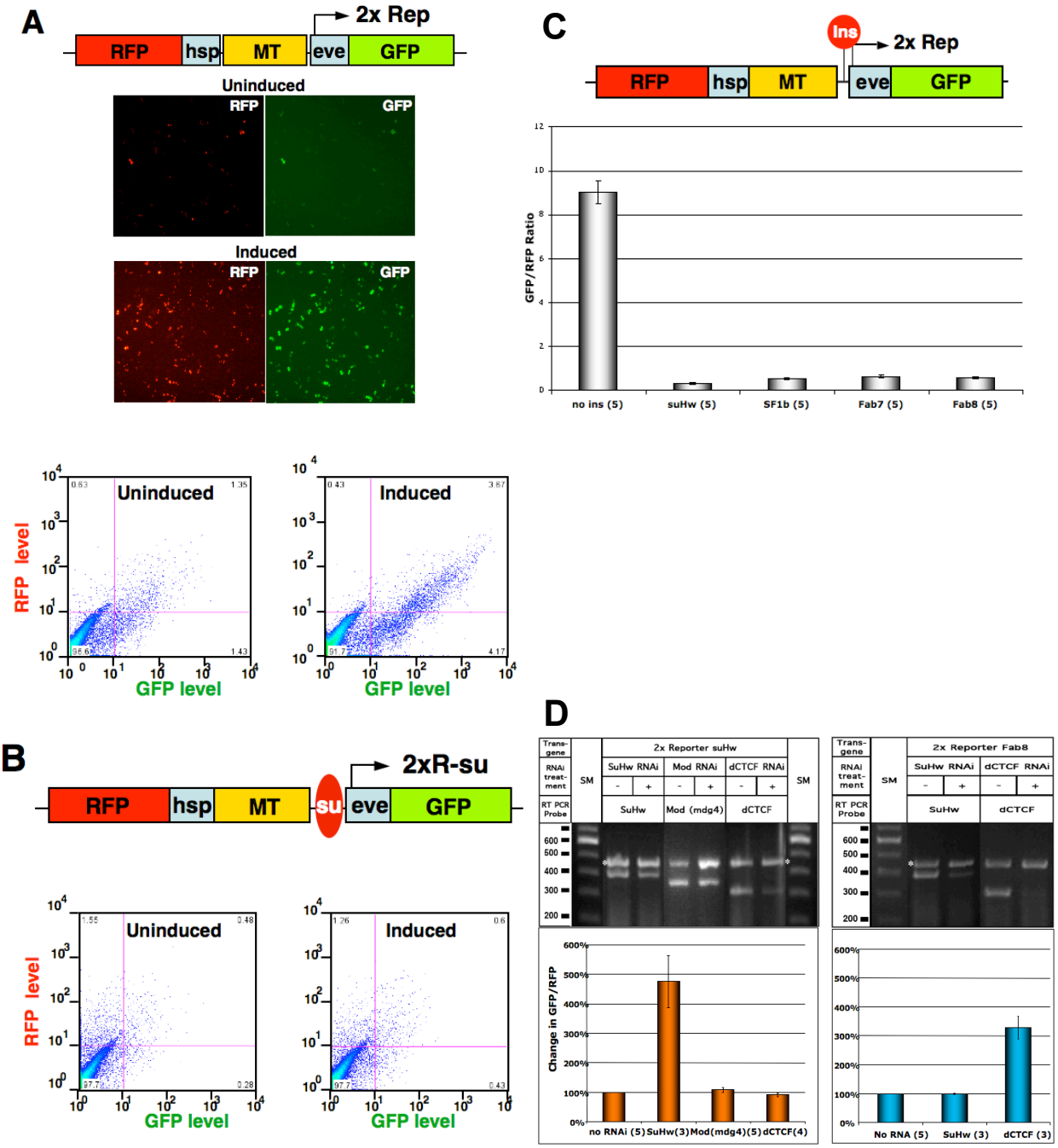
A
2x Rep
RFP
hsp
MT
eve
GFP
Uninduced
RFP
GFP
Induced
RFP
GFP
Uninduced
Induced
RFP level
GFP level
B
2xR-su
su
C
Ins
GFP/RFP Ratio
no ins (5)
suHw (5)
SF1b (5)
Fab7 (5)
Fab8 (5)
D
Trans-gene
RNAi treat-ment
RT PCR Probe
SM
2x Reporter suHw
SuHw RNAi
Mod RNAi
dCTCF RNAi
SuHw
Mod (mdg4)
dCTCF
2x Reporter Fab8
Change in GFP/RFP
no RNAi (5)
SuHw(3)
Mod(mdg4)(5)
dCTCF(4)
No RNA (5)
SuHw (3)
dCTCF (3)

Fig. 3.4 RNAi knockdown of NURF components disrupts insulator activity in S2 cell enhancer-blocking assay.

S2 cells transfected with 2xR transgene containing SF1b (A), suHw (B), Fab-7 (C) and Fab-8 (D) were treated with dsRNA against *Ebx* and *Iswi*. Top: RT-PCR of 2xR insulator-containing cells for *Ebx* and *Iswi* mRNA before (left lanes) and after (right lanes) RNAi. Multiplex RT-PCR was done using gene-specific and Actin 88f control primers. Bottom: Insulator activity (GFP/RFP, untreated cell = 100%) 2xR-insulator cells with no RNAi (left), *Ebx* (middle) and *Iswi* (right) RNAi knockdown.

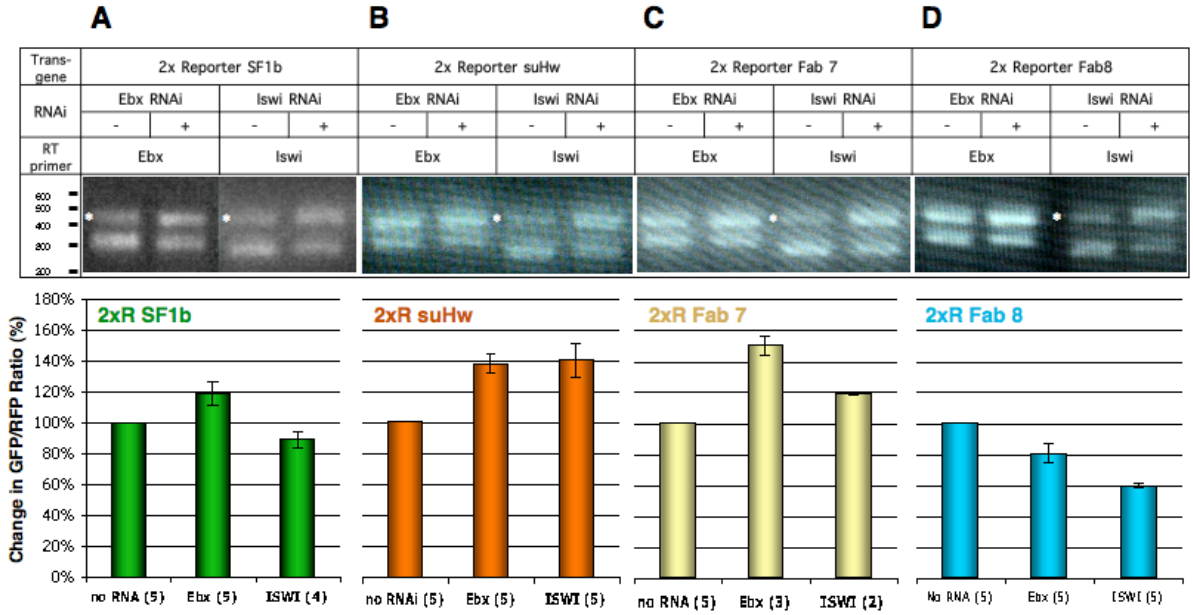
A
B
C
D
Trans-gene
2x Reporter SF1b
2x Reporter suHw
2x Reporter Fab 7
2x Reporter Fab8
RNAi
Ebx RNAi
Iswi RNAi
RT primer
Ebx
Iswi
Change in GFP/RFP Ratio (%)
2xR SF1b
2xR suHw
2xR Fab 7
2xR Fab 8
no RNA (5)
Ebx (5)
ISWI (4)
no RNAi (5)
ISWI (5)
no RNA (5)
Ebx (3)
ISWI (2)
No RNA (5)
Ebx (5)
ISWI (5)

Fig. 3.5 *Ebx* and *Iswi* mutations disrupt insulator activity in transgenic *Drosophila* embryos.

A. Whole mount in situ showing lacZ pattern in wild type and NURF mutant embryos containing the PS3 transgene. Top: Diagram of PS3 transgene, yellow circle, twist PE enhancer; blue circle, evenskipped stripe 3 enhancer, red oval, suHw insulator. Middle, lacZ reporter expression in PS3 embryos produced by wild type (left), *Ebx*^{ry122} (center) and *Iswi*^{1} (right) mutant mothers. Embryos are oriented dorsal up and anterior to the left. The distal PE enhancer is completely blocked in the wild type embryo, shown by the lack of lacZ expression in the ventral region. Partial derepression of the lacZ expression in ventral region in mutant embryos indicates reduced suHw insulator function. Bottom: Quantitative assessment of the enhancer-blocking activity of suHw in wild type and mutant embryos. Cellular blastoderm stage PS3 embryos were inspected for each genetic background and categorized into no block, weak, medium or strong block groups (see Methods). B. SF1b-containing transgene NFbFbH in wild type and NURF mutant embryos. Top: Diagram of NFbFbH transgene, yellow circle, rhomboid NEE enhancer (N); blue circle, hairy stripe 1 enhancer (H), red oval, two tandem copies of SF1b insulator. Middle, lacZ reporter expression in NFbFbH embryos produced by wild type (left), *Ebx*^{ry122} (center) and *Iswi*^{1} (right) mutant mothers. The distal NEE enhancer is completely blocked in the wild type embryo, shown by the lack of lacZ expression in the ventral lateral regions. Partial derepression of the lacZ expression in mutant embryos indicates reduced SF1b insulator function. Bottom: Quantitative assessment of the enhancer-blocking activity of SF1b in wild type and mutant embryos.

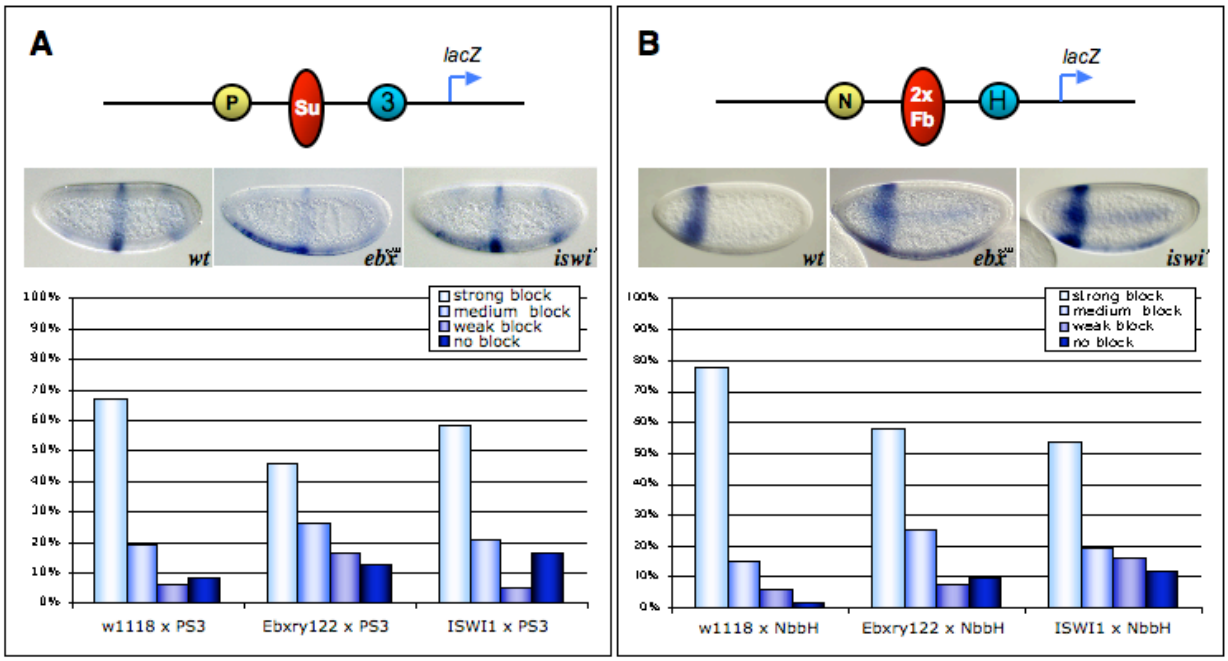
A
lacZ
P
Su
3
wt
ebx
iswi
strong block
medium block
weak block
no block
100%
90%
80%
70%
60%
50%
40%
30%
20%
10%
0%
w1118 x PS3
Ebxry122 x PS3
ISWI1 x PS3
B
lacZ
N
2x Fb
H
wt
ebx
iswi
strong block
medium block
weak block
no block
100%
90%
80%
70%
60%
50%
40%
30%
20%
10%
0%
w1118 x NbbH
Ebxry122 x NbbH
ISWI1 x NbbH

Fig. 3.6 Models for NURF's role in insulator mechanism

A. NURF facilitates insulator function by mimicking an active promoter and intercepting enhancer-promoter communications. Brown circles bound by NURF complex and H3K4M histone modification marks represent activated chromatin at an insulator (purple box) and near a downstream gene promoter (arrow). Solid and broken curve lines represent actual and potential transcription activation, respectively, from an upstream enhancer. B. NURF complex can slide or remodel nucleosomes (light brown and irregularly-spaced circles) to create flexible chromatin fiber or nucleosome-free DNA that facilitates the interactions between neighboring insulators (purple boxes) and the formation of loop domains. Alternatively, nucleosome-remodeling proteins may simultaneously interact with multiple DNA/chromatin regions to facilitate looping.

"Promoter decoy" model

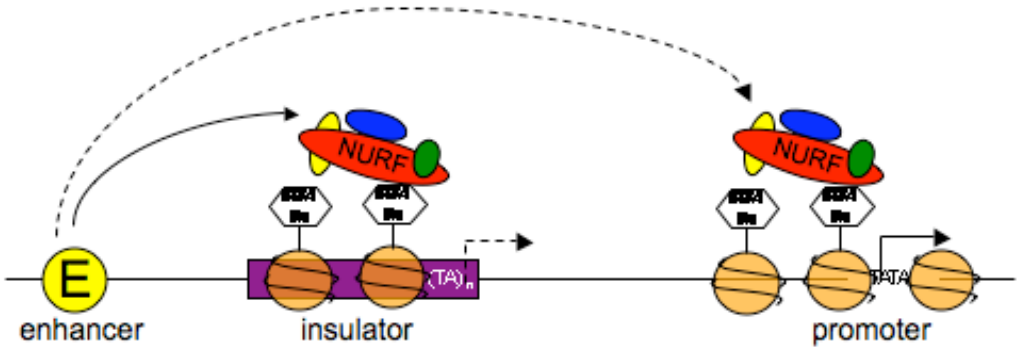

Chromatin looping model

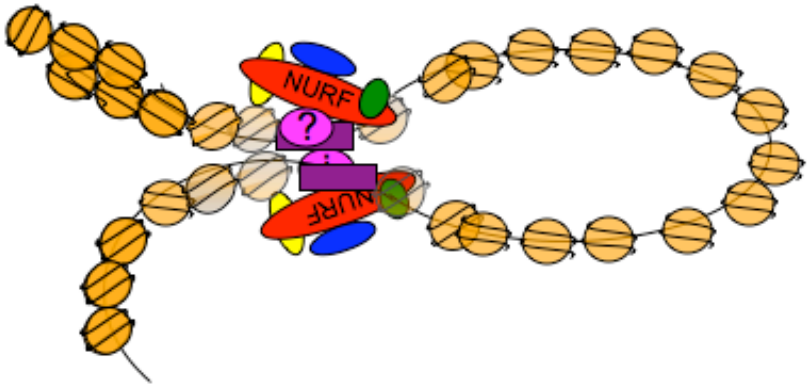

CHAPTER 4

PROBING THE GENOMIC ORGANIZATION OF DROSOPHILA HOX GENE COMPLEXES

---

[1]Mo Li and Haini N. Cai. To be submitted to *Developmental Cell*, 8/2007

ABSTRACT

The order of Hox genes on chromosome correlates with the order of their expression domains along the anterior-posterior body axis. This unique colinear relationship is conserved across diverse animal groups, suggesting a critical role of the Hox gene organization for their function. The *Drosophila* Hox genes, unlike the single contiguous Hox clusters found in vertebrates, are grouped into Antennapedia and Bithorax complexes (ANT-C and BX-C), separated by 10 million base pairs. Nonetheless, the separation does not affect the coordinated expression of the Hox genes. We have probed the role of specialized DNA such as insulators in the spatial organization and regulation of *Drosophila* Hox genes. Using the chromosome conformation capture (3C) technique, we detected interactions between the SF1 insulator and the *Antennapedia, Deformed* and *labial* gene regions in the ANT-C. The DNA regions facilitating these interactions contain boundary activity as shown by enhancer-blocking assay. Strikingly, we also detected steady interactions between the promoters of *Antp* from the ANT-C and *Abd-B* from the BX-C, suggesting a spatial linkage of the two complexes despite the linear separation. Using 3D FISH, we confirmed the interactions detected using 3C in embryonic and larval tissues. We further showed that the interaction between the *Antp* and *Abd-B* loci is developmentally regulated. It occurs in posterior tissues, where both genes are expressed, or in tissues where both genes are ectopically activated due to mutations in the Polycomb group proteins. Our data suggest that the coordinated expression of Hox genes may require physical proximity of the key regulatory elements of these genes, and that such proximity may contribute to the unprecedented conservation of Hox gene organization.

INTRODUCTION

Hox genes are a group of highly conserved genes that function in patterning the body axes. In most genomes, Hox genes are clustered and display a colinear relationship between the gene order on chromosome and spatial and/or temporal expression profile along the anterior-posterior body axis. This unique colinear relationship suggests that genomic organization plays a critical role in Hox gene regulation. A paradox of Hox gene regulation in *Drosophila* is that the *Drosophila* Hox genes are split into two complexes, the *Antennapedia* complex (ANT-C) and the *Bithorax* complex (BX-C), yet the 10 Mbp separation of the two does not affect their coordinated expression. The molecular mechanism underlying the colinear expression of Hox genes is unclear. Recent studies on the murine *HoxB* cluster suggest that Hox gene expression is coordinated in part by the formation of higher-order chromatin structures (Chambeyron and Bickmore, 2004; Chambeyron et al., 2005). In addition, higher-order chromatin structures, such as chromatin loop formation mediated by long-range interactions between cis-regulatory elements, have been demonstrated to regulate developmentally related genes including the TH1/TH2 cytokine genes, the β-*globin* genes, and the olfactory receptor genes (Ling et al., 2006; Lomvardas et al., 2006; Spilianakis et al., 2005). Another piece of the puzzle comes from a recent report on a long-range interaction between the Fab-7 insulator and the promoter of the *Abd-B* gene, both from the *Bithorax* Hox complex (Cleard et al., 2006). These findings suggest that Hox gene expression could be coordinated by interactions between cis-regulatory elements, such as promoters, enhancers and insulators. Based on this hypothesis, we probed possible long-range regulatory interactions between cis-regulatory elements in

Drosophila Hox complexes.

Hox genes are regulated by a complex system of cis-regulatory elements. For example, the Hox genes of BX-C, *Ultrabithorax (Ubx), abdominal-A (abd-A)* and *Abdominal-B (Abd-B)*, have extensive *cis*-regulatory regions that are organized into autonomous regulatory domains, each consisting of tissue-specific enhancers and Polycomb/Trithorax response element (PRE/TRE) repression/activation modules. These domains are separated by DNA elements called chromatin boundaries. Deletions of chromatin boundary in BX-C cause neighboring domains to fuse, which leads to misregulation of Hox genes and transformation of body segment identity (homeotic transformation) (Maeda and Karch, 2006). This evidence demonstrates that chromatin boundaries are important for maintaining regulatory independence of neighboring domains. Although it is unclear if the other *Drosophila* Hox cluster, ANT-C, is also organized into independent domains, the discovery of the SF-1 chromatin boundary in ANT-C seems to support the idea. SF-1 is located between the homeotic *Sex comb reduced* (*Scr*) gene and the non-homeotic *fushi tarazu* (*ftz*) gene (a map of the genomic region is depicted in Fig. 4.2). In transgenic assays, SF-1 blocks enhancer-promoter interactions and protects the *mini-white* gene from chromosomal position effects (CPE). SF-1 has been proposed to restrict the enhancers of the two neighboring genes to appropriate targets and protect *ftz* from the spread of Polycomb-mediated silent chromatin formation from nearby homeotic genes (Belozerov et al., 2003a).

The mechanism of SF-1 function is unknown. Increasing evidence supports a looping model in which boundaries function by interacting with like elements and forming chromatin loops (Blanton et al., 2003; Cai and Shen, 2001; Gerasimova et al., 2000; Muravyova et al., 2001; Tolhuis et al., 2002). This model is consistent with the fact that the function of SF-1 requires the GAGA factor, a protein capable of mediating insulator pairing through the BTB/POZ (Broad complex, Tramtrack, bric a brac/poxvirus and zinc finger) protein-dimerization domain (Belozerov et al., 2003a; Melnikova et al., 2004). We hypothesize that SF-1 may function by interacting with additional boundaries downstream of *ftz* to form an independent *ftz* transcription unit within a chromatin loop domain. Additionally, the formation of such a chromatin loop may also facilitate the function of the *Scr* distal enhancers, which are located downstream of *ftz*.

We adopted the chromosome conformation capture (3C) technique to probe for DNA sequences that could interact with SF-1 in the *ftz* downstream region. In light of a recent discovery of a boundary-promoter interaction in the BX-C (Cleard et al., 2006), we also examined possible interactions between SF-1 and the promoter and intergenic regions of Hox genes in ANT-C. Guided by the results from the SF-1 3C search, we further probed long-range interactions between Hox genes using the 3C and FISH technique, which provided new insights into the genomic organization of Drosophila Hox complexes.

RESULTS

The SF1 chromatin boundary forms chromatin loops with sequences in the *ftz-Antp* region

To test the hypothesis that SF-1 functions by forming chromatin loops with other boundaries, we applied the Chromatin Conformation Capture (3C) technique to probe for long-range interactions between SF-1 and relevant genomic regions in ANT-C. 3C is a powerful new tool for studying the spatial organization of the genome (Dekker et al., 2002). It uses formaldehyde-mediated crosslinking to capture spatial juxtaposition of DNA. The likelihood of two DNA fragments being crosslinked is an indication of spatial proximity. The crosslinking frequency is quantitated using a ligation-based PCR strategy (Fig.4-1A), and expressed as the ratio (ie. relative crosslinking frequency) of signal obtained by PCR on crosslinked template to that obtained on a control template (Fig.4-1B). The control template includes all possible ligation products present in equal quantity. It also corrects for variations in PCR amplification efficiency of different primer sets, and is universally adopted as a necessary control for 3C (Dekker, 2006). Other control experiments that omit the crosslinking or ligation steps are used to demonstrate the specificity of a positive signal. Recently, the use of 3C has revealed long-range regulatory interactions in the β-*globin*, *H19/Igf2* and olfactory receptor loci (Ling et al., 2006; Lomvardas et al., 2006; Tolhuis et al., 2002). 3C is therefore an ideal tool for studying the organization of complex genetic loci such as the Hox complexes.

First, we applied the 3C technique to *Drosophila* embryos and measured, in triplicate, relative crosslinking frequencies between the EcoRI fragment containing SF-1

and twelve EcoRI fragments that constitute a 32 kb genomic region encompassing *ftz* and its downstream sequences. The map of the region and the fragments tested in the 3C analysis are depicted in Fig. 4.2A. We identified two regions that were crosslinked to SF1 at high frequency. The first region (Peak 1) is the third EcoRI fragment located 10 Kb 3' to the *ftz* transcription start site (Fig. 4-2A). This was surprising, because a larger fragment containing Peak 1 (represented by a blue box marked with a "V" in Fig. 4.2A) showed little insulator activity in a previous attempt to search for SF-1 interacting elements using a transgenic strategy (see Fig. 4.3). Instead, we found strong enhancer-blocking activity in the sequence immediately 5' to the No.V fragment (blue box marked "IV" in Fig. 4.2A). We noted that Peak 1 is situated 3' to the ftz-DE enhancer of *ftz* (Calhoun and Levine, 2003) and 5' to the PS2 enhancer of *Scr* (Gorman and Kaufman, 1995). Although Peak 1 is not an enhancer-blocker *per se*, because of its prominent interaction with SF-1 and special genomic location, we think that Peak 1 cooperates with SF-1 to separate regulatory elements of *ftz* and *Scr* into independent domains by forming chromatin loops. The second peak (Peak 2) of crosslinking frequency contains the 10th and 11th EcoRI fragments. Despite the large linear distance (36-39 Kb) from SF-1, Peak 2 interacts with SF-1 at a significantly higher frequency than the neighboring fragments (Fig. 4.2). To test if Peak 2 contains enhancer-blocking activity, the 3.2 kb region was divided into two partially overlapping 2 kb sub-fragments and tested for enhancer-blocking activity in *Drosophila* S2 cells as described in Chapter 3. The 3' sub-fragment, ftz+28-30k, displayed strong enhancer-blocking activity that is comparable to the su(Hw) insulator, while the 5' sub-fragment, ftz+27-29k, displayed no enhancer-

blocking activity (data not shown). To verify the result *in vivo*, we generated flies carrying a transgene with the ftz28-30k fragment in the pEbNH enhancer-blocking test construct. The transgenic enhancer-blocking assay uses two tissue-specific enhancers, the *hairy* stripe 1 enhancer (H1) and the *rhomboid* neuroectoderm enhancer (NEE), which drive reporter gene expression in a transverse anterior stripe and two ventral-lateral stripes, respectively (Cai and Levine, 1997). Insertion of the ftz28-30k fragment between the two enhancers strongly blocked the NEE-directed *lacZ* expression, but not the H1-directed one, indicating enhancer-blocking activity (Nftz28-30k in Fig. 4.3B). This result revealed a novel enhancer-blocking activity in a 2 kb (1.6 kb at the 3' end of the 11th EcoRI fragment plus 400 bp of the 12th fragment) fragment at the 3' end of Peak 2. We noted that Peak 2 falls into the 3' end of a 10 kb region that has been coarsely defined as a PRE that is responsible for the maintenance of *Scr* repression in the mesothoracic and metathoracic segments (Gindhart and Kaufman, 1995). The discovery of an enhancer-blocking activity close to a PRE draws an interesting parallel to the close association between insulators and PREs in BX-C (Barges et al., 2000; Busturia et al., 2001; Mihaly et al., 1997). It is likely that the enhancer-blocker in Peak 2 functions to separate the regulatory elements of *Scr* from those of the neighboring *Antp* gene, which contains intronic enhancers and repressors; and that this function relies on the formation of a chromatin loop between SF-1 and Peak 2.

We show that SF-1 interacts with two regions downstream of *ftz*, both of which are closely associated with a novel enhancer-blocking activity. These results suggest that SF-1 forms chromatin loops with two insulators downstream of *ftz*, separating

regulatory elements of *Scr*, *ftz* and *Antp* into independent domains; and the loop formation may shorten the effective distance between the Scr promoter and its distal regulatory elements such as enhancers or PREs, therefore facilitating their function.

SF1 participates in multiple long-range interactions with sequences outside the *ftz-Antp* region in ANT-C

We next tested if SF-1 participates in long-range interactions with regulatory regions of other Hox genes in the ANT-C. In particular, we focused on genomic regions surrounding Hox promoters, because a recent report showed that the Fab-7 boundary in the BX-C participates in long-range interaction with the *Abd-Bm* promoter (Cleard et al., 2006). Our search included the promoter-proximal regions of the *Antp, Deformed (Dfd), proboscipedia (pb)* and *labial (lab)* genes. We also included the genomic region downstream of *Dfd*, because the orientation of *Dfd* in *D. melanogaster* was inverted during evolution and does not agree with the rest of the Hox genes (Negre and Ruiz, 2007). Within these regions, we consistently detected interactions between SF-1 and three EcoRI fragments, containing the promoter of *Antp*, immediately downstream of *Dfd,* and upstream of *lab*, respectively (A+1, D1 and L+4 in Fig. 4.2B). We noticed that these SF-1-interacting fragments stand out from neighboring fragments, which do not produce detectable 3C signals. We reason that this is due to a reduced background crosslinking frequency caused by the greater distance to SF-1. To screen for enhancer-blocking activity, we dissected these three fragments into partially overlapping sub-fragments of ~1.7 kb each (A+1/1 and A+1/2, D1/1 through D1/5 and L+4/1 through L+4/3 in Fig. 4.2B) and tested them for enhancer-blocking activity in S2 cells. A+1/1,

D1/4 and L+4/1 have the strongest enhancer-blocking activity among the sub-fragments from the same EcoRI fragment, while others have weak activity (Fig. 4.3A). These three sub-fragments were further tested in transgenic enhancer-blocking assay. The D1/4 and A+1/1sub-fragments showed intermediate to strong enhancer-blocking activity, while L+4/1 had little activity (ND1/4H and NA+1/1H in Fig. 4.3B).

Our data provide the first evidence of an insulator participating in multiple long-range interactions with cis-elements that contain enhancer-blocking activity in *Drosophila* Hox gene complex. This suggests that SF-1 may be involved in the regulation of other Hox genes in ANT-C through interactions with novel insulators in addition to its function in the *Scr-ftz* region.

Multiple loops exist between the *Antp* promoter and other Hox genes in ANT-C

We next asked whether the sequences that interact with SF-1 could interact with other regions of ANT-C. Using 3C, we tested long-range interactions between the promoter region of *Antp* (the A+1 fragment) and EcoRI fragments in a 300 kb genomic region downstream of the *Antp* gene. The A+1 fragment was selected, because it contains two types of regulatory elements—a promoter and an insulator. Our preliminary results show that despite the large distance the *Antp* promoter interacts with many more regions than SF-1 in the ANT-C. We observe a general trend of clustering of regions with high relative crosslinking frequencies immediately upstream and downstream of Hox genes (e.g. see the *Dfd, pb* and *lab* regions in Fig 4.4A), although there are several peaks that are located exclusively in introns (*lab, pb* and *Dfd* in Fig. 4.4A). Also, the *Antp* promoter does not interact with regions further downstream of *lab,*

which is beyond the limit of ANT-C. The interactions between the *Antp* promoter and multiple regulatory regions in ANT-C suggest that the *Antp* promoter may play an role in coordinating Hox gene expression.

Long-range interaction between the ANT-C and BX-C

Based on the observation that the *Antp* promoter interacts with regulatory regions of Hox genes in ANT-C, we probed the possible interactions between the *Antp* promoter and regions in Bithorax homeotic complex. We measured relative crosslinking frequency between the *Antp* promoter and six EcoRI fragments covering extensive flanking regions of the *Abd-Bm* gene and found a strong signal just upstream of the *Abd-Bm* promoter (Fig. 4.4B). We did not detect any other signal in the neighboring regions. The experiment was repeated three times with independent preparations of 3C samples. Our result shows that the two *Drosophila* Hox complexes physically interact with each other despite being separated by 10 Mbp, suggesting a spatial linkage between the two.

Visualizing long-range regulatory interactions in ANT-C by 3D FISH

A limitation of 3C analyses is that the crosslinking frequencies determined by the 3C technique reflect an average of the whole embryo, which contains different tissues. To confirm the long-range interactions uncovered in 3C analyses at the single-cell level, we preformed three-dimensional FISH experiments. We studied the co-localization of the SF-1 and *Antp* loci, and the *lab* and *Antp* loci in wild-type embryos at the germ band-retracted stage. We did not examine the co-localization of SF-1 and Peak 1 or Peak 2

in the FISH analysis, because the inter-probe distances would be too small to be resolved by light microscopy. First, we compared the co-localization between the *Antp* and SF-1 loci and that between the *Antp* and control loci (Antp+140k), with the control probe and the SF-1 probe being equidistant from *Antp*. In the first and second thoracic segments (T1 and T2), the average distance between the *Antp* and SF-1 signals is significantly smaller (t-test, T1: $p<2.7x10^{-5}$, T2: $p< 2.5x10^{-6}$) than that between the *Antp* and control signals. The *Antp* and SF-1 loci also co-localized 2.5 times more frequently (center-to-center distance < 0.25 μm) than the control pair (Fig. 4.5A-C). These results further confirm that the SF-1 and *Antp* loci are closely associated with each other in the nucleus. We also noticed that the inter-probe distance of both the experimental and control pairs increased slightly in T2. This difference between the two segments may be attributed to the more "open" chromatin structure of the *Antp* gene in T2, where it becomes fully activated (Zink et al., 1991).

We next examined the co-localization of the *Antp* and *lab* loci in embryos. Similarly, the distance between *Antp* and *lab* is significantly smaller (t-test, $p<2x10^{-6}$) than that between *Antp* and an equidistant control (Antp+330k). The co-localization frequency of the *Antp* and *lab* loci is 2.1 times greater than that of the control loci (Fig. 4.6A, B and E). Our data show that the *Antp* and *lab* loci frequently co-localize, confirming the results obtained using the 3C technique. We arrived at the same conclusion when imaginal discs of 3rd instar larvae were used in the same analysis (Fig. 4.6C and D). Taken together, we confirmed the long-range interactions in ANT-C detected by 3C using an independent approach (3D FISH).

Developmental regulation of the spatial organization of Drosophila Hox complexes

To study the developmental regulation of the interaction between the *Antp* and *Abd-B* gene in the two *Drosophila* Hox complexes, we performed 3D FISH experiments using probes to the *Antp* and *Abd-B* loci in tissues representing different gene expression profiles and developmental stages. In T1 of embryos, neither *Antp* nor *Abd-B* are expressed. We observed that the two loci are far apart and rarely co-localize in T1. The localization of the loci in T2, where only *Antp* is expressed, resembles that of T1. However, in the eighth abdominal segment (A8), where both *Antp* and *Abd-B* are co-expressed, we observed a 32% decrease of the inter-loci distance and a 91% increase in the frequency of co-localized loci, indicating frequent interactions (See Fig. 4.7A and C; T1, T2 and A8 for wild-type embryo in Fig. 4.7F). When we repeated the same analysis on larval imaginal discs, the results closely matched those in embryos. Interestingly, the interactions between the two loci are strengthened in posterior larval tissues (Fig. 4.7B; T1, T2 and A8 for wild-type imaginal disc in Fig. 4.7F). Perhaps this is because larval tissue is committed to differentiation for a longer period of time and therefore allows more stable interactions to form.

Since the interaction between *Antp* and *Abd-B* is tissue specific, we wondered if it could be affected by mutations that cause misregulation of Hox genes. *Polycomb* (*Pc*) and *extra sexcombs* (*esc*) belong to the Polycomb-Group (Pc-G) genes, which are required for the repression of Hox genes in regions where they must remain silent. In

mutants of Pc-G genes, homeotic genes are derepressed in tissues anterior to their normal expression domain, resulting in homeotic transformations of anterior body segments to posterior ones (Kennison, 1993; Paro, 1990; Pirrotta, 1997; Simon, 1995). In particular, *Abd-B* is derepressed in all anterior segments in *Pc*$^{-}$ embryos, transforming these segments into abdominal segments. To unambiguously identify the *Pc*$^{-}$ mutant embryos, we labeled ABD-B proteins using an anti-Abd-B antibody in FISH experiments (Fig. 4.7D and E). Both *Antp* and *Abd-B* are depressed in mutant T1 cells (Fig. 4.7E). We found that they are significantly closer (compared to wild-type, $p<0.0013$) and overlap 2.5 times more frequently than in wild-type T1, which is reminiscent of wild-type A8. In mutant T2 cells, the *Abd-B* gene is derepressed, while the *Antp* expression is unchanged (*Antp* is expressed in T2 in wild-type flies). We also did not detect any significant change of the inter-probe distance of the *Antp* and *Abd-B* loci. Similarly, in A8 of the Pc^{-} embryos, where expression of neither gene is changed, we observed little change in the co-localization frequency of the two loci (Fig. 4.7C; T1, T2 and A8 for *Pc*$^{-}$ embryo in Fig. 4.7F). Analyses in *esc*$^{-}$ embryos produced similar results to those in *Pc*$^{-}$ embryos (data not shown).

In conclusion, our data show that the interaction between the *Antp* and *Abd-B* promoters occurs in posterior tissues, where both genes are expressed, or in mutant tissues where both genes are ectopically activated. This is the first evidence of a tissue-specific and developmentally regulated physical interaction between the *Drosophila* Hox gene complexes. Our results suggest that a common activation mechanism may bring the two *Drosophila* Hox gene complexes in physical proximity in posterior body region,

which may be important for coordinating Hox gene expression.

DISCUSSION

Our 3C and transgenic analyses on the *ftz-Antp* intergenic region resulted in two important findings: first, SF-1 interacts with two DNA regions flanking the distal *Scr* regulatory elements, and second, that these two SF-1-tethering regions are associated with novel enhancer-blocking activities. These results support the hypothesis that SF-1 functions by interacting with other insulators and forming chromatin loops. The first SF-1-tethering region, Peak 1, is located in between the ftz-DE enhancer and the PS2 enhancer of *Scr*. Although Peak 1 does not block enhancers *per se*, there is a strong enhancer-blocking activity immediately 5' to it (SF2-4). We hypothesize that the tethering and enhancer-blocking activities belong to one compound cis-regulatory element that separates the *ftz* and *Scr* regulatory elements into different domains by interacting with SF-1 and forming chromatin loops. A potential problem with this model is the location of the *Scr* T1 enhancer (Gorman and Kaufman, 1995), which partially overlaps with the tethering-insulator combo (see Fig4.2A). However, when the T1 enhancer was identified 12 years ago, it was mapped only coarsely using convenient restriction sites to a relatively large 3.7 kb fragment due to technical limitations. Further molecular dissection of the 3.7 kb fragment is necessary to determine the relative position of the enhancer and insulator. The second SF-1-tethering region, Peak 2, is located at the 3' end of the distal PRE of *Scr*, and it harbors strong enhancer-blocking activity. We propose that this tethering and insulator combo block spreading of the *Scr* distal PRE-mediated silencing into the *Antp* gene domain. The *Scr* distal PRE has been

shown to repress ectopic activation of the *Scr* promoter posterior of T1 (Gindhart and Kaufman, 1995), where *Antp* is expressed. The tethering and insulator combo of Peak 2 therefore provides a mechanism of protecting *Antp* from being ectopically silenced by the *Scr* distal PRE. Peak 2 also contains a 389 bp DNA element named the distal tethering element (DTE). DTE has been shown to facilitate the *Scr* T1 enhancer in transgenic assays and is proposed to function by tethering the enhancer to the promoter (Calhoun and Levine, 2003). However, the authors placed DTE immediately next to the T1 enhancer in the assays, which is a great deviation from the 20 kb separation in the endogenous environment. Furthermore, there is did no direct evidence of interactions between DTE and the *Scr* promoter. To clarify this point, we tested possible interaction between DTE and the *Scr* promoter directly by 3C and did not detect any. Because of the above reasons, we do not think DTE mediates long-range interaction between itself and the *Scr* promoter.

The next logical question would be: do Peak 1 and Peak 2 form chromatin loops with SF-1 simultaneously in the same cell, or separately in different tissues? Unfortunately, 3C in the whole embryo does not allow us to address this question. To overcome this technical limitation, we are in the process of developing new methods to mark specific tissues by fluorescent protein expression to specifically isolate cells from these tissues using Fluorescence Activated Cell Sorting (FACS). In a preliminary test, we have successfully sorted GFP positive cells from fly embryos expressing a *Kruppel*-GFP reporter gene and used the sorted cells to reproduce the 3C results from whole embryo using 3 independent set of primers. Applying 3C technique to specific tissues

will provide us deeper insights into the dynamics of chromatin structures.

The discovery of multiple SF-1 tethering regions outside the *ftz-Antp* region suggests additional roles of SF-1 in the regulation of genes in ANT-C. Interestingly, four out of five tethering regions (including Peak 1 and Peak 2) either contain enhancer-blocking activity or are close to a region that has enhancer-blocking activity. Although the L+4 fragment does not block enhancers, we cannot exclude the possibility that its flanking regions contain insulators just like the region 5' to Peak 1. These insulators may participate in one-to-one interactions *in vivo*, or they may form a rosette-like structure similar to the proposed insulator body of su(Hw) (Gerasimova et al., 2000). Future tissue-specific 3C studies will be able to differentiate the two possibilities.

The discovery of an insulator in the *Antp* promoter region is consistent with previous genetic evidence. The $Antp^{73b}$ mutation is caused by a chromosome inversion that replaced the *Antp* promoter with a foreign promoter. Curiously, this leads to a dominant phenotype due to ectopic expression of *Antp,* although normal ANTP protein is expressed due to the activity of the foreign promoter (Schneuwly et al., 1987). Additionally, a short *Antp* promoter containing 1 kb of upstream region has been shown to be particularly sensitive to position effects in transgenic flies when compared to other *Antp* promoters with longer upstream sequences (Zink et al., 1991). Both the ectopic activation *Antp* in $Antp^{73b}$ and the sensitivity to position effect of the short *Antp* promoter can be explained by the lack of an insulator in the immediate upstream region of the *Antp* promoter. A recent study provided a hint of the *in vivo* function of some of these insulators. Mito et al. reported the distribution of histone H3.3 variant and Pc-G proteins

in *Drosophila* Hox gene complexes. We found that the Peak 2 and the *Antp* promoter regions coincide with a high level of histone H3.3 and peaks of Pc-G proteins binding. More importantly, the known chromatin boundaries of the Bithorax complex—Mcp, Fab-7 and Fab-8, all coincide with peak levels of H3.3 (Mito et al., 2007). This correlation suggests that the novel insulators identified in ANT-C may perform similar functions as the chromatin boundaries in BX-C to separate neighboring cis-regulatory domains.

We used 3C and 3D FISH as two independent yet complementary approaches to study the organization of *Drosophila* Hox gene complexes. To our knowledge, this is the first time that long-range interactions between multiple Hox genes have been studied at different developmental stages and in a tissue-specific fashion. We discovered that the *Antp* promoter interacts with the regulatory regions of all other Hox genes in the same complex, suggesting that it may be a lynchpin of the organization of Hox genes in ANT-C. Moreover, we showed that the promoter of *Antp* interacts with the promoter of *Abd-Bm*, providing the first evidence of a direct link between the two *Drosophila* Hox gene complexes, ANT-C and BX-C. We also demonstrated that the interaction between the two Hox complexes is developmentally regulated and forms primarily in posterior tissues where both *Antp* and *Abd-B* are expressed. Finally, we showed that mutations in Pc-G proteins cause *Antp* and *Abd-B* to interact in T1, where they normally do not interact.

Regulation of gene expression by higher-order chromatin structures has been long proposed to underlie the unprecedented structural conservation of Hox gene complexes. Previous genetic studies have shown that a mutation of *Antp* caused by the

insertion of a repetitive sequence near the promoter leads to dominant derepression of *Scr*, which is located 150 kb away (Southworth and Kennison, 2002). However, the molecular basis of this long-range transcriptional influence has not been elucidated to date. Our data is consistent with this result and provides a mechanism through which long-range transcriptional influence can be explained. In addition, many studies including this one show that different classes of regulatory elements including insulators, enhancers and promoters, can interact with each other, which could mediate the interaction of Hox genes (Cai and Shen, 2001; Cleard et al., 2006; Lomvardas et al., 2006). The *Antp* promoter region that interacts with regulatory regions of other Hox genes contains a promoter and an insulator. It is likely that different types of regulatory elements participate in the long-range interactions. Irrespective of the types of regulatory element involved in the interaction, a common goal might be to bring distant genes together so that they can be co-regulated.

Another conundrum of Hox gene regulation in *Drosophila* is how the colinear regulation of Hox genes is maintained when the genes are split into two complexes, separated by ~10 Mbp. Our results reveal for the first time a physical interaction between the two *Drosophila* Hox complexes. One component of this inter-complex interaction, the *Antp* promoter region, can participate in long-range interactions with multiple Hox genes in ANT-C, and therefore appears to be the hub of Hox gene organization in ANT-C. The other part, the *Abd-Bm* promoter upstream region, has also been shown to engage in long-range regulatory interactions, evidenced by its role in the transactivation of a distant enhancer and its interaction with the Fab-7 insulator (Cleard

et al., 2006; Sipos et al., 1998). The above evidence indicates that the promoter region of *Antp* and *Abd-B* may function as an organizing center for their respective Hox gene complex. Together with our discovery of a spatial link between the two Hox complexes, these results suggest a novel mechanism of coordinating gene regulation of the two Hox complexes by bringing the two together in the nuclear space.

The interaction between the *Antp* and *Abd-B* promoters occurs in posterior tissues, where both genes are expressed, or in mutant tissues where both genes are ectopically activated. This suggests a common activation mechanism may be responsible for bringing the two loci together in the nucleus. The Trithorax group (Trx-G) proteins, which are positive regulators of Hox gene expression, are possible candidates that could mediate this interaction. Future FISH analysis in Trx-G mutants should provide further insights into the developmental regulation of the interaction between Hox complexes.

Interaction between co-regulated genes is not unique to Hox gene clusters. Recent studies have suggested that it may be a common phenomenon found in many complex genetic loci that contain co-regulated genes, such as the *β-globin* genes, the olfactory receptor genes and the T_H1 and T_H2 cytokine genes (Ling et al., 2006; Lomvardas et al., 2006; Spilianakis et al., 2005). The combinatorial approach of 3C, 3D FISH and transgenic analyses described here is therefore highly valuable for studying this previously under-explored aspect of gene regulation in many development processes.

MATERIALS AND METHODS

Transgenic enhancer-blocking assay

The P-element constructs used in the embryo enhancer-blocking assays were based on the pCaSPeR or the pC4plz vector. All DNA sequences tested for enhancer blocking activity were generated by PCR and cloned into pCRII/TOPO vector (Invitrogen). The primers used: AGAGCGGAACCGAAAGC and AACTAGAGGGAATGGTATTGTCG for SF2-1; TGTTTTGCAAACATCAACCAAG and GGATCGCGGGTTCTCA for SF2-2; TATATATCTAGACAAACCATCCTCTTGTG and TATATATCTAGAGAAGCCATCC-TTACCAA for SF2-3; GGATGGCTTCGGAATATTATAAATG and GGGACTTACAT-ATATGCAATCGG for SF2-4; ATACATTGTAATAATATTCCTCAAC and TATTATT-TTTCATTTAGCACGC for SF2-5; GCGGCCGCTCCTCGATTGTGTG and TCAATT-GTGCAAAAAAAGCCA for ftz28-30k; GAATTCTCAGCTAACGGTAGCTT and GCGGCCGCTATTTTAA-GAAATTAAAAGC for A+1/1; TGTAAAACCTGATCGTAATGTTTCT and GCGGCCGCTTAACCAGATATGTACGT for D1/4; CGTAAGGTAATTTTTAAGC-ATTTCGTG and GCGGCCGCAGTCACCTCTTCTTAA for L+4/1. The ftz28-30k, A+1/1, D1/4 and L+4/1 sequences were inserted into the NotI site between the NEE and H1 enhancers in pEbNH (Cai and Levine, 1997). To generate the SF2 test constructs, the H1 enhancer was cut out from an existing clone (provided by Haini Cai) as a SpeI-BamHI fragment and inserted into the 2N vector (Cai lab). The H1 sequence was then isolated as an SpeI-NotI fragment. The SF2 candidate sequences were cut out from

respective TOPO clones as SpeI-NotI fragments. These two kinds of SpeI-NotI fragments were ligated together into a NotI site of the pC4plz to generate the final construct. The position and orientation of the enhancer and test sequences were determined by restriction digestion or PCR. P-element transformation, whole mount *in situ* hybridization and visual assessment of reporter gene expression were performed as described (Belozerov et al., 2003a).

Chromosome Conformation Capture (3C) analysis

The original 3C procedures were developed for determining chromosome conformation in yeast by Dekker et al. (Dekker et al., 2002). We used a protocol described elsewhere (Gomez et al., 2005) with adaptations to study genomic organization of Hox clusters in *Drosophila* embryos. Embryonic nuclei were prepared from collections of 0~20 hour old fly embryos according to protocols by Kamakaka R. and Blanton J et al. (Blanton et al., 2003) with small modifications. After washing and blot-drying, embryos were resuspended in Buffer I (15mM Hepes-KOH pH 7.6, 10mM KCl, 5mM $MgCl_2$, 0.1mM EDTA, 0.5mM EGTA, 0.35mM Sucrose, 1mM DTT, 1mM $Na_2S_2O_5$, 0.5-1ug/mL Antipain, Leupeptin) and immediately homogenized by 10-20 passes in a Dounce homogenizer with a B pestle. The homogenate was filtered with miracloth® and rinsed once with fresh Buffer I to collect all materials. Debris in the filtrate was removed by centrifuging at 480 xg for 9 min. The supernatant was centrifuged at 2000 xg for 10 min to collect nuclei. After resuspension in Buffer I, the nuclei pallet was carefully overlaid on top of an equal volume of Buffer II (Buffer I with

0.8 M sucrose) and centrifuged again at 2000 xg for 10 min. Nuclei were resuspended in nuclei resuspension buffer (0.34M sucrose, 10 mM Tris pH8.0, 10 mM NaCl, 1% Triton X-100, 0.25 mM PMSF, 0.1% β-Mercaptoethanol). A small aliquot of nuclei was stained with DAPI and counted under microscope using a hemocytometer. Nuclei were spun down again and resuspended in cross-link buffer (nuclei resuspension buffer contining 1% formaldehyde), or plain nuclei resuspension buffer for the no-crosslink control. Crosslinking was done on a nutator at room temperature for 5 min. The reaction was quenched by the addition of glycine to 0.125 M. The samples were washed with nuclei resuspension buffer (2X 2000 xg for 5 min) and loop assay buffer (10 mM Tris-HCl pH7.9, 5 mM $MgCl_2$, 20mM NaCl and 1mM dithiothreitol; 2000 xg, 5min) and resuspended in 1x NEB restriction buffer. The material was incubated at 37 °C for 10 min with the presence of 0.1% SDS to remove non-crosslinked proteins from DNA. Triton X-100 was added to 1% to sequester SDS. Approximately $3x10^7$ nuclei were digested by EcoR I at 37 °C over night. The restriction enzyme was heat inactivated at 65 °C for 25 min. The digested DNA was diluted 40 times and ligated by T4 DNA ligase for 20 min at room temperature followed by an overnight incubation at 16 °C. To reverse the crosslinks, the samples were incubated at 50 °C over night in the presence of 10 μg/ml proteinase K. DNA was purified by phenol-chloroform extraction and ethanol precipitation. To generate the control template, purified genomic DNA was digested with the same restriction enzyme and ligated in a concentration of ~500 ng/μl. The appropriate amount of template DNA used in PCR was determined by serial dilution. The specificity of the PCR products was ensured by a two-step nested PCR

strategy. For each restriction fragment of interest, the restriction site is always 3' to the outer and inner primers. We designed the primers to make the final PCR products all about 200-300 bp long. PCR products were analyzed on 2% agarose gels and imaged by a Biorad UV Gel Doc imager. Quantitation of PCR products was done using the Gel Analyzer function of ImageJ (Rasband, W.S. http://rsb.info.nih.gov/ij/).

Three-dimensional FISH and image analysis

FISH experiments were performed according to published protocols (Dernburg, 2000). Genomic DNA of the interested loci were cloned by PCR into the PCRII-TOPO vector (Invitrogen, CA) with the following primers: Antp 1st 5k forward: TGAAAAACAAGAG-ACCCGGCG, Antp1st 5k reverse: AAACCGTTACGGCTGCCATTT, Antp+330k 1st 5k forward: ACCCTTTATACCCAGACGACG, Antp+330k 1st 5k reverse: TCCCCTTTT-TAGAGACTTGCGC, Antp+330k 2nd 5k forward: CCCCTAGCACTAGTGCAACAA, Antp+330k 2nd 5k reverse: CCCCTAGCACTAGTGCAACAA, Antp+140k forward: TCGAGGATGTGAGAGTACGGAT, Antp+140k reverse: ATTACTCAAGCATG-GCACCCA, lab 1st 5k forward: GCAGTCGTATCGTGGTATCTACA, lab 1st 5k reverse: TGGCCTTAGACTCTTTTGACCG, lab 2nd 5k forward: AAGGCTAGGCTCCTTGGG-ATT, lab 2nd 5k reverse: GAATACTGACACAAAAAAATGCTCCT, AbdB 1st 5k forward: TGAGACCCCCCAGTTAAATGA, AbdB 1st 5k reverse: TTAATGACGGCTAC-CCAACGG, AbdB 2nd 5k forward: CCGTTGGGTAGCCGTCATTAA, AbdB 2nd 5k reverse: TTTTGCACAGTGCATGTGCTG. The probes for the *Antp, Antp+330kb, lab,*

Abd-B loci were made from two neighboring 5 kb DNA fragments that were cloned separately. The probe for the *Antp+140kb* locus was made from a single 5 kb DNA fragment. A existing SF-1 clone was used for making the SF-1 probe (Belozerov et al., 2003a). For fluorescence labeling of probes, plasmid DNA were fragmented with six 4-base-recongnizing restriction enzymes to ~100 bp and labeled with Cy3-, Cy5- or Dig-UTP in terminal transferase reactions according to manufacturer's instructions (TdT labeling kit, Roche). FISH on imaginal discs was done exactly as described (Xu et al., 2004). For embryo FISH, stage 9-13 embryos were collected and fixed in glass vials containing 4ml of heptane and 4ml of fixative (3.7% freshly prepared formaldehyde in Buffer A (Dernburg et al., 1996). Fixation was carried out by shaking the vial on an orbital shaker at maximum speed for 25 min. The hybridization and immunostaining steps were performed as described (Dernburg, 2000). An anti-ABD-B antibody (DSHB, 1A2E9) was used together with Alexa Fluor® 488 anti-mouse IgG for visualizing the ABD-B protein in wilde-type or mutant embryos in the immunostaining steps following hybridization. To simultaneously label the nuclear envelop, a rabbit anti-lamin antibody (a gift from the Fisher Lab) was used in conjunction with Alexa Fluor® 647 goat anti-rabbit IgG.

Confocal microscopy of the FISH and immunostaining experiments was done using a Zeiss laser-scanning microscope (LSM 510 META). The distance between FISH signals were calculated using the distance measurement function of the Zeiss LSM image browser software.

ACKNOWLEDGEMENT

I wish to thank Drs. Parimal Majumder and Jeremy Boss for introducing me to the 3C technique; Sapna Patel for her help on cell-sulture insulator assays; Thao Le and Diana Houng for technical assistance with embryo microinjection; Dr. Nancy Manley and Pansy Bond for their assistance with confocal microscopy; Dr. Ping Shen for sharing instruments and useful discussion. I am grateful to Sapna Patel, Sharmila Roy and Kevin Liu for critical reading of the thesis. I also thank Haini Cai and my committee for invaluable guidance and discussions on this project. This work is supported by the NIH.

Figure 4.1 Chromosome Conformation Capture

(A) Schematic outline of the 3C technique. Colored lines represent DNA fragments. Restriction sites (blue bars), gene specific primers (colored arrows) and formaldehyde-induced crosslinks (thick black bars connecting DNA fragments) are indicated. Theoretical PCR results are depicted at the bottom of the flow chart. **(B)** A schematic of the procedure for generating the control template for 3C. The elements are similarly indicated as in (A). **(C)** An example of PCR products obtained from the crosslinked template, the non-crosslinked template and the control template.

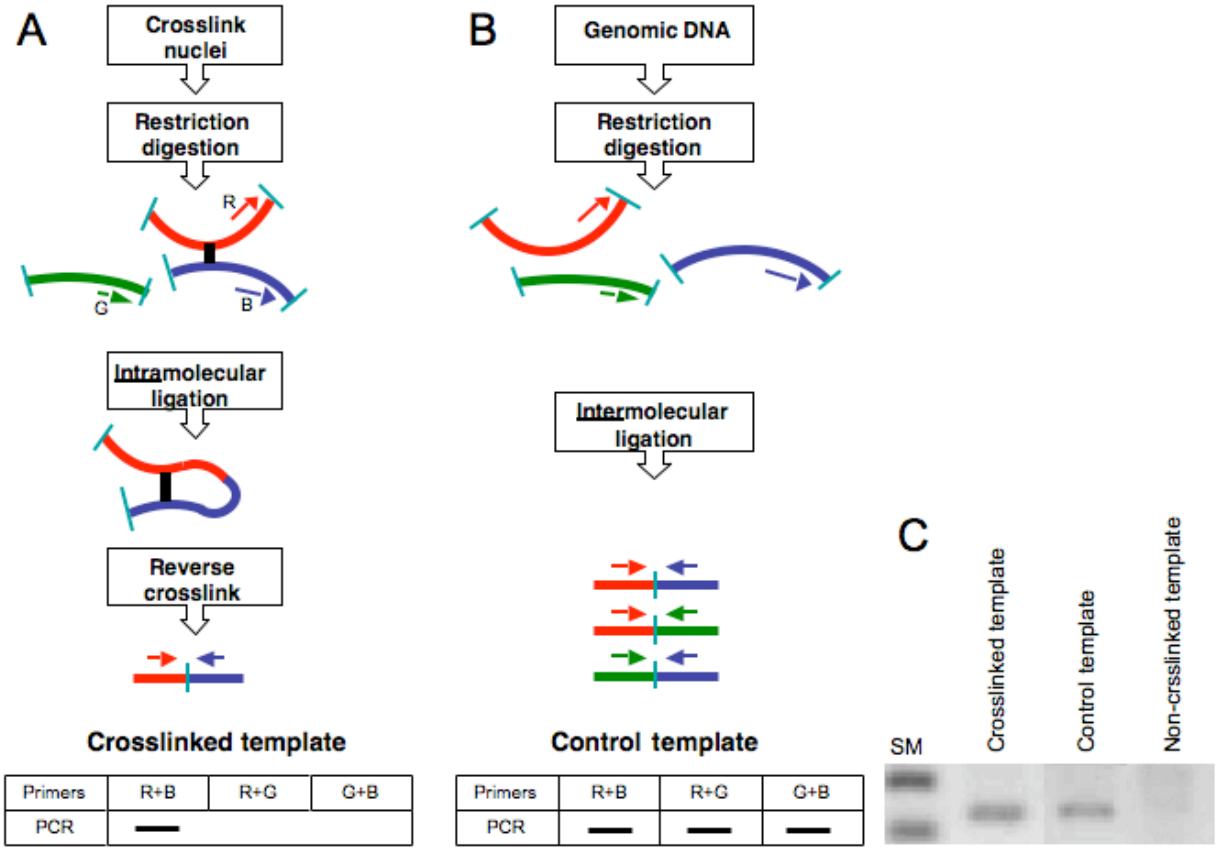

Crosslinked template

Primers	R+B	R+G	G+B
PCR	—		

Control template

Primers	R+B	R+G	G+B
PCR	—	—	—

Figure 4.2 Long-range interactions between SF-1 and genomic regions in ANT-C

(**A**) Relative crosslinking frequencies between fixed SF-1 EcoRI fragment and the *ftz-Antp* intergenic region. A schematic of the 50 kb genetic interval from the first exon of *Scr* to the last exon of *Antp* is drawn to scale at the bottom of the graph. The genes are depicted as solid colored boxes. Major cis-regulatory elements are indicated as checkerboard patterned boxes with the same color as the genes they belong to. The blue boxes with marked with Roman numerals (named SF2-I through SF2-V) are test DNA in a previous study. The distance indicated on the scale bar is to SF-1. EcoRI restriction sites are shown as short vertical bars above the scale bar. The position of the 2.3 kb EcoRI fragment that corresponds to SF-1 is marked by a red vertical line. The *y* axis is the relative crosslinking frequency. The *x* axis shows the position in the region. The height of the bars represents the relative crosslink frequency between SF-1 and the EcoRI fragments. The width of the bars reflects the length of the corresponding EcoRI fragment. The double-line break in a bar indicates that the value of relative crosslink frequency is too big to be display in the graph. The results were due to low PCR signals obtained from control template rather than high signals from crosslinked template. This may reflect a unresolved technical issue of the 3C method (Tolhuis et al., 2002). **(B)** Relative crosslinking frequencies between fixed SF-1 fragment and the *lab*, *Dfd* and *Antp* regions. The overlapping bars below the bar graph show the sub-fragments that were used in cell-culture and embryo enhancer-blocking assays.

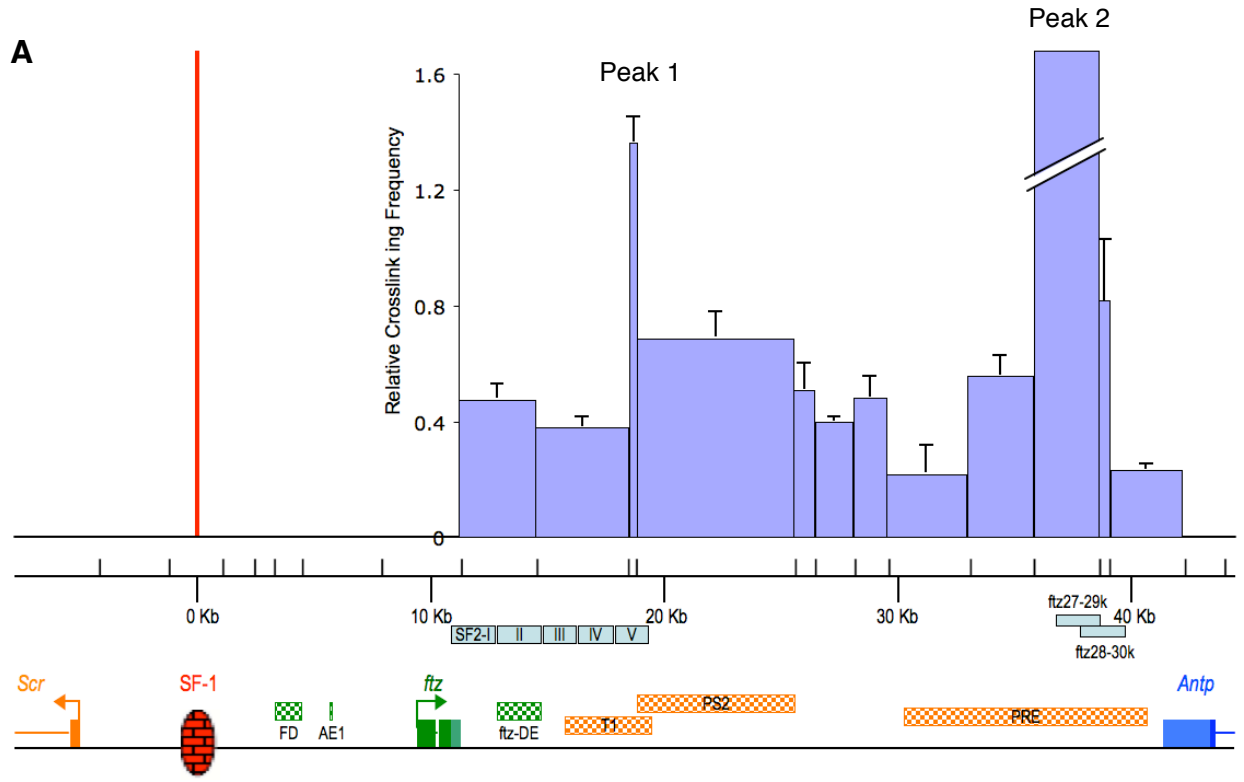
A
Peak 1
Peak 2
Relative Crosslink ing Frequency
1.6
1.2
0.8
0.4
0
0 Kb
10 Kb
20 Kb
30 Kb
40 Kb
SF2-I
II
III
IV
V
ftz27-29k
ftz28-30k
Scr
SF-1
FD
AE1
ftz
ftz-DE
T1
PS2
PRE
Antp

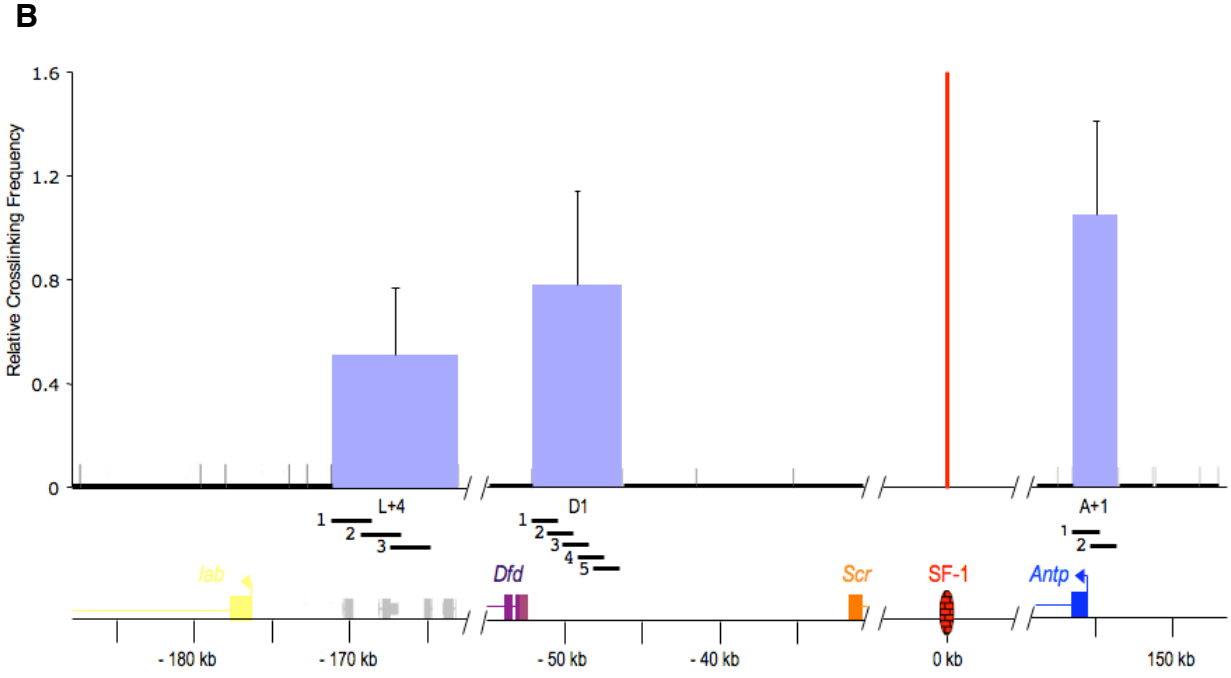
B
Relative Crosslinking Frequency
1.6
1.2
0.8
0.4
0
L+4
D1
A+1
lab
Dfd
Scr
SF-1
Antp
- 180 kb
- 170 kb
- 50 kb
- 40 kb
0 kb
150 kb

Figure 4.3 Enhancer-blocking activity of SF-1 interacting elements in ANT-C

(A) Schematic of the cell-culture enhancer-blocking test construct and summary of the enhancer-blocking test. **(B)** A schematic of the pEbNH enhancer-blocking test construct is shown on top. The reporter expression in blastoderm stage embryos is visualized by whole-mount *in situ* hybridization. The bar graph represents a quantitative assessment of the enhancer-blocking activity of the transgenes. The shades of blue from light to dark correspond to strong block, medium block, weak block and no block categories, which are separated according to the level of reporter expression. A photograph the embryo with the representative staining pattern is shown below each transgene. The NlambdaH transgene is a neutral spacer control, which contains a 1.4 kb spacer in between the nehancers. The NbbH transgene contains two tandem copies of the minimal enhancer-blocking activity of SF-1, SF-1b, and serves as a positive control. **(C)** Embryonic enhancer-blocking activity of SF2-I to V. A schematic of the transgene construct used to test enhancer-blocking activity. The *mini-white* reporter gene expression is visualized by whole-mount *in situ* hybridization in blastoderm stage embryos. The *in situ* hybridization of the endogenous *single-minded* gene, which is expressed in two ventral stripes of the embryo, is used as an internal control for staining. A quantitative assessment of the *mini-white* reporter expression in the *hairy* stripe 1 (H1) region is shown in the same bar graph format as in (B). A photograph showing the most frequently observed staining pattern is shown below each transgene. Please note that the SF2-II and SF2-III contain the ftz-DE enhancer, which represses the H1-driven reporter expression rather than blocks it.

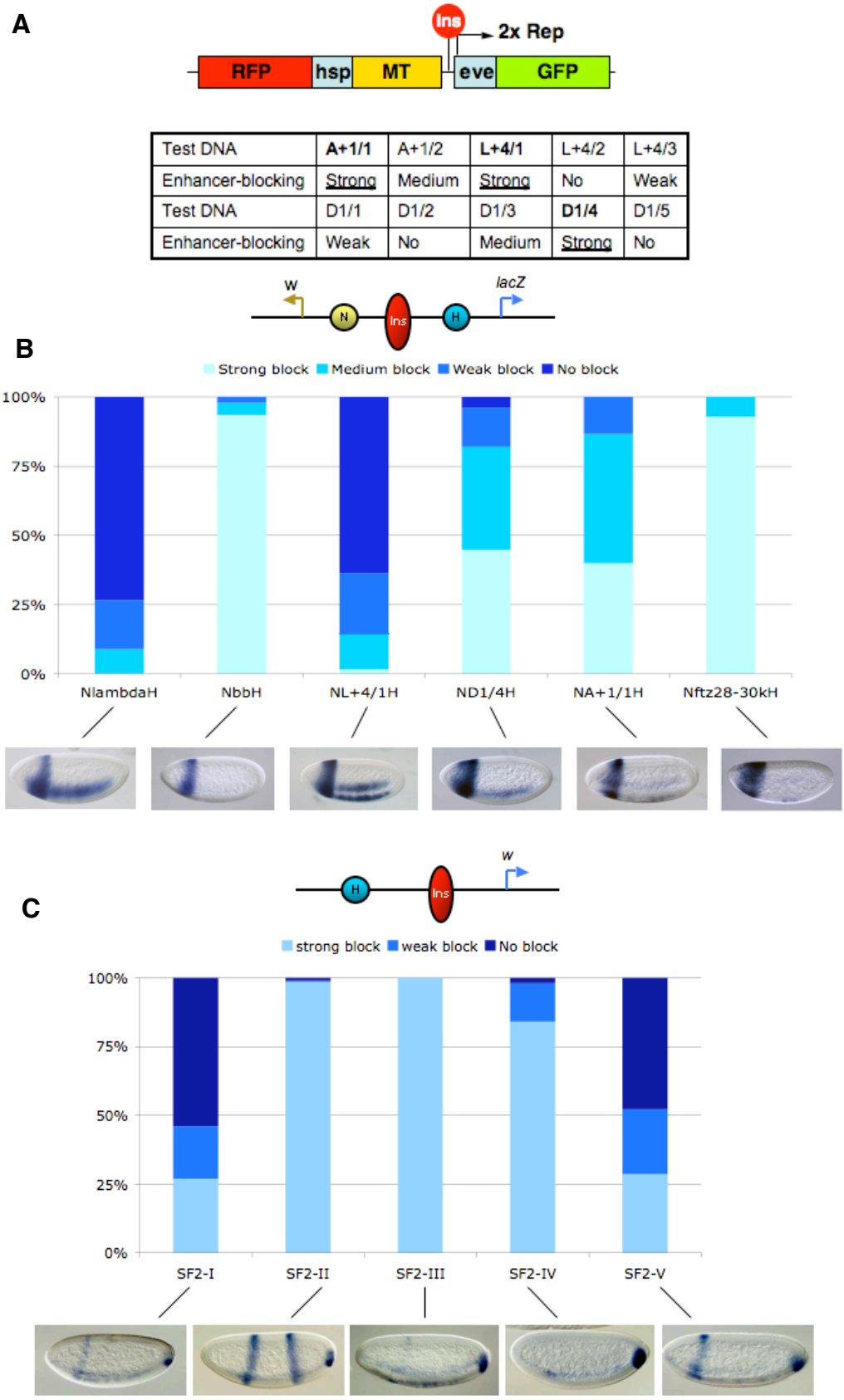
A
Ins
2x Rep
RFP
hsp
MT
eve
GFP
Test DNA | A+1/1 | A+1/2 | L+4/1 | L+4/2 | L+4/3
Enhancer-blocking | Strong | Medium | Strong | No | Weak
Test DNA | D1/1 | D1/2 | D1/3 | D1/4 | D1/5
Enhancer-blocking | Weak | No | Medium | Strong | No
w
lacZ
N
Ins
H
B
Strong block
Medium block
Weak block
No block
100%
75%
50%
25%
0%
NlambdaH
NbbH
NL+4/1H
ND1/4H
NA+1/1H
Nftz28-30kH
C
w
H
Ins
strong block
weak block
No block
100%
75%
50%
25%
0%
SF2-I
SF2-II
SF2-III
SF2-IV
SF2-V

Figure 4.4 Long-range interactions between the *Antp* promoter and genomic regions in *Drosophila* Hox gene complexes

A map of the genetic region is shown below each graph. The structure of Hox genes (colored) and non-Hox genes (grey) is indicated. Arrows mark the transcription start site of Hox genes. Distance to the *Antp* promoter is indicated on the scale. All EcoRI restriction sites are depicted as short vertical lines above the scale bar. **(A)** Relative crosslinking frequencies between fixed A+1 EcoRI fragment in the *Antp* promoter region and a 250 kb genomic region containing the other four Hox genes. Thick lines in the graph represent a value of zero. Yellow lines indicate no signals from both crosslinked template and control template. Red lines indicate that signals were obtained from crosslinked template, control template as well as the non-crosslinked template. **(B)** Relative crosslinking frequencies between fixed A+1 EcoRI fragment and a 40 kb region surrounding the *Abd-Bm* gene.

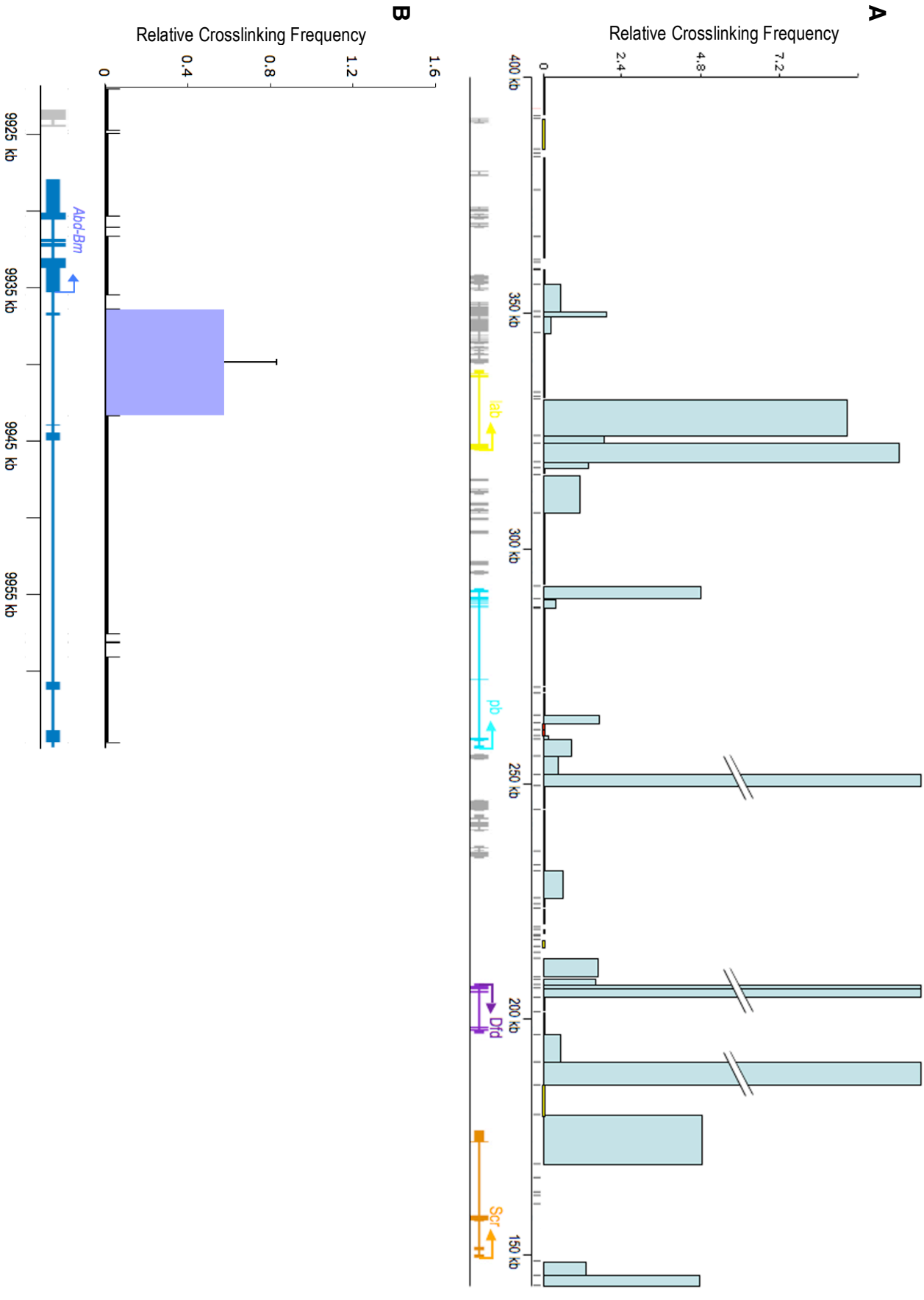
A
Relative Crosslinking Frequency
0
2.4
4.8
7.2
400 kb
350 kb
300 kb
250 kb
200 kb
150 kb
lab
pb
Dfd
Scr
B
Relative Crosslinking Frequency
0
0.4
0.8
1.2
1.6
9925 kb
9935 kb
9945 kb
9955 kb
Abd-Bm

Figure 4.5 Co-localization of the *Antp* and SF-1 loci as revealed by 3D FISH

A schematic showing the location of FISH probes is depicted on top of each graph. **(A)** Hybridization of wild-type embryos with Cy3-dUTP-labeled SF-1 probe (red) for the SF-1 locus and digoxigenin(DIG)-dUTP-labeled *Antp* probe for the *Antp* promoter region. The *Antp* probe was visualized by staining with an anti-DIG-FITC antibody (green). The outline of individual nucleus was determined from a DIC image of the same confocal section and depicted as ovals in the picture. White arrowheads indicate co-localization of the two probes. **(B)** Hybridization of wild-type embryos with Cy5-dUTP-labeled Antp+140k probe (blue) and DIG-dUTP-labeled *Antp* probe. **(C)** Quantitative representation of inter-probe distance (solid bars) and co-localization frequency (hatched bars) of the *Antp* and SF-1 loci (blue) and that of the *Antp* and Antp+140k loci (red) in T1 and T2 of *Drosophila* embryos.

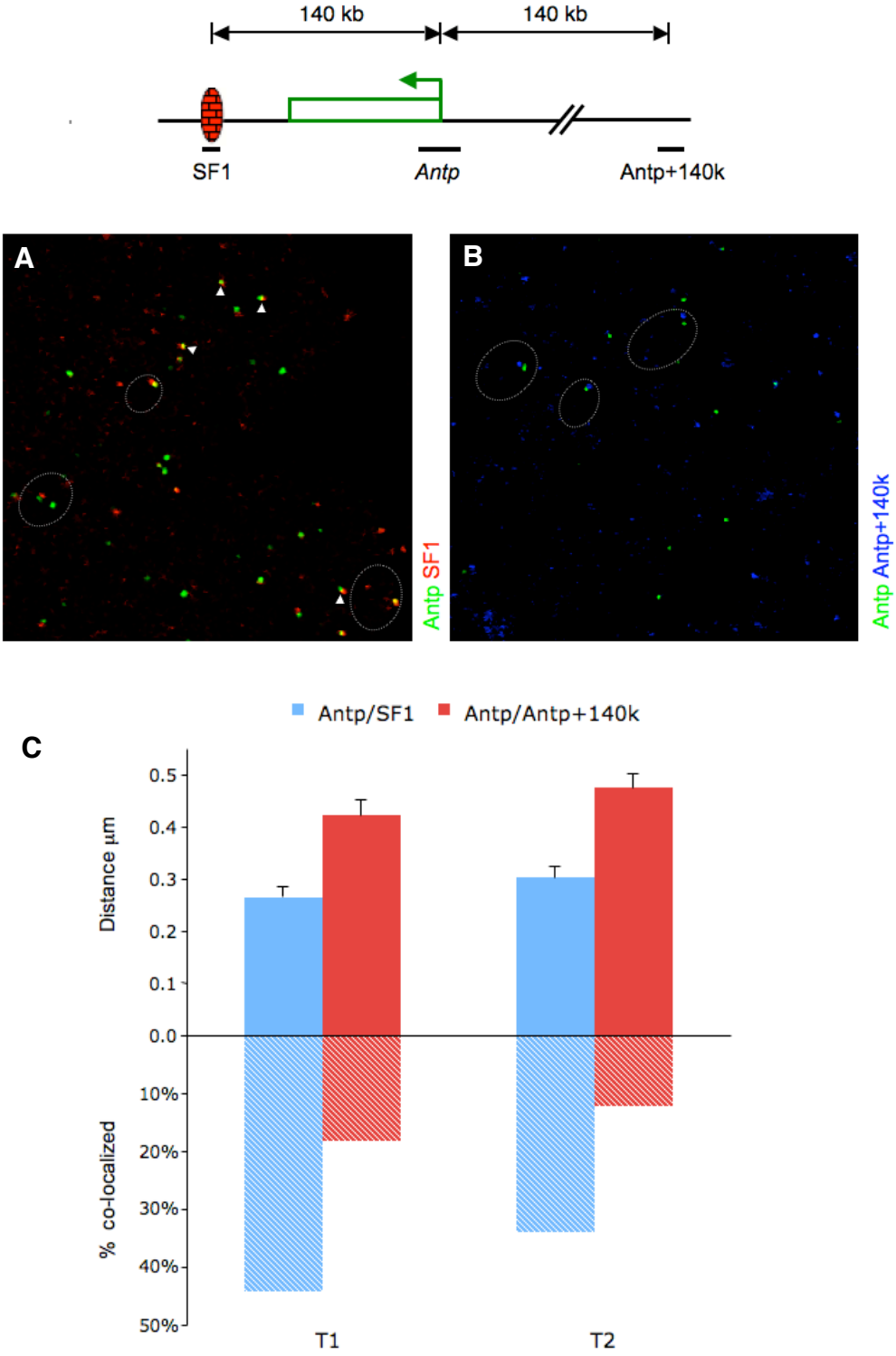
140 kb
140 kb
SF1
Antp
Antp+140k
A
B
Antp SF1
Antp Antp+140k
C
Antp/SF1
Antp/Antp+140k
Distance µm
% co-localized
0.5
0.4
0.3
0.2
0.1
0.0
10%
20%
30%
40%
50%
T1
T2

Figure 4.6 Co-localization of the *Antp* and *lab* loci as revealed by 3D FISH

(A) Hybridization of wild-type embryos with Cy3-dUTP-labelled *Antp* probe (red), DIG-dUTP-labeled *lab* probe (green) and Cy5-dUTP-labeled SF-1 probe (blue). **(B)** Hybridization of wild-type embryos with Cy3-dUTP-labeled *Antp* probe (red) and Cy5-dUTP-labeled Antp+330k probe (blue). **(C)** Hybridization of wild-type imaginal discs with Cy3-dUTP-labeled *Antp* probe (red) and DIG-dUTP-labeled *lab* probe (green). To simultaneously label the nuclear envelop, a rabbit anti-lamin antibody (a gift from the Fisher Lab) was used in conjunction with Alexa Fluor® 647 goat anti-rabbit IgG (blue). **(D)** Hybridization of wild-type imaginal discs with Cy3-dUTP-labeled *Antp* probe (red) and DIG-dUTP-labeled Antp+330k probe (green). Nuclear envelop was labeled blue. **(E)** Quantitative representation of inter-probe distance (solid bars) and co-localization frequency (hatched bars) of the *Antp* and *lab* loci (orange) and that of the *Antp* and Antp+330k loci (green) in T1 and T2 of *Drosophila* embryos. ND, not done.

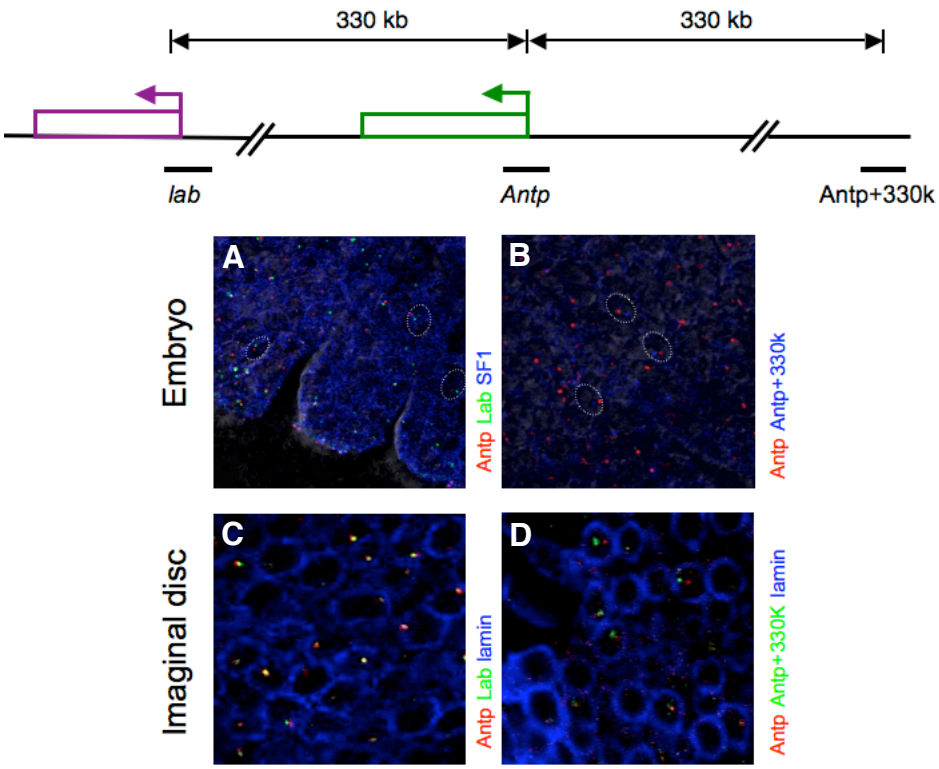
330 kb
330 kb
lab
Antp
Antp+330k
A
B
C
D
Embryo
Imaginal disc
Antp Lab SF1
Antp Antp+330k
Antp Lab lamin
Antp Antp+330K lamin

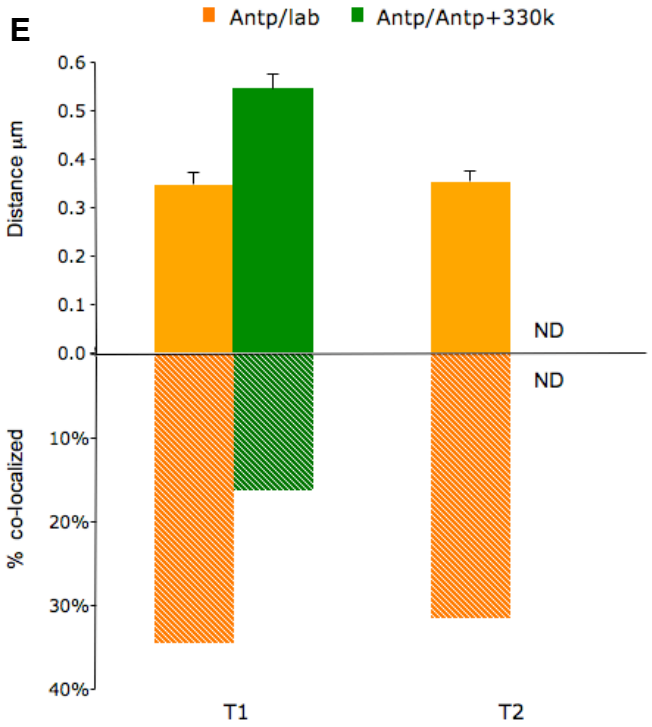
E
Antp/lab
Antp/Antp+330k
Distance µm
% co-localized
0.6
0.5
0.4
0.3
0.2
0.1
0.0
10%
20%
30%
40%
ND
ND
T1
T2

Figure 4.7 Interaction between *Antp* and *Abd-B* is developmentally regulated

(A) Hybridization of wild-type embryos with Cy3-dUTP-labelled *Abd-B* probe (red) and Cy5-dUTP-labeled *Antp* probe (blue). **(B)** Hybridization of wild-type imaginal discs with Cy3-dUTP-labelled *Abd-B* probe (red) and DIG-dUTP-labeled *Antp* probe (blue). **(C)** Hybridization of *Pc*$^{-}$ embryos with Cy3-dUTP-labelled *Antp* probe (red) and Cy5-dUTP-labeled *Abd-B* probe (blue). **(D)** Localization of the ABD-B protein in wild-type embryos. The ABD-B protein was visualized using an anti-ABD-B monoclonal antibody in conjunction with Alexa Fluor® 488 anti-mouse IgG. The photograph is an overlay of the green fluorescence channel and the DIC channel, which shows the segments of the embryo. Arrowheads indicate the position of T1 and A8. **(E)** Localization of the ABD-B protein in *Pc*$^{-}$ embryos. **(F)** Quantitative representation of inter-probe distance (solid bars) and co-localization frequency (hatched bars) of the *Antp* and *Abd-B* loci in T1 ((light blue), T2 (intermidiate shade of blue), and A8 (dark blue), of wild-type embryos, wild-type imaginal discs and *Pc*$^{-}$ embryos.

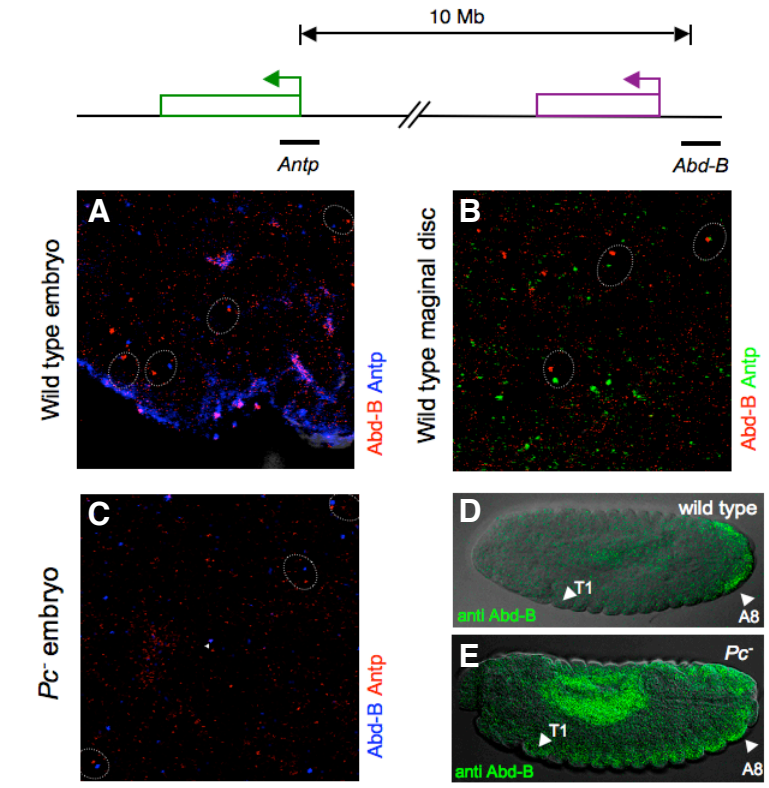
10 Mb
Antp
Abd-B
A
Wild type embryo
Abd-B Antp
B
Wild type maginal disc
Abd-B Antp
C
Pc- embryo
Abd-B Antp
D
wild type
T1
anti Abd-B
A8
E
Pc-
T1
anti Abd-B
A8

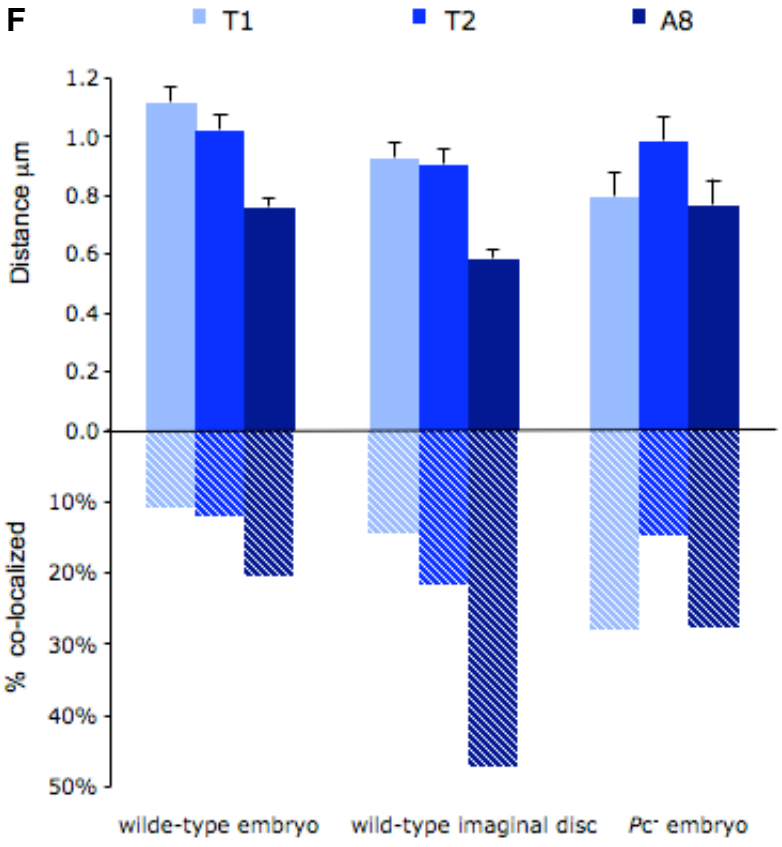
F
T1
T2
A8
Distance µm
1.2
1.0
0.8
0.6
0.4
0.2
0.0
% co-localized
10%
20%
30%
40%
50%
wilde-type embryo
wild-type imaginal disc
Pc- embryo

CHAPTER 5

CONCLUSION

My work has focused on understanding the biological function and molecular mechanism of chromatin boundaries, especially in the *Drosophila* Hox gene complexes. Chromatin boundaries or insulators partition the genome into structurally and functionally autonomous domains. The su(Hw) insulator is one of the best characterized *Drosophila* insulators. However, little is known about the mechanism underlying its insulator activity. Increasing evidence suggests that insulators may function via interactions with other insulators in the genome. For example, our group found that two tandem suHw insulators abolish the enhancer-blocking activity of each other, suggesting that interactions between neighboring insulators may be important for enhancer-blocking, and that tandem repeats preclude such interactions. This notion is supported by the observation that the su(Hw) insulator proteins, SUHW and MOD(MDG4), are found to co-localize at hundreds of sites on polytene chromosomes, but only appear in about 20 nuclear loci at the nuclear periphery. Further, the *gypsy* retrotransposon, which contains the 340 bp SUHW binding site, has also been found to locate to these peripheral loci. Based on these observations it was proposed that the function of su(Hw) depends on its localization to the nuclear periphery. To investigate whether tethering of su(Hw) insulator to the nuclear periphery is necessary or sufficient for its enhancer-blocking function, we visualized the nuclear location of transgenes that

contains either single-copy functional insulator or tandem-copy non-functional insulators. Using fluorescent in situ hybridization (FISH), we show that transgenes containing the su(Hw) insulator(s) do not preferentially localize near nuclear periphery. Immunostainings show that SUHW and MOD(MDG4) are not restricted to the nuclear periphery. Additionally, the enhancer-blocking activity of su(Hw) remains intact during heat shock, which disrupts the cluster of insulator proteins at nuclear periphery. Our data show that su(Hw) can function in the nuclear interior, possibly through interactions with other insulators or nuclear structures.

SF-1, an insulator our group discovered in the Drosophila Hox gene cluster, *Antennapedia* complex (ANT-C), is used as a model to investigate how endogenous insulators regulate gene expression. SF-1 is located in the intergenic region between the Hox gene *Sex comb reduced (Scr)*, and the non-homeotic gene *fushi tarazu (ftz)* in ANT-C. We hypothesize that SF-1 plays three roles to ensure the independent regulation of *ftz* and the neighboring *Scr* and *Antp* Hox genes. 1. It blocks *ftz* and *Scr* enhancers from influencing the neighboring promoters; 2. It interacts with other boundary-like elements located downstream of the *ftz* gene to form an independent chromatin loop domain that protects the *ftz* gene from Polycomb-mediated gene silencing known to be essential for the Hox gene regulation; and 3. The loop formation facilitates the distal *Scr* enhancers.

To understand the biological function and molecular mechanism of SF-1, I studied the trans factors of SF-1 using a novel cell-based enhancer-blocking assay, and searched for cis-elements that interact with SF-1 using the Chromosome Conformation

Capture (3C) method. Using a cell-based insulator assay, we show that Ebx/NURF301 and Iswi modulate the activity of multiple Drosophila insulators including SF-1, su(Hw), Fab-7 and Fab-8. Reduced level of Ebx/NURF301 or Iswi also disrupts the enhancer-blocking activity of SF1 and su(Hw) in transgenic embryos. Our findings provide the first evidence that a nucleosome-remodeling complex participates in the enhancer-blocking mechanism of insulators. It also suggests that diverse types of *Drosophila* insulators, previously known to depend on distinct cis and trans components, share a common mechanism that can mobilize nucleosomes and create open and flexible chromatin.

I used the Chromosome Conformation Capture (3C) technique in ANT-C to search for cis-elements that could interact with SF-1. First, we find that SF-1 interacts with two regions downstream of *ftz*, both of which are closely associated with a novel enhancer-blocking activity. Our data suggest that SF-1 forms chromatin loops with two insulators downstream of *ftz*, separating regulatory elements of *Scr*, *ftz* and *Antp* into independent domains; and the loop formation may shorten the effective distance between the Scr promoter and its distal regulatory elements such as enhancers or PREs, therefore facilitating their function. Second, we find that SF-1 interacts with additional sequences in the *lab, Dfd* and *Antp* regulatory regions. Furthermore, most of these sequences contain novel enhancer-blocking activity. Our data provide the first evidence of an insulator participating in multiple long-range regulatory interactions in the *Drosophila* Hox gene complex. This suggests that SF-1 may be involved in the regulation of other Hox genes in ANT-C through interactions with novel boundaries in addition to its function in the *Scr-ftz* region.

To gain insights into the genomic organization of Drosophila Hox complexes, I used the 3C and FISH technique to probe long-range interactions between Hox genes. We find that the *lab* and *Antp* gene in ANT-C are closely associated with each other inside the nucleus despite the large linear distance. We also detect an interaction between promoter regions of *Antp* in ATN-C and *Abd-B* in BX-C. We further show that the interaction between the *Antp* and *Abd-B* loci is developmentally regulated. It occurs in posterior tissues, where both genes are expressed, or in tissues where both genes are ectopically activated due to mutations in the Polycomb group proteins. This is the first documented example of a developmentally regulated, long-range physical interaction between Hox clusters. Our data suggest that the coordinated expression of Hox genes may require physical proximity of the key regulatory elements of these genes.

Interaction between co-regulated genes is not unique to Hox gene clusters. Recent studies have suggested that it may be a common phenomenon found in many complex genetic loci that contain co-regulated genes, such as the *β-globin* genes, the olfactory receptor genes and the T_H1 and T_H2 cytokine genes. The combinatorial approach of 3C, 3D FISH and transgenic analyses described here is therefore highly valuable for studying this previously under-explored aspect of gene regulation in many development processes.

The findings presented in this dissertation support the looping model of insulator function, which proposes that insulators function by interacting with each other. Interactions between insulators may influence gene transcription in multiple ways,

including separating genes into independent chromatin loop domains, bringing distant genes together to be co-regulated and facilitating or repressing transcription by localizing genes in special nuclear compartments. Our data also demonstrate that interactions between insulators are not only involved in local gene regulation, but also important for coordinating the regulation of distant genomic loci. Future experiments aimed at identifying the protein factors that facilitate interactions between insulators should provide deeper insights into how these interactions regulate gene expression.

REFERENCES

Ameres, S.L., Drueppel, L., Pfleiderer, K., Schmidt, A., Hillen, W., and Berens, C. (2005). Inducible DNA-loop formation blocks transcriptional activation by an SV40 enhancer. Embo J *24*, 358-367.

Antes, T.J., Namciu, S.J., Fournier, R.E., and Levy-Wilson, B. (2001). The 5' boundary of the human apolipoprotein B chromatin domain in intestinal cells. Biochemistry *40*, 6731-6742.

Ashe, H.L., Monks, J., Wijgerde, M., Fraser, P., and Proudfoot, N.J. (1997). Intergenic transcription and transinduction of the human beta-globin locus. Genes Dev *11*, 2494-2509.

Avramova, Z., and Tikhonov, A. (1999). Are scs and scs' 'neutral' chromatin domain boundaries of the locus? Trends Genet *15*, 138-139.

Babu, P., Selvakumar, K.S., and Bhosekar, S. (1987). Studies on transvection at the bithorax complex in Drosophila melanogaster. Mol Gen Genet *210*, 557-563.

Badenhorst, P., Voas, M., Rebay, I., and Wu, C. (2002). Biological functions of the ISWI chromatin remodeling complex NURF. Genes Dev *16*, 3186-3198.

Barges, S., Mihaly, J., Galloni, M., Hagstrom, K., Muller, M., Shanower, G., Schedl, P., Gyurkovics, H., and Karch, F. (2000). The Fab-8 boundary defines the distal limit of the bithorax complex iab-7 domain and insulates iab-7 from initiation elements and a PRE in the adjacent iab-8 domain. Development *127*, 779-790.

Barolo, S., Castro, B., and Posakony, J.W. (2004). New Drosophila transgenic reporters: insulated P-element vectors expressing fast-maturing RFP. Biotechniques *36*, 436-440, 442.

Bell, A.C., and Felsenfeld, G. (2000). Methylation of a CTCF-dependent boundary controls imprinted expression of the Igf2 gene. Nature *405*, 482-485.

Bell, A.C., West, A.G., and Felsenfeld, G. (1999). The protein CTCF is required for the enhancer blocking activity of vertebrate insulators. Cell *98*, 387-396.

Belmont, A.S. (2001). Visualizing chromosome dynamics with GFP. Trends Cell Biol *11*, 250-257.

Belozerov, V.E., Majumder, P., Shen, P., and Cai, H.N. (2003a). A novel boundary element may facilitate independent gene regulation in the Antennapedia complex of Drosophila. Embo J *22*, 3113-3121.

Belozerov, V.E., Majumder, P., Shen, P., and Cai, H.N. (2003b). A novel boundary element may facilitate independent gene regulation in the Antennapedia Complex of Drosophila. EMBO J *22*.

Belozerov, V.E., P. Majumder, P. Shen and H.N. Cai (2003). A novel boundary element may facilitate independent gene regulation in the Antennapedia complex of Drosophila. The EMBO Journal *22*, 3113-3121.

Bevis, B.J., and Glick, B.S. (2002). Rapidly maturing variants of the Discosoma red fluorescent protein (DsRed). Nat Biotechnol *20*, 83-87.

Bi, X., and Broach, J.R. (1999). UASrpg can function as a heterochromatin boundary element in yeast. Genes Dev *13*, 1089-1101.

Bi, X., and Broach, J.R. (2001). Chromosomal boundaries in S. cerevisiae. Curr Opin Genet Dev *11*, 199-204.

Blanton, J., Gaszner, M., and Schedl, P. (2003). Protein:protein interactions and the pairing of boundary elements in vivo. Genes Dev *17*, 664-675.

Boutros, M., Kiger, A.A., Armknecht, S., Kerr, K., Hild, M., Koch, B., Haas, S.A., Consortium, H.F., Paro, R., and Perrimon, N. (2004). Genome-wide RNAi analysis of growth and viability in Drosophila cells. Science *303*, 832-835.

Bunch, T.A., Grinblat, Y., and Goldstein, L.S. (1988). Characterization and use of the Drosophila metallothionein promoter in cultured Drosophila melanogaster cells. Nucleic Acids Res *16*, 1043-1061.

Busturia, A., Lloyd, A., Bejarano, F., Zavortink, M., Xin, H., and Sakonju, S. (2001). The MCP silencer of the Drosophila Abd-B gene requires both Pleiohomeotic and GAGA factor for the maintenance of repression. Development *128*, 2163-2173.

Cai, H., Kiefel, P., Yee, J., and Duncan, I. (1994). A yeast artificial chromosome clone map of the Drosophila genome. Genetics *136*, 1385-1399.

Cai, H., and Levine, M. (1995). Modulation of enhancer-promoter interactions by insulators in the Drosophila embryo. Nature *376*, 533-536.

Cai, H.N. (2006). Function and mechanism of chromatin boundaries. In Gene Expression and Regulation, J. Ma, ed. (Beijing, Higher Education Press).

Cai, H.N., and Levine, M. (1997). The gypsy insulator can function as a promoter-specific silencer in the Drosophila embryo. EMBO J *16*, 1732-1741.

Cai, H.N., and Shen, P. (2001). Effects of cis arrangement of chromatin insulators on enhancer-blocking activity. Science *291*, 493-495.

Cai, H.N., Zhang, Z., Adams, J.R., and Shen, P. (2001). Genomic context modulates insulator activity through promoter competition. Development *128*, 4339-4347.

Calhoun, V.C., and Levine, M. (2003). Long-range enhancer-promoter interactions in the Scr-Antp interval of the Drosophila Antennapedia complex. Proc Natl Acad Sci U S A *100*, 9878-9883.

Calvi, B.R., and Spradling, A.C. (2001). The nuclear location and chromatin organization of active chorion amplification origins. Chromosoma *110*, 159-172.

Caplen, N.J., Fleenor, J., Fire, A., and Morgan, R.A. (2000). dsRNA-mediated gene silencing in cultured Drosophila cells: a tissue culture model for the analysis of RNA interference. Gene *252*, 95-105.

Celniker, S.E., and Drewell, R.A. (2007). Chromatin looping mediates boundary element promoter interactions. Bioessays *29*, 7-10.

Chambeyron, S., and Bickmore, W.A. (2004). Chromatin decondensation and nuclear reorganization of the HoxB locus upon induction of transcription. Genes Dev *18*, 1119-1130.

Chambeyron, S., Da Silva, N.R., Lawson, K.A., and Bickmore, W.A. (2005). Nuclear re-organisation of the Hoxb complex during mouse embryonic development. Development *132*, 2215-2223.

Chen, Q., Lin, L., Smith, S., Lin, Q., and Zhou, J. (2005). Multiple Promoter Targeting Sequences exist in Abdominal-B to regulate long-range gene activation. Developmental biology *286*, 629-636.

Cheng, L.W., Viala, J.P., Stuurman, N., Wiedemann, U., Vale, R.D., and Portnoy, D.A. (2005). Use of RNA interference in Drosophila S2 cells to identify host pathways controlling compartmentalization of an intracellular pathogen. Proc Natl Acad Sci U S A *102*, 13646-13651.

Chernukhin, I., Shamsuddin, S., Kang, S.Y., Bergstrom, R., Kwon, Y.W., Yu, W., Whitehead, J., Mukhopadhyay, R., Docquier, F., Farrar, D.*, et al.* (2007). CTCF interacts with and recruits the largest subunit of RNA polymerase II to CTCF target sites genome-wide. Mol Cell Biol *27*, 1631-1648.

Chubb, J.R., and Bickmore, W.A. (2003). Considering nuclear compartmentalization in the light of nuclear dynamics. Cell *112*, 403-406.

Chubb, J.R., Boyle, S., Perry, P., and Bickmore, W.A. (2002). Chromatin motion is constrained by association with nuclear compartments in human cells. Curr Biol *12*, 439-445.

Chung, J.H., Whiteley, M., and Felsenfeld, G. (1993). A 5' element of the chicken beta-globin domain serves as an insulator in human erythroid cells and protects against position effect in Drosophila. Cell *74*, 505-514.

Cleard, F., Moshkin, Y., Karch, F., and Maeda, R.K. (2006). Probing long-distance regulatory interactions in the Drosophila melanogaster bithorax complex using Dam identification. Nat Genet *38*, 931-935.

Cremer, T., and Cremer, C. (2001). Chromosome territories, nuclear architecture and gene regulation in mammalian cells. Nat Rev Genet *2*, 292-301.

Cremer, T., Kreth, G., Koester, H., Fink, R.H., Heintzmann, R., Cremer, M., Solovei, I., Zink, D., and Cremer, C. (2000). Chromosome territories, interchromatin domain compartment, and nuclear matrix: an integrated view of the functional nuclear architecture. Crit Rev Eukaryot Gene Expr *10*, 179-212.

Croft, J.A., Bridger, J.M., Boyle, S., Perry, P., Teague, P., and Bickmore, W.A. (1999). Differences in the localization and morphology of chromosomes in the human nucleus. J Cell Biol *145*, 1119-1131.

Dearolf, C.R., Topol, J., and Parker, C.S. (1989). Transcriptional control of Drosophila fushi tarazu zebra stripe expression. Genes Dev *3*, 384-398.

Dearolf, C.R., Topol, J., and Parker, C.S. (1990). Transcriptional regulation of the Drosophila segmentation gene fushi tarazu (ftz). Bioessays *12*, 109-113.

Dekker, J. (2006). The three 'C' s of chromosome conformation capture: controls, controls, controls. Nature methods *3*, 17-21.

Dekker, J., Rippe, K., Dekker, M., and Kleckner, N. (2002). Capturing chromosome conformation. Science *295*, 1306-1311.

Dernburg, A.F. (2000). In situ hybridization to somatic chromosoes, Vol 1, 1 edn (CSHL, New York, CSHL Press).

Dernburg, A.F., Daily, D.R., Yook, K.J., Corbin, J.A., Sedat, J.W., and Sullivan, W. (1996). Selective loss of sperm bearing a compound chromosome in the Drosophila female. Genetics *143*, 1629-1642.

Deuring, R., Fanti, L., Armstrong, J.A., Sarte, M., Papoulas, O., Prestel, M., Daubresse, G., Verardo, M., Moseley, S.L., Berloco, M.*, et al.* (2000). The ISWI chromatin-remodeling protein is required for gene expression and the maintenance of higher order chromatin structure in vivo. Mol Cell *5*, 355-365.

Dillon, N., and Festenstein, R. (2002). Unravelling heterochromatin: competition between positive and negative factors regulates accessibility. Trends Genet *18*, 252-258.

Donze, D., Adams, C.R., Rine, J., and Kamakaka, R.T. (1999). The boundaries of the silenced HMR domain in Saccharomyces cerevisiae. Genes Dev *13*, 698-708.

Donze, D., and Kamakaka, R.T. (2001). RNA polymerase III and RNA polymerase II promoter complexes are heterochromatin barriers in Saccharomyces cerevisiae. Embo J *20*, 520-531.

Dorsett, D. (1993). Distance-independent inactivation of an enhancer by the suppressor of Hairy-wing DNA-binding protein of Drosophila. Genetics *134*, 1135-1144.

Dorsett, D. (1999). Distant liaisons: long-range enhancer-promoter interactions in Drosophila. Curr Opin Genet Dev *9*, 505-514.

Dunn, K.L., Zhao, H., and Davie, J.R. (2003). The insulator binding protein CTCF associates with the nuclear matrix. Exp Cell Res *288*, 218-223.

Elefant, F., Cooke, N.E., and Liebhaber, S.A. (2000a). Targeted recruitment of histone acetyltransferase activity to a locus control region. J Biol Chem *275*, 13827-13834.

Elefant, F., Su, Y., Liebhaber, S.A., and Cooke, N.E. (2000b). Patterns of histone acetylation suggest dual pathways for gene activation by a bifunctional locus control region. Embo J *19*, 6814-6822.

Elfring, L.K., Deuring, R., McCallum, C.M., Peterson, C.L., and Tamkun, J.W. (1994). Identification and characterization of Drosophila relatives of the yeast transcriptional activator SNF2/SWI2. Mol Cell Biol *14*, 2225-2234.

Ferrari, S., Simmen, K.C., Dusserre, Y., Muller, K., Fourel, G., Gilson, E., and Mermod, N. (2004). Chromatin domain boundaries delimited by a histone-binding protein in yeast. J Biol Chem *279*, 55520-55530.

Feuerbach, F., Galy, V., Trelles-Sticken, E., Fromont-Racine, M., Jacquier, A., Gilson, E., Olivo-Marin, J.C., Scherthan, H., and Nehrbass, U. (2002). Nuclear architecture and spatial positioning help establish transcriptional states of telomeres in yeast. Nat Cell Biol *4*, 214-221.

Filippova, G.N., Cheng, M.K., Moore, J.M., Truong, J.P., Hu, Y.J., Nguyen, D.K., Tsuchiya, K.D., and Disteche, C.M. (2005). Boundaries between chromosomal domains of X inactivation and escape bind CTCF and lack CpG methylation during early development. Developmental cell *8*, 31-42.

Fyodorov, D.V., Blower, M.D., Karpen, G.H., and Kadonaga, J.T. (2004). Acf1 confers unique activities to ACF/CHRAC and promotes the formation rather than disruption of chromatin in vivo. Genes Dev *18*, 170-183.

Galloni, M., Gyurkovics, H., Schedl, P., and Karch, F. (1993). The bluetail transposon: evidence for independent cis-regulatory domains and domain boundaries in the bithorax complex. Embo J *12*, 1087-1097.

Galy, V., Olivo-Marin, J.C., Scherthan, H., Doye, V., Rascalou, N., and Nehrbass, U. (2000). Nuclear pore complexes in the organization of silent telomeric chromatin. Nature *403*, 108-112.

Gasser, S.M. (2002). Visualizing chromatin dynamics in interphase nuclei. Science *296*, 1412-1416.

Gaszner, M., and Felsenfeld, G. (2006). Insulators: exploiting transcriptional and epigenetic mechanisms. Nat Rev Genet *7*, 703-713.

Gause, M., Morcillo, P., and Dorsett, D. (2001). Insulation of enhancer-promoter communication by a gypsy transposon insert in the Drosophila cut gene: cooperation between suppressor of hairy-wing and modifier of mdg4 proteins. Mol Cell Biol *21*, 4807-4817.

Gerasimova, T.I., Byrd, K., and Corces, V.G. (2000). A chromatin insulator determines the nuclear localization of DNA. Mol Cell *6*, 1025-1035.

Gerasimova, T.I., and Corces, V.G. (1998). Polycomb and trithorax group proteins mediate the function of a chromatin insulator. Cell *92*, 511-521.

Gerasimova, T.I., and Corces, V.G. (2001). Chromatin insulators and boundaries: effects on transcription and nuclear organization. Annu Rev Genet *35*, 193-208.

Gerasimova, T.I., Gdula, D.A., Gerasimov, D.V., Simonova, O., and Corces, V.G. (1995). A Drosophila protein that imparts directionality on a chromatin insulator is an enhancer of position-effect variegation. Cell *82*, 587-597.

Geyer, P.K. (1997a). The role of insulator elements in defining domains of gene expression. Curr Opin Genet Dev *7*, 242-248.

Geyer, P.K. (1997b). The role of insulator elements in defining domains of gene expression. Curr Opin Genet Dev *7*, 242-248.

Geyer, P.K., and Clark, I. (2002). Protecting against promiscuity: the regulatory role of insulators. Cell Mol Life Sci *59*, 2112-2127.

Geyer, P.K., and Corces, V.G. (1987). Separate regulatory elements are responsible for the complex pattern of tissue-specific and developmental transcription of the yellow locus in Drosophila melanogaster. Genes Dev *1*, 996-1004.

Gindhart, J.G., Jr., and Kaufman, T.C. (1995). Identification of Polycomb and trithorax group responsive elements in the regulatory region of the Drosophila homeotic gene Sex combs reduced. Genetics *139*, 797-814.

Gomez, J.A., Majumder, P., Nagarajan, U.M., and Boss, J.M. (2005). X box-like sequences in the MHC class II region maintain regulatory function. J Immunol *175*, 1030-1040.

Gorman, M.J., and Kaufman, T.C. (1995). Genetic analysis of embryonic cis-acting regulatory elements of the Drosophila homeotic gene sex combs reduced. Genetics *140*, 557-572.

Gribnau, J., Diderich, K., Pruzina, S., Calzolari, R., and Fraser, P. (2000). Intergenic transcription and developmental remodeling of chromatin subdomains in the human beta-globin locus. Mol Cell *5*, 377-386.

Grunstein, M. (1998). Yeast heterochromatin: regulation of its assembly and inheritance by histones. Cell *93*, 325-328.

Gruzdeva, N., Kyrchanova, O., Parshikov, A., Kullyev, A., and Georgiev, P. (2005). The Mcp Element from the bithorax Complex Contains an Insulator That Is Capable of Pairwise Interactions and Can Facilitate Enhancer-Promoter Communication. Mol Cell Biol *25*, 3682-3689.

Gyurkovics, H., Gausz, J., Kummer, J., and Karch, F. (1990). A new homeotic mutation in the Drosophila bithorax complex removes a boundary separating two domains of regulation. Embo J *9*, 2579-2585.

Haber, J.E. (1998). Mating-type gene switching in Saccharomyces cerevisiae. Annu Rev Genet *32*, 561-599.

Hagstrom, K., Muller, M., and Schedl, P. (1996). Fab-7 functions as a chromatin domain boundary to ensure proper segment specification by the Drosophila bithorax complex. Genes Dev *10*, 3202-3215.

Hammond, S.M., Bernstein, E., Beach, D., and Hannon, G.J. (2000). An RNA-directed nuclease mediates post-transcriptional gene silencing in Drosophila cells. Nature *404*, 293-296.

Hark, A.T., Schoenherr, C.J., Katz, D.J., Ingram, R.S., Levorse, J.M., and Tilghman, S.M. (2000). CTCF mediates methylation-sensitive enhancer-blocking activity at the H19/Igf2 locus. Nature *405*, 486-489.

Heun, P., Taddei, A., and Gasser, S.M. (2001). From snapshots to moving pictures: new perspectives on nuclear organization. Trends Cell Biol *11*, 519-525.

Ho, Y., Elefant, F., Cooke, N., and Liebhaber, S. (2002). A defined locus control region determinant links chromatin domain acetylation with long-range gene activation. Mol Cell *9*, 291-302.

Hogga, I., and Karch, F. (2002). Transcription through the iab-7 cis-regulatory domain of the bithorax complex interferes with maintenance of Polycomb-mediated silencing. Development *129*, 4915-4922.

Hopmann, R., Duncan, D., and Duncan, I. (1995). Transvection in the iab-5,6,7 region of the bithorax complex of Drosophila: homology independent interactions in trans. Genetics *139*, 815-833.

Ishii, K., Arib, G., Lin, C., Van Houwe, G., and Laemmli, U.K. (2002). Chromatin boundaries in budding yeast: the nuclear pore connection. Cell *109*, 551-562.

Ishii, K., and Laemmli, U.K. (2003). Structural and dynamic functions establish chromatin domains. Mol Cell *11*, 237-248.

Ito, T., Bulger, M., Pazin, M.J., Kobayashi, R., and Kadonaga, J.T. (1997). ACF, an ISWI-containing and ATP-utilizing chromatin assembly and remodeling factor. Cell *90*, 145-155.

Jack, J., and DeLotto, Y. (1995). Structure and regulation of a complex locus: the cut gene of Drosophila. Genetics *139*, 1689-1700.

Johnson, K.D., Grass, J.A., Park, C., Im, H., Choi, K., and Bresnick, E.H. (2003). Highly restricted localization of RNA polymerase II within a locus control region of a tissue-specific chromatin domain. Mol Cell Biol *23*, 6484-6493.

Karch, F., Galloni, M., Sipos, L., Gausz, J., Gyurkovics, H., and Schedl, P. (1994). Mcp and Fab-7: molecular analysis of putative boundaries of cis-regulatory domains in the bithorax complex of Drosophila melanogaster. Nucleic Acids Res *22*, 3138-3146.

Katsani, K.R., Hajibagheri, M.A., and Verrijzer, C.P. (1999). Co-operative DNA binding by GAGA transcription factor requires the conserved BTB/POZ domain and reorganizes promoter topology. Embo J *18*, 698-708.

Kellum, R., and Schedl, P. (1991). A position-effect assay for boundaries of higher order chromosomal domains. Cell *64*, 941-950.

Kellum, R., and Schedl, P. (1992a). A group of scs elements function as domain boundaries in an enhancer- blocking assay. Mol Cell Biol *12*, 2424-2431.

Kellum, R., and Schedl, P. (1992b). A group of scs elements function as domain boundaries in an enhancer-blocking assay. Mol Cell Biol *12*, 2424-2431.

Kennison, J.A. (1993). Transcriptional activation of Drosophila homeotic genes from distant regulatory elements. Trends Genet *9*, 75-79.

Kyrchanova, O., Toshchakov, S., Parshikov, A., and Georgiev, P. (2007). Study of the functional interaction between Mcp insulators from the Drosophila bithorax complex:

effects of insulator pairing on enhancer-promoter communication. Mol Cell Biol *27*, 3035-3043.

Labrador, M., and Corces, V.G. (2002). Setting the boundaries of chromatin domains and nuclear organization. Cell *111*, 151-154.

Lanctot, C., Cheutin, T., Cremer, M., Cavalli, G., and Cremer, T. (2007). Dynamic genome architecture in the nuclear space: regulation of gene expression in three dimensions. Nat Rev Genet *8*, 104-115.

Ling, J.Q., Li, T., Hu, J.F., Vu, T.H., Chen, H.L., Qiu, X.W., Cherry, A.M., and Hoffman, A.R. (2006). CTCF mediates interchromosomal colocalization between Igf2/H19 and Wsb1/Nf1. Science *312*, 269-272.

Liu, S., McLeod, E., and Jack, J. (1991). Four distinct regulatory regions of the cut locus and their effect on cell type specification in Drosophila. Genetics *127*, 151-159.

Lomvardas, S., Barnea, G., Pisapia, D.J., Mendelsohn, M., Kirkland, J., and Axel, R. (2006). Interchromosomal interactions and olfactory receptor choice. Cell *126*, 403-413.

Maeda, R.K., and Karch, F. (2006). The ABC of the BX-C: the bithorax complex explained. Development *133*, 1413-1422.

Mahmoudi, T., Katsani, K.R., and Verrijzer, C.P. (2002). GAGA can mediate enhancer function in trans by linking two separate DNA molecules. Embo J *21*, 1775-1781.

Mahy, N.L., Perry, P.E., and Bickmore, W.A. (2002a). Gene density and transcription influence the localization of chromatin outside of chromosome territories detectable by FISH. J Cell Biol *159*, 753-763.

Mahy, N.L., Perry, P.E., Gilchrist, S., Baldock, R.A., and Bickmore, W.A. (2002b). Spatial organization of active and inactive genes and noncoding DNA within chromosome territories. J Cell Biol *157*, 579-589.

Marshall, W.F., Marko, J.F., Agard, D.A., and Sedat, J.W. (2001). Chromosome elasticity and mitotic polar ejection force measured in living Drosophila embryos by four-dimensional microscopy-based motion analysis. Curr Biol *11*, 569-578.

Melnikova, L., Juge, F., Gruzdeva, N., Mazur, A., Cavalli, G., and Georgiev, P. (2004). Interaction between the GAGA factor and Mod(mdg4) proteins promotes insulator bypass in Drosophila. Proc Natl Acad Sci U S A *101*, 14806-14811.

Mihaly, J., Barges, S., Sipos, L., Maeda, R., Cleard, F., Hogga, I., Bender, W., Gyurkovics, H., and Karch, F. (2006). Dissecting the regulatory landscape of the Abd-B gene of the bithorax complex. Development *133*, 2983-2993.

Mihaly, J., Hogga, I., Barges, S., Galloni, M., Mishra, R.K., Hagstrom, K., Muller, M., Schedl, P., Sipos, L., Gausz, J.*, et al.* (1998). Chromatin domain boundaries in the Bithorax complex. Cell Mol Life Sci *54*, 60-70.

Mihaly, J., Hogga, I., Gausz, J., Gyurkovics, H., and Karch, F. (1997). In situ dissection of the Fab-7 region of the bithorax complex into a chromatin domain boundary and a Polycomb-response element. Development *124*, 1809-1820.

Mito, Y., Henikoff, J.G., and Henikoff, S. (2007). Histone replacement marks the boundaries of cis-regulatory domains. Science *315*, 1408-1411.

Mlynarova, L., Loonen, A., Mietkiewska, E., Jansen, R.C., and Nap, J.P. (2002). Assembly of two transgenes in an artificial chromatin domain gives highly coordinated expression in tobacco. Genetics *160*, 727-740.

Moazed, D. (2001). Enzymatic activities of Sir2 and chromatin silencing. Current opinion in cell biology *13*, 232-238.

Moon, H., Filippova, G., Loukinov, D., Pugacheva, E., Chen, Q., Smith, S.T., Munhall, A., Grewe, B., Bartkuhn, M., Arnold, R.*, et al.* (2005). CTCF is conserved from Drosophila to humans and confers enhancer blocking of the Fab-8 insulator. EMBO Rep *6*, 165-170.

Morcillo, P., Rosen, C., Baylies, M.K., and Dorsett, D. (1997). Chip, a widely expressed chromosomal protein required for segmentation and activity of a remote wing margin enhancer in Drosophila. Genes Dev *11*, 2729-2740.

Morcillo, P., Rosen, C., and Dorsett, D. (1996). Genes regulating the remote wing margin enhancer in the Drosophila cut locus. Genetics *144*, 1143-1154.

Muravyova, E., Golovnin, A., Gracheva, E., Parshikov, A., Belenkaya, T., Pirrotta, V., and Georgiev, P. (2001). Loss of insulator activity by paired Su(Hw) chromatin insulators. Science *291*, 495-498.

Nabirochkin, S., Ossokina, M., and Heidmann, T. (1998). A nuclear matrix/scaffold attachment region co-localizes with the gypsy retrotransposon insulator sequence. J Biol Chem *273*, 2473-2479.

Nakayama, T., Nishioka, K., Dong, Y.X., Shimojima, T., and Hirose, S. (2007). Drosophila GAGA factor directs histone H3.3 replacement that prevents the heterochromatin spreading. Genes Dev *21*, 552-561.

Negre, B., and Ruiz, A. (2007). HOM-C evolution in Drosophila: is there a need for Hox gene clustering? Trends Genet *23*, 55-59.

Noma, K., Allis, C.D., and Grewal, S.I. (2001). Transitions in distinct histone H3 methylation patterns at the heterochromatin domain boundaries. Science *293*, 1150-1155.

Ohtsuki, S., and Levine, M. (1998a). GAGA mediates the enhancer blocking activity of the eve promoter in the Drosophila embryo. Genes Dev *12*, 3325-3330.

Ohtsuki, S., and Levine, M. (1998b). GAGA mediates the enhancer blocking activity of the eve promoter in the Drosophila embryo. Genes Dev *12*, 3325-3330.

Okada, M., and Hirose, S. (1998). Chromatin remodeling mediated by Drosophila GAGA factor and ISWI activates fushi tarazu gene transcription in vitro. Mol Cell Biol *18*, 2455-2461.

Oki, M., and Kamakaka, R.T. (2005). Barrier function at HMR. Mol Cell *19*, 707-716.

Oki, M., Valenzuela, L., Chiba, T., Ito, T., and Kamakaka, R.T. (2004). Barrier proteins remodel and modify chromatin to restrict silenced domains. Mol Cell Biol *24*, 1956-1967.

Parada, L., and Misteli, T. (2002). Chromosome positioning in the interphase nucleus. Trends Cell Biol *12*, 425-432.

Parkhurst, S.M., Harrison, D.A., Remington, M.P., Spana, C., Kelley, R.L., Coyne, R.S., and Corces, V.G. (1988). The Drosophila su(Hw) gene, which controls the phenotypic

effect of the gypsy transposable element, encodes a putative DNA-binding protein. Genes Dev *2*, 1205-1215.

Paro, R. (1990). Imprinting a determined state into the chromatin of Drosophila. Trends Genet *6*, 416-421.

Pikaart, M.J., Recillas-Targa, F., and Felsenfeld, G. (1998). Loss of transcriptional activity of a transgene is accompanied by DNA methylation and histone deacetylation and is prevented by insulators. Genes Dev *12*, 2852-2862.

Pirrotta, V. (1997). Chromatin-silencing mechanisms in Drosophila maintain patterns of gene expression. Trends Genet *13*, 314-318.

Rea, S., Eisenhaber, F., O'Carroll, D., Strahl, B.D., Sun, Z.W., Schmid, M., Opravil, S., Mechtler, K., Ponting, C.P., Allis, C.D.*, et al.* (2000). Regulation of chromatin structure by site-specific histone H3 methyltransferases. Nature *406*, 593-599.

Recillas-Targa, F., Pikaart, M.J., Burgess-Beusse, B., Bell, A.C., Litt, M.D., West, A.G., Gaszner, M., and Felsenfeld, G. (2002). Position-effect protection and enhancer blocking by the chicken beta-globin insulator are separable activities. Proc Natl Acad Sci U S A *99*, 6883-6888.

Rollins, R.A., Korom, M., Aulner, N., Martens, A., and Dorsett, D. (2004). Drosophila nipped-B protein supports sister chromatid cohesion and opposes the stromalin/Scc3 cohesion factor to facilitate long-range activation of the cut gene. Mol Cell Biol *24*, 3100-3111.

Routledge, S.J., and Proudfoot, N.J. (2002). Definition of transcriptional promoters in the human beta globin locus control region. J Mol Biol *323*, 601-611.

Schneuwly, S., Kuroiwa, A., and Gehring, W.J. (1987). Molecular analysis of the dominant homeotic Antennapedia phenotype. Embo J *6*, 201-206.

Schweinsberg, S., Hagstrom, K., Gohl, D., Schedl, P., Kumar, R.P., Mishra, R., and Karch, F. (2004). The enhancer-blocking activity of the Fab-7 boundary from the Drosophila bithorax complex requires GAGA-factor-binding sites. Genetics *168*, 1371-1384.

Segal, D., Cherbas, L., and Cherbas, P. (1996). Genetic transformation of Drosophila cells in culture by P element-mediated transposition. Somat Cell Mol Genet *22*, 159-165.

Simon, J. (1995). Locking in stable states of gene expression: transcriptional control during Drosophila development. Current opinion in cell biology *7*, 376-385.

Sipos, L., and Gyurkovics, H. (2005). Long-distance interactions between enhancers and promoters. Febs J *272*, 3253-3259.

Sipos, L., Mihaly, J., Karch, F., Schedl, P., Gausz, J., and Gyurkovics, H. (1998). Transvection in the Drosophila Abd-B domain: extensive upstream sequences are involved in anchoring distant cis-regulatory regions to the promoter. Genetics *149*, 1031-1050.

Small, S., Blair, A., and Levine, M. (1992). Regulation of even-skipped stripe 2 in the Drosophila embryo. Embo J *11*, 4047-4057.

Southworth, J.W., and Kennison, J.A. (2002). Transvection and silencing of the Scr homeotic gene of Drosophila melanogaster. Genetics *161*, 733-746.

Spana, C., Harrison, D.A., and Corces, V.G. (1988). The Drosophila melanogaster suppressor of Hairy-wing protein binds to specific sequences of the gypsy retrotransposon. Genes Dev *2*, 1414-1423.

Spector, D.L., and Gasser, S.M. (2003). A molecular dissection of nuclear function. EMBO Rep *4*, 18-23.

Spilianakis, C.G., Lalioti, M.D., Town, T., Lee, G.R., and Flavell, R.A. (2005). Interchromosomal associations between alternatively expressed loci. Nature *435*, 637-645.

Splinter, E., Heath, H., Kooren, J., Palstra, R.J., Klous, P., Grosveld, F., Galjart, N., and de Laat, W. (2006). CTCF mediates long-range chromatin looping and local histone modification in the beta-globin locus. Genes Dev *20*, 2349-2354.

Stief, A., Winter, D.M., Stratling, W.H., and Sippel, A.E. (1989). A nuclear DNA attachment element mediates elevated and position-independent gene activity. Nature *341*, 343-345.

Strohner, R., Wachsmuth, M., Dachauer, K., Mazurkiewicz, J., Hochstatter, J., Rippe, K., and Langst, G. (2005). A 'loop recapture' mechanism for ACF-dependent nucleosome remodeling. Nat Struct Mol Biol *12*, 683-690.

Suka, N., Suka, Y., Carmen, A.A., Wu, J., and Grunstein, M. (2001). Highly specific antibodies determine histone acetylation site usage in yeast heterochromatin and euchromatin. Mol Cell *8*, 473-479.

Tanabe, H., Habermann, F.A., Solovei, I., Cremer, M., and Cremer, T. (2002). Non-random radial arrangements of interphase chromosome territories: evolutionary considerations and functional implications. Mutat Res *504*, 37-45.

Tautz, D., and Pfeifle, C. (1989). A non-radioactive in situ hybridization method for the localization of specific RNAs in Drosophila embryos reveals translational control of the segmentation gene hunchback. Chromosoma *98*, 81-85.

Tolhuis, B., Palstra, R.J., Splinter, E., Grosveld, F., and de Laat, W. (2002). Looping and interaction between hypersensitive sites in the active beta-globin locus. Mol Cell *10*, 1453-1465.

Torigoi, E., Bennani-Baiti, I.M., Rosen, C., Gonzalez, K., Morcillo, P., Ptashne, M., and Dorsett, D. (2000). Chip interacts with diverse homeodomain proteins and potentiates bicoid activity in vivo. Proc Natl Acad Sci U S A *97*, 2686-2691.

Tsukiyama, T., Becker, P.B., and Wu, C. (1994). ATP-dependent nucleosome disruption at a heat-shock promoter mediated by binding of GAGA transcription factor. Nature *367*, 525-532.

Tsukiyama, T., Daniel, C., Tamkun, J., and Wu, C. (1995). ISWI, a member of the SWI2/SNF2 ATPase family, encodes the 140 kDa subunit of the nucleosome remodeling factor. Cell *83*, 1021-1026.

Tsukiyama, T., and Wu, C. (1995). Purification and properties of an ATP-dependent nucleosome remodeling factor. Cell *83*, 1011-1020.

Tuan, D., Kong, S., and Hu, K. (1992). Transcription of the hypersensitive site HS2 enhancer in erythroid cells. Proc Natl Acad Sci U S A *89*, 11219-11223.

Udvardy, A., Maine, E., and Schedl, P. (1985). The 87A7 chromomere. Identification of novel chromatin structures flanking the heat shock locus that may define the boundaries of higher order domains. J Mol Biol *185*, 341-358.

Varga-Weisz, P.D., and Becker, P.B. (2006). Regulation of higher-order chromatin structures by nucleosome-remodelling factors. Curr Opin Genet Dev *16*, 151-156.

Varga-Weisz, P.D., Blank, T.A., and Becker, P.B. (1995). Energy-dependent chromatin accessibility and nucleosome mobility in a cell-free system. Embo J *14*, 2209-2216.

Varga-Weisz, P.D., Wilm, M., Bonte, E., Dumas, K., Mann, M., and Becker, P.B. (1997). Chromatin-remodelling factor CHRAC contains the ATPases ISWI and topoisomerase II. Nature *388*, 598-602.

Vazquez, J., Belmont, A.S., and Sedat, J.W. (2001). Multiple regimes of constrained chromosome motion are regulated in the interphase Drosophila nucleus. Curr Biol *11*, 1227-1239.

Vazquez, J., and Schedl, P. (2000). Deletion of an insulator element by the mutation facet-strawberry in Drosophila melanogaster. Genetics *155*, 1297-1311.

Walter, J., Schermelleh, L., Cremer, M., Tashiro, S., and Cremer, T. (2003). Chromosome order in HeLa cells changes during mitosis and early G1, but is stably maintained during subsequent interphase stages. J Cell Biol *160*, 685-697.

Wang, M.M., and Reed, R.R. (1993). Molecular cloning of the olfactory neuronal transcription factor Olf-1 by genetic selection in yeast. Nature *364*, 121-126.

Wei, G.H., Liu de, P., and Liang, C.C. (2005). Chromatin domain boundaries: insulators and beyond. Cell Res *15*, 292-300.

West, A.G., and Fraser, P. (2005). Remote control of gene transcription. Hum Mol Genet *14 Spec No 1*, R101-111.

West, A.G., Gaszner, M., and Felsenfeld, G. (2002). Insulators: many functions, many mechanisms. Genes Dev *16*, 271-288.

West, A.G., Huang, S., Gaszner, M., Litt, M.D., and Felsenfeld, G. (2004). Recruitment of histone modifications by USF proteins at a vertebrate barrier element. Mol Cell *16*, 453-463.

Wilkie, G.S., and Davis, I. (2001). Drosophila wingless and pair-rule transcripts localize apically by dynein-mediated transport of RNA particles. Cell *105*, 209-219.

Wilkie, G.S., Shermoen, A.W., O'Farrell, P.H., and Davis, I. (1999). Transcribed genes are localized according to chromosomal position within polarized Drosophila embryonic nuclei. Curr Biol *9*, 1263-1266.

Xiao, H., Sandaltzopoulos, R., Wang, H.M., Hamiche, A., Ranallo, R., Lee, K.M., Fu, D., and Wu, C. (2001). Dual functions of largest NURF subunit NURF301 in nucleosome sliding and transcription factor interactions. Mol Cell *8*, 531-543.

Xu, Q., Li, M., Adams, J., and Cai, H.N. (2004). Nuclear location of a chromatin insulator in Drosophila melanogaster. J Cell Sci *117*, 1025-1032.

Yasui, D., Miyano, M., Cai, S., Varga-Weisz, P., and Kohwi-Shigematsu, T. (2002). SATB1 targets chromatin remodelling to regulate genes over long distances. Nature *419*, 641-645.

Yoon, Y.S., Jeong, S., Rong, Q., Park, K.Y., Chung, J.H., and Pfeifer, K. (2007). Analysis of the H19ICR insulator. Mol Cell Biol *27*, 3499-3510.

Yoshida, C., Tokumasu, F., Hohmura, K.I., Bungert, J., Hayashi, N., Nagasawa, T., Engel, J.D., Yamamoto, M., Takeyasu, K., and Igarashi, K. (1999). Long range interaction of cis-DNA elements mediated by architectural transcription factor Bach1. Genes Cells *4*, 643-655.

Zhao, H., and Dean, A. (2004). An insulator blocks spreading of histone acetylation and interferes with RNA polymerase II transfer between an enhancer and gene. Nucleic Acids Res *32*, 4903-4919.

Zhao, H., Kim, A., Song, S.H., and Dean, A. (2006). Enhancer blocking by chicken beta-globin 5'-HS4: role of enhancer strength and insulator nucleosome depletion. J Biol Chem *281*, 30573-30580.

Zhao, K., Hart, C.M., and Laemmli, U.K. (1995). Visualization of chromosomal domains with boundary element-associated factor BEAF-32. Cell *81*, 879-889.

Zhou, J., Barolo, S., Szymanski, P., and Levine, M. (1996). The Fab-7 element of the bithorax complex attenuates enhancer-promoter interactions in the Drosophila embryo. Genes Dev *10*, 3195-3201.

Zhou, J., and Levine, M. (1999). A novel cis-regulatory element, the PTS, mediates an anti-insulator activity in the Drosophila embryo. Cell *99*, 567-575.

Zink, B., Engstrom, Y., Gehring, W.J., and Paro, R. (1991). Direct interaction of the Polycomb protein with Antennapedia regulatory sequences in polytene chromosomes of Drosophila melanogaster. Embo J *10*, 153-162.